# CHARACTERIZATION OF OSFTIP9 IN REGULATING RICE TILLERING BEHAVIOUR

**ZHOU XUAN**

*(B. Sc. (Hons.), NUS)*

**A THESIS SUBMITTED**

**FOR THE DEGREE OF DOCTOR OF PHILOSOPHY**

**DEPARTMENT OF BIOLOGICAL SCIENCES**

**NATIONAL UNIVERSITY OF SINGAPORE**

2019

Supervisor :
Proferssor Yu Hao

Examiners:
Dr Yin Zhongchao
Professor Prakash P Kumar
Professor Mao Chuanzao, Zhejiang University

**DECLARATION**

I hereby declare that this thesis is my original work and
it has been written by me in its entirety.
I have duly acknowledged all the sources of information
which have been used in the thesis.

This thesis has also not been submitted for any degree in any university previously.

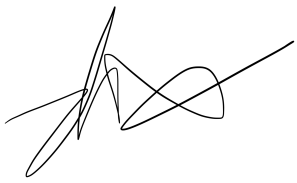

ZHOU XUAN
5 August 2019

# Acknowledgements

I would like to express the sincerest and deepest gratitude to Professor Yu Hao, for being my supervisor, who granted me such a precious opportunity to conduct my doctorate research in his laboratory. He was the one introduced me to the field of molecular biology, and his constant, unfailing encouragement throughout these years walked me out of all the difficulties that I was or was not prepared for. He had been a knowledgeable, patient, and supportive supervisor, from whom I received not only trainings over proper scientific researches, but also lessons of being a capable researcher. In a nutshell, Professor Yu Hao had mentored me in all ways that a mentee can be supervised, which would definitely be the treasures to be carried throughout my research life.

I would also like to thank Professor Prakash Kumar, and Dr. Yin Zhongchao, for being my TAC members for years. Their valuable comments helped me navigate better in project designing and experiment performance, and their patience and kindness had been giving me much support. I would also thank Associate Professor Liou Yih Cherng, for his being my good friend who enlightened my research life in campus.

I am extremely grateful for the Research Scholarship offered by the Department of Biological Sciences (DBS), National University of Singapore, without which the project could never be done. And it was highly appreciated for the department to

provide with those common facilities, which was beneficial for all the researchers in DBS.

Last but never the least, I would like to express my utmost appreciation and gratitude to all the friends and fellow lab members, Dr. Liang Zhe, Li Yan, Dr. Shen Lisha, Dr. Gong Ximing, Dr. Bao Shengjie, Dr. Wang Yanwen, Dr. Zhang Bin, Dr. Wang Qian, for their lovely company and precious friendship. Special thanks to Dr. Liu Lu and Dr. Norman Teo Zhi Wei, for their generous support and valuable advice throughout.

Diamonds don't shine; they reflect. I was, am, and will always be in deep love with my parents, without whom I could never grow into who I am today. Their endless love has been giving me enormous courage and confidence, and will be my support forever.

August 2019

Zhou Xuan

# Table of Contents

# Summary

Multiple C2 domain and transmembrane region proteins (MCTPs) are involved in macromolecular trafficking, which play important roles in various plant developmental stages. In this study, we focused on the investigation of one of the rice (*Oryza Sativa L.*) MCTPs, FT-INTERACTING PROTEIN 9 (OsFTIP9). Using CRISPR-Cas9 system, we generated two loss-of-function mutant of *OsFTIP9*, namely *Osftip9-1* and *Osftip9-2*. The *Osftip9-1* had increased number of secondary tillers, which could be rescued by genomic fragment of *OsFTIP9*. The mutant phenotype was consistent with *OsFTIP9* RNAi lines and the co-suppression lines. Also, *in situ* hybridization revealed the mRNA expression of *OsFTIP9* in the shoot apical meristem (SAM) and axillary buds.

Yeast two-hybrid (Y2H) screening was performed using different truncated forms of OsFTIP9 containing various numbers of C2 domains. Potential interacting partners included Fine Culm 1 (FC1), DWARF 14 (D14) and DWARF 14-LIKE (D14L). The interaction between OsFTIP9 and the potential interacting partners were then validated through several methods. Y2H assay showed that both FC1 and D14L interacted with truncated OsFTIP9 containing three C2 domains, while D14 interacted with truncated OsFTIP9 containing two C2 domains. BiFC and pull-down assay also showed that OsFTIP9 interacted with FC1 and D14L. We also obtained the deletion mutants, *fc1-2* and *d14*, in the *Nipponbare* background from other laboratories, and confirmed that the tillering phenotypes of both mutants were similar to *Osftip9-1*. Given the similarity level of the phenotypes and validity of available evidence, we focused on elucidating

the interaction between OsFTIP9 and FC1. And thus, *FC1* RNAi lines were generated as a crosscheck, and FC1 antibodies were also produced for the detection of FC1 protein.

We firstly found that the expression pattern of FC1 at the tissue level was not changed in *Osftip9-1* mutant background across different growth stages, suggesting that OsFTIP9 might not transport FC1 across tissues. However, the stability of FC1 was reduced in *Osftip9-1* as compared to wild-type (WT), as detected by the Western Blot results. Thus, OsFTIP9 might help stabilize FC1 protein. We also found that the Subcellular localization of FC1 was changed in *Osftip9-1* protoplast cells as compared to WT: FC1 was localized completely to the nucleus in WT protoplast cells, but the signal was present in the whole cell of *Osftip9-1* mutant backround. We further found that the expressions of two FC1 downstream target genes were changed in *Osftip9-1* and *fc1-2*, which were *D14*, and *RICE GRASSY TILLERS 1* (*OsGT1*). Taken together, our results suggested that OsFTIP9 played important roles in stabilizing FC1 protein and mediating the transportation of FC1 into the nucleus, thus affecting the expression of FC1 downstream target genes to regulate rice tillering behaviour.

# List of Tables

# List of Figures

# Chapter 1

# Literature Review

# Chapter 1 Literature Review

## 1.1 Rice attracts great research interest as an important staple food

### 1.1.1 Global rice consumption urges the need for scientific research

Rice is one of the most important food sources worldwide, which sustains more than half of the world's population, especially as an important staple food in the Asian countries (Khush, 2005). Up to 90% of rice is consumed by Asians, which constitutes about 60% of the world's total population, and what makes the challenges worse is that this population is still in booming growth (Khush, 2005). Currently, rice, including food made using rice, accounts for 1/3 to 2/3 of the total calorie intake by Asians, reflecting the importance of rice in the Asian diet (Khush, 2005).

However, this still does not resolve the food crisis facing the whole world, given two persisting problems: 1. The rice production is yet too low to meet the consumption need, despite the fast growth rate; 2. The population growth in rice-consuming countries is expected to be growing at a faster speed than rice supply. In fact, the food crisis is still one of the biggest problems globally. More than 1 person dies from hunger every minute, and for those who are still alive, chronic hunger and nutrition-deficiency are also causing life threatening conditions to them (Khush, 2005). With the booming development of the economy, the population growth is getting increasingly diverse

among various countries. For countries in the developed areas, they are having less and even negative growth, while for less-developed countries, the population is till shooting up.

The demand for rice is expected to further grow in the future, in terms of both quantity and quality: for developed countries, they are demanding for better rice such as higher nutrition and better taste; while for developing countries, they are striving for feeding more people with food growth in the limited arable lands. It is projected that up to 40% more rice will be needed by 2030, in order to be able to catch up with the growing consumption demand, yet the lands suitable for farming has been extensively exploited (Khush, 2005). Facing such a challenge of producing more rice with limited arable lands, several ways have been proposed: wide hybridization, hybrid breeding, conventional hybridization & selection, genetic engineering and ideotype breeding (Khush, 2005). Some of them have already been employed the rice production, such as the crossing of wild rice species with the cultivated ones. It should be noticed that these methods can be combined in order to achieve better results, for example, genetically modified rice with better ideotype.

### 1.1.2 The architecture of rice has direct impacts on the yield

The architecture of a rice plant has a substantial influence over rice production, especially in terms of yield. Modern rice has been characterized as semi-dwarf, with

larger leaf area but relatively large number of non-productive tillers. Tillers refer to the branches in monocotyledonous plants, such as rice, which determine the space requirement of a plant. A tiller typically emerges from the leaf axil, usually on the basal internodes that are not elongated yet. To further increase rice production, it is proposed that the future of rice traits contains several characteristics: 1. Relatively low tiller number of about 10; 2. All the tillers are productive, and each panicle produces around 250 grains; 3. The leaves are relatively erect, with dark green color for better photosynthesis; 4. The root system is deep and vigorous (Khush, 2005).

In fact, the study of crop plant architecture has long been attracting interests, as it does not only affect the yield, but also decides the survival ability. Rice plant architecture is mainly described by the panicle morphology, height, and tillers. For tiller-related trait, it is further discussed in terms of tiller angle and tiller number. On one hand, tiller angle refers to the angle between a tiller and the main culm (Xu, McCouch, & Shen, 1998). For a rice plant with large tiller angle, it requires large space due to the big canopy, while for a rice plant with too small tiller angle, the total area receiving light is rather small, leading to insufficient photosynthesis. On the other hand, tiller number refers to the number of branches that develop from the axillary meristems, which plays a substantial role in determining the architecture (Wang & Li, 2005).

### 1.2 FTIP family proteins exert transportation function

### 1.2.1 MCTPs are critical for macromolecular trafficking

The C2 domain, a lipid-binding domain, has long been considered to have important potential functions in eukaryotes, as this conserved domain possesses the ability to target proteins to the membrane (Nalefski & Falke, 1996). The structure of a C2 domain typically constitutes a β-sandwich made by 8 anti-parallel strands, and displays two distinct topologies (Nalefski & Falke, 1996). Despite the functional structure, as well as the prevalent presence of C2 domain-containing genes in plant genomes, only a few have been found to actually exert the macromolecular trafficking *in planta* (Liu, Zhu, Shen, & Yu, 2013). Among those genes, each one of them contains various numbers of C2 domains with or without a transmembrane domain. Apart from proteins containing one C2 domain, most of them belong to the family named multiple C2 domains and transmembrane region proteins (MCTPs). Despite the relatively small number of MCTPs in the animal genomes, they are more abundant in the plant genomes, and moreover, they are highly conserved especially in angiosperms (Liu et al., 2012). MCTP family is further divided into subfamilies, including the FTIP1-like MCTPs and synaptotagmins (Liu et al., 2012).

The FTIP1-like MCTP family was first identified in *Arabidopsis*, all 16 members of which encode several C2 domains followed by one or several transmembrane domains (Liu et al., 2013). FTIP1 and QUIRKY (QKY) protein were reported to have the transportation function in the vascular tissue. It is also found that QKY might regulate

the signalling of STRUBBELIG (SUB) through a non-cell-autonomous manner (Fulton et al., 2009). More recently, two other members from the FTIP1-like MCTPs, FTIP3 and FTIP4, are found to prevent the intercellular trafficking of SHOOTMERISTEMLESS (STM) in the shoot apical meristems (Liu et al., 2018).

### 1.2.2 FTIP1 regulates flowering time by mediating FT transport in *Arabidopsis*

FT- INTERACTING PROTEIN 1 (FTIP1) was reported to regulate flowering time of *Arabidopsis* through transportation of the florigen encoded by *FLOWERING LOCUS T (FT)* (Liu et al., 2012). During the early developmental stage, the reiterative primordial production of SAM contributes to the accumulation of biomass (Bowman & Eshed, 2000). The architecture of a plant was planned at the stage of embryogenesis, while SAM executes the pre-set body plan by giving rise to such vegetative organs as leaves and tillers (Levy & Dean, 1998). When the ambient environment signals are sensed, such as light and temperature, a mature rice plant will switch to the reproductive stage. At this stage, SAM will change from producing vegetative organs to reproductive organs, such as flowers (Hastings & Follett, 2001). This process is the flowering transition, during which both exogenous and endogenous signals were perceived (Hastings & Follett, 2001). Given the importance of the flowering transition, it has been attracting research focus for long, and 4 pathways are proposed to play regulatory roles, which are autonomous pathways, photoperiodic pathways, gibberellin pathways and vernalization pathways (Hastings & Follett, 2001). Furthermore, it is found that all

these 4 pathways do not function independently, as they converge to a few common integrators, known as florigen. In *Arabidopsis*, *FT* is found to encode the protein that functions as the so-called florigen, and following this, orthologs of *FT* in other plant species are reported with similar functions in flowering transition (Corbesier et al., 2007; Jaeger & Wigge, 2007; M. K. Lin et al., 2007; Mathieu, Warthmann, Kuttner, & Schmid, 2007; Tamaki, Matsuo, Wong, Yokoi, & Shimamoto, 2007). Despite the elucidation of the genetic pathways, the missing linkage remains in the transportation of FT: while it makes sense that FT is synthesized in the leaf tissue as the photoperiodic signal is perceived, the distance from leaves to SAM required carriers of FT (Bernier & Perilleux, 2005; Zeevaart, 1962).

FTIP1 encodes a protein containing three C2 domains and a phosphoribosyltransferase C-terminal domain (PRT_C). It is localized to the endoplasmic reticulum (ER), which overlaps with the localization of FT (Liu et al., 2013). Given the function of ER forming a membrane vesicle network bridging the sieve element and companion cells, FTIP1 might possess the function of transporting FT from companion cells to the sieve elements, probably through plasmodesmata (Liu et al., 2013). The FTIP1's function of membrane trafficking, as well as the protein structure, resemble the synaptotagmins. Synaptotagmins are a protein family characterized by two C2 domains, a variable linker and a N-terminal transmemvrane region, ane such a structure enables the membrane-trafficking function (Liu et al., 2013). And an increasing amount of evidence shows that

MCTPs do have the potential of transportation, which is significant for plant development.

### 1.2.3 Rice OsFTIPs also possess transportation functions in various genetic pathways

Shortly after the publication of FTIP1, its ortholog in rice, OsFTIP1, was reported to have similar transportation function that regulates the flowering transition in rice (Liu et al., 2012; Song et al., 2017). OsFTIP1 belongs to the FTIP1-like MCTPs found in rice, namely, the OsFTIPs. With the similar protein structure of 3 C2 domains followed by one PRT_C domain, *Osftip1* loss-of-function mutant shows late-flowering phenotype under long day (LD) condition. It is found to interact with the LD florigen, RFT1. Similar to the FTIP1 and FT, colocalization of RFT1 and OsFTIP9 on the ER is reported (Song et al., 2017). It is further found that OsFTIP9 is only present in the companion cells, indicating that OsFTIP9 might be responsible for transporting RFT1 out of companion cells (Song et al., 2017). Although it is difficult to directly examine the presence of OsFTIP1 in the plasmodesmata, available evidence still indicates that the transportation of RFT1 into the sieve element is via the plasmodesmata, in consideration of the similarity between FTIP1 and OsFTIP1.

More recently, another member of OsFTIPs, OsFTIP7, was also reported to regulate the nuclear translocation process of *Oryza sativa* HOMEOBOX 1 (OSH1) (Song et al.,

2018a). OSH1 is a transcription factor that supresses *OsYUCCA4*, which controls the synthesis of auxin (Song et al., 2018b). And thus, the loss-of-function mutant of *Osftip7* exhibits anther indehiscence phenotype, which eventually affects the rice grain production (Song et al., 2018b).

### 1.2.4 OsFTIP9 is MCTP protein in rice with potential functions in membrane trafficking

Among the 12 OsFTIP members, only OsFTIP1 and OsFTIP7 are identified with transportation roles. All OsFTIP proteins contain 3 or 4 C2 domains, followed by a various number of transmembrane regions forming the PRT_C domain. Such a conserved protein structure indicates that other member of OsFTIPs may also have similar functions of macromolecular trafficking as OsFTIP1 and OsFTIP7.

Among the OsFTIPs, OsFTIP9 is the closest ortholog to the *Arabidopsis* QKY. QKY plays a role in the cell-to-cell communication, and its loss-of-function mutant exhibits abnormally developed floral organ, leaves, stems and siliques (Fulton et al., 2009; Vaddepalli et al., 2014). It is further proposed that QKY regulates vascular transport through plasmodesmata (Epel, 1994; Vaddepalli et al., 2014). The above mentioned evidence suggested a conserved function of macromolecular trafficking of OsFTIP9.

## 1.3 Tillering behaviours of rice

### 1.3.1 Molecular perspective of tillering in rice

Despite the fact that tillering behaviour has been an attracting research focus and some rice mutants exhibiting tillering phenotype were identified quite early, genetic research uncovering the underlying molecular mechanisms remains insufficient. It has been mysterious that why some rice breeds showed elevated or reduced tiller numbers, until more recently, more tiller-related genes, such as *MONOCULM 1* (*MOC1)* and *Oryza sativa TEOSINTE BRANCHED 1* (*OsTB1)*, are reported (Liang, Shang, Lin, Lou, & Zhang, 2014; C. Xu et al., 2012).

*MOC1* is the first gene found as a key regulator controlling rice tillering (X. Li et al., 2003). It is orthologous to the *LATERAL SUPPRESSORS* (*LAS*) in *Arabidopsis* and tomato, which is a member of the GRAS family (Greb et al., 2003; Pysh, Wysocka-Diller, Camilleri, Bouchez, & Benfey, 1999; Schumacher, Schmitt, Rossberg, Schmitz, & Theres, 1999). MOC1 is expressed inn the axillary buds and mainly regulats the emergence of axillary meristem (Liang et al., 2014). The *moc1* mutant fails to generate axillary buds, resulting in merely a monoculm. Thus, MOC1 is proposed to be a positive regulator of tillering (Liang et al., 2014). More recently, *TILLERING AND DWARF* 1 (*TAD1*) and *TILLER ENHANCER* (*TE*) are found to be coexpressed with *MOC1*. The *tad1* loss-of-function mutant shows increased tiller number and dwarfism phenotype;

while *te* loss-of-fuction mutant also exhibits significantly increased tiller number (Lin et al., 2012; C. Xu et al., 2012). TAD1 forms a complex with other genes before interacting with MOC1, while TE also interacts with MOC1 in a similar way by forming the complex of APC/$C^{TE}$ (Lin et al., 2012). The final complex formation that consists MOC1 degrades in a cell-cycle-dependent manner, which eventually controls the rice yield through regulating the axillary tiller growth (Lin et al., 2012; C. Xu et al., 2012).

*LAX PANICLE 1* (*LAX1*) is another gene reported to be a regulator in the tillering pathway, through controlling of the emergence and maintenance of the the axillary meristem (Komatsu et al., 2003). It is showed that LAX1 accumulates in the emerging axillary meristem transiently at the plastochron 4 stage, and it plays a role in the tillering pathway by controlling the protein trafficking (Oikawa & Kyozuka, 2009). LAX2 is subsequently found to be involved in the same pathway through interaction with LAX1 (Tabuchi et al., 2011).

### 1.3.2 Strigolactone pathway, a novel pathway newly discovered to regulate rice tillering

Strigolactones (SLs) are primarily identified in the root exudates that stimulated germination (Cook, Whichard, Turner, Wall, & Egley, 1966). They are carotenoid-derived hormones present in a wide range of plants with various functions (Waters, Gutjahr, Bennett, & Nelson, 2017). More recently, SLs are found to regulate the plant

tillering behaviour by acting as repressors (Gomez-Roldan et al., 2008; Umehara et al., 2008). The most well-known mechanism through which SLs control tillering is the D14-MAX2-D53 signalling pathway, yet it remains to be further elucidated regarding the downstream events ((Waters, Gutjahr, Bennett, & Nelson, 2017).

There are two proposed models: 1. SLs might regulate the transcription of *BRANCHED1* (*BRC1*), a transcription factor belonging to the TCP family; 2. SLs might regulate the PIN1 protein, which is an auxin efflux carrier, at the plasmamembrane (De Cuyper et al., 2015; Dun, de Saint Germain, Rameau, & Beveridge, 2012). For the first model, it is hypothesized that SLs and cytokinin are synthesized in the root and then transported to the bud via xylem (Brewer, Dun, Gui, Mason, & Beveridge, 2015; Dun et al., 2012). Furthermore, SLs is hypothesized to be the secondary messengers of auxin, which represses axillary tillers indirectly (Domagalska & Leyser, 2011). SLs and cytokinin both regulate BRC1. The *brc1* mutant exhibit higher tillering ability and is insensitive to SL treatment. Moreover, treatment with GR24 (an SLs analog) significantly upregulates the expression of *BRC1*, which suggests that BRC1 acts as a target of SLs (Waters et al., 2017). For the other model, auxin is proposed to be synthesized in the bud and then exported out. In this model, axillary buds need to canalize auxin out to the root, in order to be released from the suppression effects brought by the auxin, and thus, a transport link connecting bud to the main stem is expected to be established (Prusinkiewicz et al., 2009). It is also hypothesized that several buds will form a competition for the strength of the auxin sources. Published

data supported that PIN1 is regulated by SLs, yet there is still insufficient data directly proved that the regulation of SLs on PIN1 determines the tillering berhaviour (Bennett et al., 2016; Bennett et al., 2006).

### 1.3.3 Rice *FC1* gene plays a critial role in regulation tillering-related genes

*FINE CULM 1* (*FC1*) was primarily named as *OsTB1*, which is orthologous to *TB1* in maize. It encodes a protein belonging to the TCP family protein, a transcription factor with a length of 388 amino acids (Minakuchi et al., 2010). To be more specific, FC1 belongs to the CYC/TB1 subfamily, with two more rice genes belonging to this family (Martin-Trillo & Cubas, 2010; Yuan et al., 2009). A recessive allele, *fc1-2*, is in the *Nipponbare* background (Minakuchi et al., 2010). This mutant contained two deletions adding up to 27 bp within the TCP domain, which is the reserved functional domain. *fc1-2* exhibits increased tiller number as well as mild dwarfism phenotypes (Arite et al., 2007). More importantly, the mutant phenotypes cannot be rescued by the application of exogenous GR24, which suggests that FC1 might be essential for SLs pathway (Minakuchi et al., 2010). The Functioning of SLs requires the presence of FC1 protein, so that the tiller dormancy can be maintained (Minakuchi et al., 2010).

In addition, the mRNA expression of *FC1* is examined in the bud of WT rice plants. It was found that *FC1* mRNA is expressed in the shoot apical meristem area, including the surrounding leaves and vascular tissues, as well as the emerging axillary buds,

especially the primordia (Minakuchi et al., 2010). Furthermore, hormonal treatments, including IAA and SLs, do not affect the expression pattern of *FC1* in various tissues, indicating that the expression of *FC1* is not under direct regulation of SLs (Minakuchi et al., 2010).

Taken together, it is proposed that FC1 acts downstream of both SLs pathway and cytokinin pathway to inhibit the emergence and growth of axillary buds. And SLs promote, while cytokinin inhibits, the function of FC1. FC1 functions as a transcription factor to directly regulate the most end-stream genes related to tillering phenotypes.

### 1.3.4 Rice *D14* gene is a critical receptor of SLs

A series of dwarf mutants with more tillering phenotype has been reported, including *dwarf 3* (*d3*), *d10*, *dwarf 17* (*d17*). While *D10* is orthologous to *MAX4/RMS1/DAD1*, *D3* is orthologous to *MAX2/RMS4*. And *D17* is orthologous to the *MAX3/RMS5* (Arite et al., 2009). The D14 gene, characterised as a receptor of SLs, belongs to the α/β-hydrolase superfamily (Arite et al., 2009). The *d14* mutant is reported to contain a single substitution, acting as a recessive mutant (Arite et al., 2009). It shows much higher tiller number than WT, as well as drastic dwarfism phenotype (Arite et al., 2007). Genetic experiments prove that D14 is also involved in the SLs pathway as the double mutant of *d10-1* and *d14-1* shows no differentiable phenotype as that of *d10-1* or *d14-1*, while D10 has been reported to function in the SLs synthesis (Arite et al., 2009; Ishikawa et

al., 2005). *d14* is SL-insensitive when being applied with exogenous GR24, indicating an impaired SL signaling (Arite et al., 2009). The *D14* mRNA showed high expression in the buds as well as leaves, yet GUS staining indicates that the transcription of *D14* is mainly in the vasculature, including the axillary buds, stems and parenchyma cells (Arite et al., 2009). Furthermore, AtD14 is reported to act as a receptor of SLs in *Arabidopsis*, as it forms the AtD14–D3–ASK1 complex to exert the function of SLs (Yao et al., 2016).

# Chapter 2

# Materials & Methods

# Chapter 2 Materials & Methods

## 2.1 Plant materials & growth conditions

All rice (*Oryza sativa* ssp *japonica*, cultivar *Nipponbare*) plants were grown under long days with 14 h light and 10 h dark condition, at the temperature of 32°C and 25°C, respectively. The relative humidity was ~70%.

Fertiliser was supplied when the seedlings were 4 weeks old, using POLY Fert 21-21-21 produced by New Eastern (1971) PTE LTD. Fertuliser powder was dissolved in water (10% w/v) as 10X prepared stock. A total volume of 50ml 1X diluted fertiliser solution was added to each rice pot to ensure equal amount, at the early development stage.

## 2.2 Plasmid construction

### 2.2.1 Polymerase Chain Reaction (PCR) amplification and cloning

Target Fragments were amplified using PCR. The reaction system was set as: 1 µl reaction template (genomic DNA, cDNA or even plasmids dependent on the desired PCR fragments), 0.2 mM dNTP mix, 1X PCR buffer, 10 pmol of each of the forward and reverse primers (designed to be specific to the targeted fragments), and lastly, 0.5U

PfuTurbo® (Stratagene, USA). The reaction was topped up to the desired volume with sterile water and went through thermal cycling. The programme was set as: pre-denaturation for 10 min at 95 °C; 40 cycles of denaturation for 30 s at 95 °C, annealing (temperature and time length depended on the primer sets and length of products), extension for 5 min at 72 °C; final extension for 10 min at 72 °C. The product was kept at -20 °C or immediately run through agarose gel electrophoresis, of which the gel concentration depended on the size of the bands, followed by visualisation by ethidium bromide (EtBr) staining.

After confirming the existence of the desired band, the PCR product was purified using Gel/PCR DNA fragments extraction kit (Geneaid) or PCR purification kit, depending on the products being PCR products or recycled agarose gel containing the band. To purify the PCR product, it was mixed with 5 volume of the DF buffer, and then transferred to the DF column. The column went through centrifugation for 1 min at the maximum speed. The column was washed with 350 µl Wash Buffer twice, and then spin dry for 3 min at the maximum speed. The column was added with 30-50 µl elution buffer and the eluted product was collected by 1 min centrifugation at the top speed. On the other hand, for the gel purification, the desired band was contained in the agarose gel. 2X volume of the Buffer DF was added to the gel tube. The tube was placed at 60 °C for 30 min until the gel dissolved completely. The mixture then underwent the same procedures as PCR product purification. The purified product was examined using nanodrop to check the concentration and quality.

The fragment was then digested in preparation ligation. Up to 2000 ng purified fragment was mixed with 6X CutSmart buffer and 2 µl desired restriction enzyme if single digestion or 2 µl each of the desired restriction enzymes if double digestion. The reaction was topped up to 60 µl with sterile water and mixed well by gentle pipetting. The digestion was carried out at 37°C for 2 h, and the product went through the same PCR purification procedures as described in the previous section. The linearized fragment was then ligated using T4 DNA ligase to the vector linearized with matching restriction enzymes. The reaction system was set as: 100 ng linearized fragment, 20 ng linearized vector, 10X T4 ligase buffer and 2 µl T4 DNA ligase enzyme (Fermentas). It was mixed well by gentle tapping and incubated at 16 °C for 6 hr. The ligation product was then ready to be delivered into the *E. coli* competent cells for positive screening and colony PCR.

### 2.2.2 Heat shock transformation

The ready-made *E. coli* competent cells (Strain XL1-blue) were thawed on ice for up to 15 min and then mixed with the ligation products or plasmids. The mixture was gently tapped several times in order to be mixed well and then incubated on ice for another 10 min period. The tube was then transferred to 42°C incubator for 60 s, followed by immediate cooling on ice for 15 min. The bacteria were supplied with 700 µl of LB medium and incubated at 37 °C for 30 min with shaking. Cultured bacteria

were then collected as pellet through centrifugation of 1 min at the speed of 3000 rpm, and then resuspended with 70 µl LB medium. The bacteria were spread evenly over LB agar plate containing appropriate antibiotics as a selection. Positive colonies were visible after overnight incubation at 37°C.

### 2.2.3 Clone verification through PCR

In order to verify the positive colonies that contained the desired plasmid, they were picked and resuspended individually in 10 µl sterile water, 1 µl of which was used as the PCR amplification template. Each of the 10 µl reaction system also contained 1 unit Taq DNA polymerase, 0.2 mM dNTP, an adequate amount of water and 0.2 mM primer sets. The primer set consisted of one specific to the vector and the other specific to the DNA insertion fragment. PCR cycles were set accordingly, depending on the amplification length, melting temperature and etc. The PCR products were analysed by gel electrophoresis, in order to check the presence of the desired bands. Finally, verified colonies were further incubated in 2 ml LB medium overnight at 37°C for plasmid DNA extraction.

### 2.2.4 Plasmid DNA extraction

Amplified bacterial culture was extracted using the High-Speed Plasmid Minikit (Geneaid, Taiwan), and the steps were the same as the manufacturer's instruction.

Cultured bacteria was collected as pellets by centrifuging for 1 min at the maximum speed, followed by resuspension with 250 µl PD1 buffer. 350 µl PD2 buffer was then added and the tube was gently inverted several times for a complete mixture. 350 µl PD3 buffer was shortly added thereafter, followed by the same inversion procedure. The whole lysate went through centrifugation for 10 min at the maximum speed, followed by transferring of the supernatant to the PD column assembled with the collection tube. Centrifugation was then applied in order to pass the liquid down through the column, and the PD column was further washed with 350 µl W1 buffer once and 700 µl Washing buffer twice. The column was further dried up by spinning for 3 mins at the top speed. The appropriate amount of elution buffer (30-200 µl) was used to elute out the plasmids. The concentration and quality of the extraction were measured by nanodrop and stored at -20°C for future usage.

### 2.2.5 DNA sequencing & analysis

In order to further validate the insertion fragment, DNA sequencing was performed using the BigDye® Terminator v3.1 CycleSequencing Kit (Applied Biosystems). 1 µl (100-300 ng for plasmids and 10-20 ng for PCR fragments) of the sequencing template was added into the 10 µl reaction mix, which also contained: 5 µl 2X Big Dye Enzyme, appropriate amount of sterile water and 2 pmol selected primer that targets the desired sequencing site. Sequencing PCR cycles were set accordingly, usually as follows: 10 s denaturation at 96°C for 25 cycles, 5 s annealing at 50 °C, and 3 min extension at 60°C.

The reaction product was then sent to the DBS sequencing lab for sequencing, and the results were analysed through the BLAST function on National Centre for Biotechnology Information (NCBI, http://www.ncbi.nlm.nih.gov/).

### 2.3 Plant transformation & tissue culture

#### 2.3.1 Preparation of *Agrobacterium tumefaciens* AGL1 competent cell

A single colony of *A. tumefaciens* AGL1 was picked from the medium plate and inoculated into 2 ml LB liquid medium for overnight culturing at 28 °C with gentle shaking. It was further transferred into 100 ml LB liquid medium and continued to be cultured at the same temperature until the $OD_{600}$ reached around 0.6. The bacteria were cooled down on ice and collected as pellet through centrifugation of 10 min at 3000 rpm, 4 °C. The pellet was further rinsed for multiple times with ice cold sterile water and resuspended to a final volume of 8 ml. It was then aliquoted into sterilized 1.5 ml tubes in a portion of 50 μl with quick freezing in liquid nitrogen. The competent cells were stored at -80 °C for future usage.

#### 2.3.2 Generation of rice calluses

Rice calluses were induced prior to the *Agrobacterium*-mediated transformation, which could be from WT seeds or seeds of other desired transgenic materials. The seed husks were peeled off and healthy, white seeds were sterilized in 30% bleach solution for 30 min with vigorous shaking, and then the seeds were transferred to a laminar flow, and rinsed with sterile water for 10 times, 1 min each, in order to remove the detergent completely. The seeds were then placed on a stack of sterilized filter paper for the excessive water to be absorbed. In order to reach maximum induction efficiency, the seeds were left on the filter paper inside the laminar flow for 2 h. N6D medium was then prepared as follows: every 1 L of the N6D medium contains 3 g Chu ($N_6$) Basal Salt Mixture, 5 ml MS Organic, 2 mg 2,4-D, 0.3 g casein hydrolase, 2.878 g L-proline, 30 g sucrose and 3 g phytagel; the PH was adjusted to 5.8 and the medium was autoclaved at 121 °C for 20 min, before being poured to petri dishes and solidified. The sterilized seeds were then placed on the N6D medium, and the plates were sealed and placed inside a growth chamber under the condition of all-day light and constant temperature of 32 °C.

The calluses were visible after 3-5 days, and their quality reached the optimum status after 2-3 weeks. The calluses were excised from the gernminated seeds, and then carefully transferred to a new batch of N6D medium plates. The plates were again sealed and placed back to the chamber for another 5-7 days before being used for *Agrobacterium*-mediated transformation.

### 2.3.3 Transformation of *Agrobacterium* competent cells with plasmids

The AGL1 *Agrobacterium* competent cell was taken out from -80 °C and allowed to thaw on ice for 10 min. And then, 5 µl of the constructs (1,000 ng) was added into the competent cell and mixed well through gentle tapping. The mixture was then placed on ice for 5 min before being put into liquid nitrogen for another 5 min. The frozen tube was then transferred immediately to 37 °C incubator for 10 min. 700 µl LB broth medium was added and the bacteria culture were cultured in 28 °C for 1 hr with gentle shaking. The bacteria were collected as a pellet by centrifugation of 30 s at the maximum speed, and resuspended with 100 µl LB broth medium. LB agar plate containing the desired antibiotics was then used to culture the bacteria, followed by incubation at 28 °C for 2-3 days before positive colonies were visible.

The colonies were verified for positive transformation through PCR using similar colony PCR method as described previously.

### 2.3.4 *Agrobacterium*-mediated transformation

Several media were prepared prior to the *Agrobacterium*-mediated transformation: 1. 1 L of N6D-Co-As medium contained 50 ml N6D macro, 5 ml N6D micro, 5 ml MS organic, 5 ml Fe-EDTA, 2 mg 2,4-D, 0.3 g casein hydrolate, 30 g sucrose, 10 g glucose, 3 g phytagel. 2. 1L of N6D-AAM contained 50 ml AAM Macro, 5 ml AAM Micro, 5

ml AAM Organic, 100 ml AAM Amino acid, 5 ml Fe-EDTA, 68.5 g sucrose, 0.5 g casein hydrolate, 36 g glucose. The PH of both mediums were adjusted to 5.2. It was to be noticed that the glucose was dissolved as a separate solution for both mediums, and everything was autoclaved at 121 °C for 20 min. Then the glucose solutions were added respectively into the mediums and mixed well. For both mediums, 20mg acetosyringone was added when the medium was not extremely hot, in order to improve transformation efficiency. N6D-Co-As medium was poured into petri dishes for solidification. Selection medium was also prepared, which was basically the same as N6D medium, with extra addition of 25 mg/L hygromycin B and 600 mg/L cefotaxime. Additionally, all the flasks, pipette tips, filer papers were autoclaved at 121 °C for 20 min for sterilization.

Single *Agrobacterium* colony was picked and inoculated into 2 ml LB liquid medium with respective antibiotics. After overnight shaking, they were transferred into 50 ml LB liquid medium, and continue to be cultured for 3-5 h until $OD_{600}$ reached 0.8. The bacteria were then collected through centrifugation of 10 min at the speed of 4,000 rpm at room temperature. Supernatant was removed completely and the pellet was rinsed with 30 ml sterilized water twice, in order to further remove the LB medium residue. The pellet was resuspended in 50-100 ml N6D-AAM medium, which was ready to be used for trans-infection of the rice calluses. At the same time, rice calluses were scraped off the N6D medium and collected into a flask. The N6D-AAM medium containing *Agrobacterium* was then poured in until the calluses were completely submerged. The

flask was sealed and incubated at 28 °C for half an hour with gentle shaking. At the same time, a stack of round-shaped filter paper was soaked into the fresh N6D-AAM medium, and then, each N6D-Co-As plate was placed with a piece of soaked filter paper over the medium. The liquid AAM medium was then filtered out from the co-cultured calluses, and the calluses were placed over the prepared N6D-Co-As plate with filter paper.

The plates were then sealed and placed in the darkness for 3 days at 25 °C, before the *Agrobacteria* were washed off. The calluses were firstly scraped off the filter paper and collected into a flask. Sterilized water was added to rinse the calluses for 1 min. This process was repeated for 10 to 15 times until the water became clear. And the calluses was soaked into water containing cefatoxime at a concentration of 500 mg/L, and put on a shaker at 28 °C for half an hour. The calluses were then taken out from the flask and placed over a stack of filter paper for the absorption of the liquid. For the best washing effect and removal of *Agrobacteria*, the calluses were left inside the laminar flow over a new stack of dry filter paper, and blow dried for 3-5 h.

The calluses were then ready to be placed on the selection medium. The plates were sealed and placed inside a growth chamber with the same condition as calluses induction for 2-3 weeks. The selection effects were visible after 2 weeks, but might extend to 4 weeks, and thus, if necessary, the positive calluses were transferred into a

batch of new selection medium after week 3 for a constant supply of nutrition and selection antibiotics.

### 2.3.5 Generation of transgenic lines through tissue culture

Calluses with the successful delivery of plasmids were able to grow and reproduce on the selection medium. In order to induce differentiation, the positive calluses were carefully picked and transferred to the regenerative RE medium. 1 L of RE medium contained 3 g MS salt, 5 ml RE organic, 50 mg hygromycin B, 30 g sucrose, 30 g D-Sorbitol, 2 g casein hydrolate, 2 mg kinetin, 0.02 mg 1-Naphthaleneacetic acid, and 3 g phytagel. The pH was adjusted to 5.8 and the medium was autoclaved at 121 °C for 20 min before solidification in the petri dishes. The RE plates with positive calluses were put back to the growth chamber and green buddings were visible the earliest after 3 weeks. It was to be noticed that the differentiation might take up to 6-8 weeks, and thus, the calluses were to be subcultured to ensure a constant supply of medium.

For the differentiated cells that eventually gave rise to buddings and roots, they were picked out from the RE medium and planted into root induction medium in sterilized boxes for growth space and better induction of roots. The root induction medium contained 3 g MS salt, 5 ml RE organic, 30 g sucrose and 3 g phytagel with the pH at 5.8. The seedlings were grown inside the same root induction boxes placed inside the

growth chamber, until they reached 15 cm tall. And they were then transferred to the outdoor soil pots.

## 2.4 Genotyping

### 2.4.1 Genomic DNA extraction

DNA extraction buffer was prepared prior to the extraction, with a formula as: 0.2 M Tris-HCl at pH 9.5; 25 mM EDTA; 0.4 M LiCl; 1% SDS (w/v). An appropriate amount of the rice plant sample (usually leaves) was collected and grounded in a 1.5 ml Eppendorf tube in liquid nitrogen. 300 µl of the DNA extraction buffer was added into the finely grounded sample and mixed well by a vortex mixer. The solution was supposed to become green. And then the whole tube was centrifuged at the maximum speed for 10 min. A new tube was prepared with 300 µl isopropanol inside, and the supernatant was transferred in. After mixing the supernatant with the isopropanol, the new solution was further centrifuged at the top speed for 10 min. The supernatant was then discarded carefully using a pipette and the remaining pellet was rinsed with 700 µl 70% ethanol. And the pellet was collected again through centrifugation, and dried up in the vacuum. 50-100 µl of sterile water was added to dissolve the dried DNA and the concentration was measured using a nanodrop.

### 2.4.2 Genotyping PCR

PCR was used to test the transgenic lines in order to check the presence of the constructs. The extracted genomic DNA was used as the template. In order to check the presence of various constructs, different primers were designed for the genotyping PCR. For example, the construct-specific region was designed to be amplified for transgenic lines such as GUS lines or tagging lines, followed by gel electrophoresis for the confirmation of the desired band; and for CRISPR-Cas9 lines, targeted mutation region of the gene was amplified and sent for sequencing analysis in order to screen for mutations.

## 2.5 Expression analysis

### 2.5.1 RNA extraction and cDNA synthesis

FavorPrep$^{TM}$ Plant Total RNA Mini Kit (FAVORGEN) was used for the extraction of RNA from rice samples, with steps following the manufacturer's instruction. An appropriate amount of rice tissue sample was collected into a sterile 1.5 ml Eppendorf tube and fast frozen in liquid nitrogen. RNase-free DNase (Roche) was used as a treatment for the elimination of genomic DNA. The extracted RNA went through reverse-transcription using M-MLV transcriptase system (Promega), and the reaction setting followed the manufacturer's instruction.

### 2.5.2 Quantitative real-time PCR

In order to quantify the RNA expression of a targeted gene, quantitative real-time PCR was performed using the reserve transcription product as a template. Maxima® SYBR Green/ROX qPCR Master Mix (Fermentas) was used as an enzyme mixture, with the formula to be the same as instructed. The RT-PCR primers were designed to be gene specific and three duplicates were performed using the 7900HT Fast Real-Time PCR system (Applied Biosystems). Rice *UBIQUITIN (UBQ)* was used as a housekeeping gene for the purpose of normalization and an appropriate control sample was applied as a reference control. And the results were analysed using the Bio-Rad CFX Manager software. In order to obtain the relative expression level. The specificity of the primers was also checked by the dissociation curve.

## 2.6 Yeast two-hybrid assay

### 2.6.1 Preparation of yeast competent cells

Yeastmaker™ Yeast Transformation System 2 (Clontech, USA) was used to conduct the Y2H assay. The procedures followed the manufacturer's instructions, using the AH109 yeast strain. A single colony was picked into 50 ml of the YPDA liquid medium,

containing 10 g/L yeast extract; 0.0003% adenine hemisulfate; 20 g/L difco peptone; 2% glucose, and incubated at 30 °C overnight until $OD_{600}$ reached 0.15-0.3. The yeast cells were then collected in pellet through centrifugation at 3,000 rpm for 1 min, and then, resuspended using an adequate amount of fresh YPDA liquid medium ($OD_{600}$ to be measured at 0.4-0.8). The culture was again centrifuged at 3,000 rpm for 1 min, followed by the pellet being washed twice using sterile water. 1.1×TE/LiAc solution was prepared as: 1.1 ml 0.1 M Tris pH 7.5; 1.1 ml 1M LiAc pH 7.5; 10 mM EDTA, topped up to 10 ml with sterile water. An adequate amount of 1.1×TE/LiAc solution was added to wash the yeast cells, and then, the yeast competent cells were resuspended in ice-cooled 1.1×TE/LiAc solution.

### 2.6.2 Yeast transformation

All vectors, such as pGADT7 and pGBKT7, used in this lab were from Clontech, and the transformation procedure was performed according to the Yeastmaker™ Yeast Transformation System 2 User Manual. Appropriate amount of vectors containing the desired DNA were mixed with 50 µl of the competent cells together with 5 µM denatured Herring Testes Carrier DNA and 0.5 ml PEG/LiAC (1 M LiAc; 50% PEG 3350; 10% 10×TE buffer). The mixture went through vortex and then incubated for 30 min at 30 °C with gentle shaking. Afterwards, 20 µl of DMSO was added and mixed well. The tubes were further placed in 42 °C for 15 min with gentle shaking. The transformed yeast cells were collected in pellet through centrifugation at the maximum

speed, followed by one time rinse with NaCl solution (0.9% (w/v)). The resuspended yeast cells were dropped on three agar plates containing the following: SD/-Trp/-Leu, SD/-His/-Trp/-Leu, SD/-Ade/-His/-Trp/-Leu. Results were checked after the plates were placed at 30 °C for 3 days.

### 2.6.3 Yeast two-hybrid screening

In order to find out the interacting proteins of OsFTIP9, desired sequences were inserted into the pGBKT7 vector and then delivered into the yeast competent cells as described, and grown on an SD/-Trp plate. Single colony was picked and inoculated into 2 ml liquid SD/-Trp medium to grow overnight, and then transferred into larger volume of liquid SD/-Trp medium (50 to 100 ml) and continue to be cultured until $OD_{600}$ reached 0.8. In order to mate the yeast cell containing OsFTIP9 coding sequences with the cDNA library, 10 μg cDNA library (pre-made by Prof Yu Hao's laboratory colleagues) was mixed with 20 μl denatured Herring Testes Carrier DNA, 600 μl yeast competent cells and 2.5 ml PEG/LiAc. After complete mixing by gentle shaking, the mixture was cultured at 30 °C for about 30 min, followed by adding adequate amount of DMSO. The final mixture was further placed at 42 °C heat bath for 20 min with gentle shaking. Then, the culture went through centrifugation of 10 min at the speed of 3,000 rpm. The pellet was resuspended in 5 ml YPD plus liquid medium (Clonetch, USA), and cultured for 2 h at 30 °C. It was again collected through the same procedure of centrifugation and rinsed once with sterile 0.9% (w/v) NaCl solution. In order to quantify the

transformation efficiency, 20 µl of the final cell suspension was taken out and diluted into 10X, 100X and 1,000X portions. They were further spread on SD/-Trp/-Leu plates to be cultured at 30 °C for up to 5 days. And the rest of the mating mixture was grown on SD/-His/-Trp/-Leu plates containing 5 mM 3-amino-1,2,4-triazole (3-AT) to eliminate the false positive colonies. The plated were cultured at 30 °C for up to 5 days before being picked up for sequencing analysis.

To identify the exact DNA fragment that produced the interaction protein with OsFTIP9, survival colonies were picked and dissolved into 10 µl sterile water. 1 µl was used as a template for PCR amplification in preparation for sequencing analysis. The primer set was chosen to sit on the vector due to the uncertainty of fragment insertion, and the exact sequences were: pGAD-forward: 5'-CTATTCGATGATGAAGATACCCCACCAAACCC-3'; pGAF-reverse: 5'-AGTGAACTTGCGGGGTTTTTCAGTATCTACGAT-3'. Clones were verification through PCR. And successful amplification of the insertion DNA fragment was validated through gel electrophoresis, and only those with a single, clear band were purified and sent for sequencing analysis, using the method described in section 2.2.5. DNA sequencing & analysis.

### 2.6.4 Yeast two-hybrid assay

Y2H assay was performed in order to validate the interacting partners, which could also detect the exact interacting coding area. Various lengths of the coding sequence of OsFTIP9 were introduced into the pGBKT7 vector separately. And the gene fragment of the potential interacting protein candidates were inserted into the pGADT7 vector. Various combinations of the AD and BD constructs were delivered into the yeast competent cells using the same protocol as 2.6.2. Yeast transformation. And results were checked after 3-day culturing. Positive interacting results should be a composite of: all colonies grow on DDO plates; only interacting combinations grow on TDO plates with negative controls being empty; and interaction combinations may or may not grow on QDT plates.

## 2.7 *In vitro* pull-down assay

### 2.7.1 Protein expression in *E. coli*

In order to validate the protein-protein interaction between OsFTIP9 and its interacting partners, *in vitro* pull-down assay was performed. The coding sequences of both genes were cloned to pGEX-4T-1 vector (Pharmacia) and pMAL-c2X vector, and the constructs were delivered into *E. coli* Rosetta (DE3) (Novagen) cells for protein expression. Single colony was picked and inoculated into 50 ml LB medium with desired selection antibiotics, and cultured at 37 °C until $OD_{600}$ reached 0.6. Protein

expression was induced by IPTG of a range of 0.2-2 mM concentration, and continued to be cultured at 16 °C with low-speed shaking. In order to obtain the expressed protein lysis, lysis buffer was prepared as: 1% TritonX-100; 50 mM NaCl; 10 mM Tris-HCl at pH 8.0; 1 mM EDTA; 10 mM PMSF. The induced cells were collected through centrifugation at 3,000 rpm for 5 min, and resuspended with adequate amount of lysis buffer. The cells went through sonication followed by centrifugation at the maximum speed for 10 min at 4 °C. The released protein was soluble in the supernatant, which was carefully transferred to a new tube for future usage.

### 2.7.2 *In vitro* pull-down assay

Prior to the *in vitro* pull-down assay, desired protein was immobilized to the glutathione sepharose beads (Amersham Biosciences). It was done by adding the beads to the protein lysis collected from the previous step, and incubated at 4 °C for 2 h with gentle shaking. The beads ligated with the desired protein were collected through centrifugation at 3,000 rpm for 1 min at 4 °C, followed by three to five time wash with the lysis buffer. It was then added into the lysis of the interacting candidate protein, and went through incubation at 4 °C for 2 h with gentle shaking. IP buffer was prepared and used as a reaction solution as: 0.05% SDS; 10 μM $ZnSO_4$; 1% Triton X-100; 150 mM KCl; 50 mM Hepes at PH 7.5; 5 mM $MgCl_2$. The final beads with immobilized proteins were washed 10 times using the IP buffer repetitively. And the final product was used

as an input for the Western blot analysis in order to detect the presence of the desired bands.

### 2.8 Total protein extraction

CelLyticTM P Cell Lysis Reagent (Sigma Cat. No. C2360) was used to extract the total protein from rice tissues. The rice tissue was cut off and quick frozen in liquid nitrogen, and homogenised. The tissue powder was then mixed with the lysis solution (50 µl lysis solution for every 0.02 g sample powder), with a supply of 50X protease inhibitors (Roche) that prevents protein degradation. The mixture was placed on ice for 20 min in order for a complete release of protein, and then centrifuged at the top speed for 20 min at 4°C. The supernatant containing the total protein extraction was transferred into a new sterile tube, and was stored at -80 °C for future usage.

### 2.9 Western blot

Several things were prepared for the western blot analysis: 8 to 12% polyacrylamide gels were casted following the manufacturer's manual from Bio-Rad; 6X SDS-PAGE loading buffer was also purchased from Bio-Rad; SDS-PAGE running buffer contained 20 mM Tris-base, 150 mM glycine and 0.1% SDS; blotting buffer was prepared containing 20 mM Tris-base, 150 mM glycine, 20% methanol as well as 0.1% SDS;

PBS buffer contained 1.3 M NaCl and 70 mM $Na_2HPO_4$, pH 7.4. To start, 20 to 40 µl protein sample was mixed with the appropriate amount of loading buffer, and boiled at 98 °C for 5 min, followed by immediate cooling on ice. After the samples were denatured, they were loaded into the polyacrylamide gel in a pre-designed sequence and run in the SDS-PAGE buffer at 30 mA until the protein bands were fully separated. The gel was then electro-transferred to the immune-Blot™ PVDF membrane (Bio-Rad) in the blotting buffer at 100 V, 1hr. The membrane was then blocked using PBS buffer containing 5% (w/v) dry milk for 1.5 hr with gentle shaking at room temperature. And then, the membrane was changed to PBS buffer with dry milk containing 1:5000 (w/v) diluted antibody, and continue to be incubated for 1 h. Depending on the necessary, the second antibody might be applied with one time wash with PBST buffer (PBS buffer supplied with 0.05% Tween-10) in between. And the membrane was finally rinsed in PBST buffer for three times, 15 min each, and the signal was detected by incubating the membrane with the ECL Western Blotting Substrate (Pierce) or SuperSignal West Femto Chemiluminescent Substrate (Pierce), depending on the signal strength.

### 2.10 Non-radioactive *in situ* hybridization

#### 2.10.1 Sample fixation & embedding

1X PBS solution was prepared containing 0.13 M NaCl, 7 mM $Na_2HPO_4$ and 3 mM $NaH_2PO_4$, at pH 7.0. In order to dissolve the paraformaldehyde, the PBS solution was preheated to 60 °C and adjusted to pH 10-11. Paraformaldehyde was added to a final concentration of 4% (w/v), and then the clear solution was cooled down on ice, and adjusted back to pH 7 with $H_2SO_4$.

Plant tissues were collected and soaked in the pre-chilled paraformaldehyde solution, followed by 20 min vacuum treatment for the purpose of full penetration. The vacuum treatment was repeated several times until the tissues sunk to the bottom, which indicated that the fixation buffer completely penetrated into the tissue cells. Then the samples were changed to new fixation buffer and placed at 4 °C overnight with gentle agitation. The samples were then changed to 1X PBS buffer for 30 min agitation at 4 °C, and then, the samples went through 1 h ethanol dehydration at 4 °C in a series of concentrations: 30%, 40%, 50%, 60%, 70% and 85%. Then, 95% ethanol containing adequate amount of eosin was supplied for overnight treatment, in order to stain the samples. The samples were transferred to room temperature in 100% ethanol containing same amount of eosin for 1 h with gentle agitation, and repeated for four times. The buffer was then changed to histoclear using similar concentration series as ethanol. The samples were changed to a mixture of 75% ethanol and 25% histoclear for 1h, and then changed to a mixture of 50% ethanol and 50% histoclear for the same time length, and finally to 25% ethanol with 75% histoclear. The samples were changed to 100% ethanol and washed for 1 h for three times. Next, paraplast chips were directly added into the

histoclear solution to around 1/4 volume, and the whole mixture was placed at room temperature overnight, which was then transferred to 42 °C incubator for complete melting of the paraplast chips. The paraplast concentration was topped up to 1/2 volume at 42 °C until complete melting. Then the samples were moved to 55 °C for several hours before being changed to 100% melted paraplast solutions. For the following 7 - 14 days, fresh paraplast melt was changed twice a day, and finally the temperature was brought back to room temperature. And the solidification containing the samples was then fixed in the moulding cassette and stored at 4 °C for future use.

### 2.10.2 Sectioning

The samples were to be sectioned to a thickness of 8 μm using a microtome. ProbeOn Plus slides (Fisher Biotechnology, USA) were used to hold the sections for hybridization, and they were made to be capable of being sandwiched together for easiness of hybridization performance.

The slides were preheated to 42 °C and kept warm on the flat incubator, with several drops of DEPC-treated water. The sample cassette was placed on the microtome and sectioned in continuous mode so that the sections formed a ribbon. And then the ribbons were transferred to the DEPC-treated water so that they floated over the charged sides of the slides. Excessive water was removed so that the ribbons will be attached on the slides without air bubbles in between. And the slides were further incubated at 42 °C

overnight so that the water evaporated completely and the ribbons of samples adhered to the slides tightly. The slides were ready to be used or stored at 4 °C with desiccant.

### 2.10.3 Synthesis of RNA probes

In order to synthesize the RNA probes, including both sense and anti-sense, a length of 250 bp gene-specific region was chosen from the cDNA sequence. The fragment was amplified through PCR with appropriate primer sets and cloned to pGEM-T easy vector following the protocols introduced in the context above. The pGEM-T easy vector contains both T7 and SP6 promoters on each side of the multiple cloning site, which enabled us to synthesize both the sense and anti-sense probe from the opposite directions using appropriate restriction enzymes. The plasmid was thus, double digested, which left no 3' overhang. The digestion product was purified using the Gel/PCR DNA fragment purification kit, which was used as the DNA template for the following *in vitro* transcription. The *in vitro* transcription reaction was set up as following: 1 μg of the DNA template, 10X DIG labelling mix (Roche, Germany), 5X transcription buffer, RNase inhibitor (Promega, USA), T7 or SP6 RNA polymerase (Promega, USA), and topped up with the appropriate amount of DEPC-treated water. The reaction mixture was incubated at 37 °C for 2 h and topped up with 40 U of RNase-free DNase (Roche, Germany), followed by 30 min incubation. 1 μl of the reaction product was taken out and run through gel electrophoresis in order to check whether the transcription generated the desired probes.

The DIG-labeled RNA probes were chopped into shorter lengths between 75 and 150 bp through carbonate hydrolysis. And then the reaction mixture was topped up to 100 µl with DEPC-treated water together with 100 µl of 2X $CO_3^-$ buffer containing 80 mM $NaHCO_3$ and 120 mM $Na_2CO_3$. The duration of the 60 °C incubation was calculated based on the formula: Time (min) = (Li-Lf)/0.11*Li*Lf, (Li refers to initial length of probe in kb and Lf refers to the final length of the probe). 10 µl 10% acetic acid (v/v) was added to terminate the carbonate hydrolysis, and further added with 2 µl of tRNA (10 mg/ml), 1/10 volume of 3 M NaAc at pH 5.2, and 2.5 volumes of ethanol. After complete mixing, the product was placed at -20 °C overnight. The precipitated RNA was collected through centrifugation for 30 min at 4 °C at the maximum speed, rinsed with 70% ethanol, and finally dissolved in 50% formamide (v/v), which was ready for use or stored at -80 °C.

### 2.10.4 Pre-hybridization treatments

All the equipment and consumables used in the *in situ* hybridization was autoclaved twice at 121 °C for 1 hr in order to remove RNase. And those could not be autoclaved were placed in 0.1M NaOH overnight before being rinsed with DEPC-treated water.

The slides went through deparaffination with 10 min wash in histoclear, and slides were rinsed with gentle agitation for complete rinse and the process was repeated once. The

sample slides were also rehydrated in the ethanol concentration series with a length of 1 min each: two times rinse each in 100%, 95%, 90%, 80%, 60%, 30% concentration, and lastly placed in sterile water for 2 min. The slides were then immersed into 2X SSC buffer containing 0.3 M NaCl and 30 mM sodium citrate for gentle agitation of 20 min. A mixture of 100 mM Tris pH 8.0 and 50 mM EDTA was pre-warmed to 37 °C and proteinase K (1μg/ml) was added freshly just before the slides were transferred in. They were placed in 37 °C for 30 min with gentle agitation. The samples were then taken out to room temperature and transferred to PBS buffer containing glycine (2 mg/ml). After 2 min short immersion, fresh PBS buffer was changed twice for 2 min each. The slides were then immersed into PBS buffer containing 4% (w/v) paraformaldehyde for 10 min, and again, rinsed with fresh PBD for twice, 5 min each time. At the same time, 2.68 ml of triethanolamine into 200 ml DEPC-treated water, followed by addition of 0.8 ml HCl, 1ml acetic anhydride in sequence, and lastly the mixture was mixed vigorously. The slides were then immersed into this solution for 30 min at room temperature, and then completely rinsed with PBS buffer twice shortly. Lastly, the slides were dehydrated again in the ethanol concentration series of 30%, 60%, 80%, 90%, 95%, 100% and another 100%, similar as being described in the previous context. The slides were then ready to be used for *in situ* hybridization after the ethanol evaporated completely.

### 2.10.5 *In situ* hybridization

Several solutions were prepared during the process of *in situ* hybridization: 10X *in situ* salt containing 100 mM sodium phosphate at pH 6.8, 3 M NaCl, 50 mM EDTA, 100 mM Tris at pH 8; 50% dextran sulfate (Sigma, USA); deionized formamide (Sigma, USA), 50X denhardts solution, 10 mg/ml tRNA. 1 µl of the synthesised RNA probe was mixed with deionized formamide and topped up with DEPC-treated water to make a final deionized formamide concentration of 50% and total volume of 60 µl, which was sufficient for the hybridization of 2 pairs of slides. The probe solution was heated at 85 °C for 5 min and immediately cooled down on ice. At the same time, hybe solution was prepared by mixing 100 µl of 10X *in situ* salt, 200 µl 50% dextran sulfate, 400 µl deionized formamide, and 20 µl 50X denhardts solution, which made a final volume sufficient for the hybridization of 3 pairs of slides. 240 µl of the hybe solution was mixed with every 60 µl of the probe solution, and the complete mixture was ready to be applied on the slides. In order to save probes and ensure complete contact between the samples and the reaction mixture, slides treated with the same probes were to be sandwiched in pairs with the samples facing inwards. 200 µl of the mixture was applied into the middle of the slide sandwich without any air bubbles in between. The sandwiches were then elevated above wet towels inside an RNase-free container, and incubated at 55°C overnight.

### 2.10.6 Post-hybridization treatments

The slides were separated carefully in 0.2X SSC solution at 55 °C, and then further rinsed in fresh 0.2X SSC for 3 times and 1 hr each at 55 °C with gentle agitation. The slides were transferred into 1X PBD solution and rinsed at room temperature for 5 min. At the same time, blocking buffer was prepared by dissolving 1% Boehringer block into 100 mM Tris pH 7.5 and 150 mM NaCl. The slides were blocked at room temperature for 45 min, at the same time of which, 1.0% Bovine Serum Albumin (BSA) was dissolved in 150 mM NaCl, 100 mM Tris at pH 7.5 and 0.3% Triton X-100. The slides were then treated with this solution for another 45 min, before being incubated with anti-dig antibody (Roche, Germany). The antibody was diluted with a ratio of 1:500 in the same solution. In order to save the antibody, the slides were again sandwiched together with one side put into the antibody solution to allow capillary action to pull up the solution over the samples. The sandwiches were then dried up with a clean tissue placed at the other side, and the same capillary process was repeated once more without air bubbles in between. The sandwiches were again placed above wet tower paper inside a clean container, and left at room temperature for 2 h. After the incubation, the slides were separated again and placed into the BSA/Tris/NaCl/Triton solution for 15 min with gentle agitation. Then the BSA/Tris/NaCl/Triton solution was changed three more times with 15 min wash each time. The slides were further transferred into a new solution containing 50 mM $MgCl_2$, 100 mM Tris at pH 9.5 and 100 mM NaCl for 10 min wash for two times. After the detergent was washed off, the slides were ready to be detected for signals. Tris/NaCl/PVA solution was prepared as follows: 10% (w/v) polyvinyl alcohol (PVA, Sigma) was dissolved into the

Tris/NaCl/$MgCl_2$ solution, and further, Tris/NaCl/PVA solution was mixed well with 2% NBT/BCIP stock solution (Roche, Germany), and placed in the darkness for several minutes in order for the air bubbles to settle. 300 µl of the mixture was dropped over the slides and the same sandwiching method was applied. Similarly, the slides placed above wet tower paper inside a clean container, and put in the darkness overnight until the signal was visible. The termination of the reaction on the next day was rather easy, in that the slides were separated and rinsed directly with tap water. After the reaction buffer was rinsed off completely, the slides went through ethanol dehydration process directly starting from 70% concentration, followed by twice of 100%. The dehydrating process was performed fast, as the signal was soluble in ethanol and might get rinsed off. The air-dried slides were then ready to be examined under microscope. In order to preserve the signal for a longer time, they were mounted with 50% glycerol, which could keep the signal for several months to years.

### 2.11 Transient expression of proteins in rice protoplast cells

#### 2.11.1 Preparation of protoplast cells

Rice protoplast cells were prepared for the transient expression of various constructs for different experimental purposes. The hulls of the rice seeds were peeled off, and the seeds were sterilized in 30% bleach solution. They were rinsed several times with

sterilized water, following the same procedure as described in the calli induction process. The sterilized seeds were sowed over the root induction medium and grown in the growth chamber with the condition of 12 h light at 32 °C and 12 h darkness at 28 °C. After 7 to 10 days, strong seedlings were taken out from the medium and washed clean for protoplast isolation.

Around 80 seedlings were chosen and only the sheath part was sectioned into small pieces with the width of 0.5 mm with a sharp blade. The cut strips were then immersed in 0.6 M mannitol solution immediately. After all the seedlings were sectioned, vacuum was applied for 10 min in order for the mannitol to penetrate into the tissues, followed by dark treatment at room temperature for 10 min. At the same time, enzyme digestion solution was prepared as follows: a mixture of 0.6 M mannitol and 10 mM MES was heated up to 55 °C and added with 1.5 % Cellulase RS ( Yakult, Japan) and 0.75 % Macerozyme R-10 (Yakult, Japan). The mixture was incubated at 55 °C for 10 min and cooled down to room temperature, and finally added with 10 mM $CaCl_2$ and 0.1% BSA. The darkness-treated strips were then transferred into the enzyme digestion solution and placed in darkness for 4 -5 hr treatment with gentle agitation at the speed of 60 rpm. The temperature was to be controlled at around 28 °C, not exceeding 30 °C.

During the digestion time, other subsequent solutions were to be prepared: 1). W5 solution contained 154 mM NaCl, 125 mM $CaCl_2$, 5mM and 2 mM MES, with the PH to be adjusted to 5.7. 2). PEG solution contained 0.2 M mannitol, 40% (W/V) PEG

4000, and 0.1 M $CaCl_2$. 3). MMG solution contained 0.4 M mannitol, 4 mM MES and 15 mM $MgCl_2$ with the pH adjusted to 5.7. 4). WI solution contained 0.5 M mannitol, 4 mM MES and 20 mM KCl with the pH adjusted to 5.7.

After the digestion was done, the solution was supposed to be greenish, and equal volume of the W5 solution was added in order to stop the digestion. The mixture was shaken vigorously for 10 s. The solution was filtered through 40 μm nylon meshes in order to remove the strips. The meshes and strips were rinsed with W5 solution several times for complete collection of protoplast cells, and the flow-through was collected into round-bottom tubes. Protoplast cells were then collected through centrifugation at 1,500 rpm for 3 min. The supernatant was removed and the cells were resuspended in adequate amount of MMG solution. The concentrations of the resuspended protoplast cells were calculated with a haematocytometer, and it should be no less than $2 \times 10^6$ cells/ml. The cells were kept on ice for further experimental use.

### 2.11.2 Delivery of constructs

The constructs were delivered into the protoplast cells as soon as possible, as the cells were very fragile. 10 μg of one or several kinds of plasmids, depending on the experimental purposes, were added into a 2 ml Eppendorf tube, with the total volume not exceeding 20 μl. 100 μl of the protoplast cells were then added and mixed gently with the plasmids, and further, 110 μl PEG solution was added and mixed well by gentle

tapping. The mixture was then placed in the darkness at 25 °C for 15 min. After that, 440 μl W5 solution was added and mixed well in order to stop the reaction. The cells were then collected by centrifuging at 1,500 rpm for 3 min, and the supernatant was removed as much as possible. The cells were then resuspended in 1 ml WI solution and transferred into 6-well plate. The plate was then cultured for 12 h, or longer as needed, in darkness or under light depending on experimental purposes. And then the cells were transferred into 2 ml Eppendorf tube and concentrated through centrifugation at 1,500 rpm for 3 min.

**Table 1. List of primers used in this research**

| Primer name | Sequence |
|---|---|
| 1300P1 | CCAGGCTTTACACTTTATGC |
| 1300P2 | GCGATTAAGTTGGGTAACGC |
| AD Seq-Rev | AGATGGTGCACGATGCACAG |
| AD-D14_F | AAACATTAGATGCTGCGATCGACGCATCCGCC |
| AD-D14_R | AAAGAATTCAAATCAAGATTGCCCACATCGTCGGGC |
| d14-2-genotyping_F | ATGCTGCGATCGACGCATCCGCC |
| d14-2-genotyping_R | CGAGAGCGCGGCGGAGCACCTG |
| D14L-BiFC_F | CTCAAGCTTCGAATTCTGCAATGGGGATCGTGGAGGAGGCG |
| D14L-BiFC_R | GATCCCGGGCCCGCGGTACCGACCGCAATGTCATGCTGGATGTGT |
| FC1_NmCherry_F_ | ATCGAATTCCTGCAGATGCTTCCTTTCTTCGATTCCCCAA |
| FC1_NmCherry_R_ | ACCACTAGTGGATCCGCAGTAGTGCCGCGAATTGGC |
| fc1-2-gnotyping_F | GTGCCCTTCGGCGTCGACGGAGC |
| fc1-2-gnotyping_R | GATGGCGGCCTTGGACATGTTGAGG |
| FC1-BiFC_F | CTCAAGCTTCGAATTCTGCAATGCTTCCTTTCTTCGATTCCCCAA |
| FC1-BiFC_R | GATCCCGGGCCCGCGGTACCGCAGTAGTGCCGCGAATTGGC |
| FC1-Ri#1_F1 | AAAGAGCTCATGCTTCCTTTCTTCGATTCCCCAAGC |
| FC1-Ri#1_R1 | AAAACTAGTGGCGACGGCGAGGCGATCGT |
| FC1-Ri#2_F1 | AAAGAGCTCGGCCATGCACCCCTTCATGGACTTG |
| FC1-Ri#2_R1 | AAAACTAGTGCATCCGCCGGTCCCTCATCC |
| FTIP9 seq_1254 | TAACGCCTTTCTCATTCAGT |
| FTIP9 seq_1798 | TCGCATAGAAACCACGAGAT |
| FTIP9 seq_2472 | CTCCGAGAAGGATACAACAC |
| FTIP9 seq_2908 | GAGCCTCACATCATAAGCGA |
| FTIP9 seq_3640 | CCTGTCATCATCGTGGAAGA |
| FTIP9 seq_4460 | GCTCCAAGGTGTACCAGTCG |
| FTIP9 seq_449 | CTTTTGGCTATATCACTGGG |
| FTIP9 seq_5098 | AAGTACGGCAAGAAGTGGGT |

| | |
|---|---|
| FTIP9 seq_5896 | GACGACCTGGAGGAGGAGTT |
| FTIP9 seq_6398 | TTTGCCACTTTTGAAATGAT |
| FTIP9 seq_6890 | TGATAGAACCGCTTTGATGT |
| FTIP9 seq_7384 | CTTCTCAAGGACCGTAAAAT |
| FTIP9 seq_7962 | AACTCCCAAGTGTGATTTTC |
| FTIP9 seq_8586 | GTATCACATTGGTGGTAGGA |
| FTIP9_Cas9_ID_F | ACCATAGTATGATAGTAGCAGCTGC |
| FTIP9_Cas9_ID_R | GAAGTACACGATCCCCTCCTCC |
| FTIP9_GFP_CDS_F | ATCGAATTCCTGCAGATGGCGGCCGGTGCGCCC |
| FTIP9_GFP_CDS_R | ACCACTAGTGGATCCTCAGAGCATCCTGTCGGAGAGGCTG |
| FTIP9_OE__R | GACCGGAGCGTGTGCGGGCCGGCCT |
| FTIP9_OE_F | GAATTCCTGCAGCCCATGGCGGCCGGTGCGCCCC |
| FTIP9_RNAi_F | AAAGGTACCGAGCTCAATTCAGATCACACCGGCATCAC |
| FTIP9_RNAi_R | AAAAGATCTACTAGTGGAGAGAGTGGCGAATGGAATAGG |
| FTIP9_sgRNA_F(P3) | TTCGCCGTCGTGGACTTCGAGTTTTAGAGCTAGAAATAGCAAGTT |
| FTIP9_sgRNA_R(P4) | TCGAAGTCCACGACGGCGAAGCCACGGATCATCTGCACAACTCTT |
| FTIP9_Y2H_F_head | NAACCATATGCAAAGGATGGCGGCCGGTGCGC |
| FTIP9_Y2H_R_1 | CGGAATTCCGGGACCTCAGGCGGCGGCG |
| FTIP9_Y2H_R_12 | CGGAATTCCGGCGCGTCGGTGTTCCACGC |
| FTIP9_Y2H_R_123 | CGGAATTCCGGCCTCCACAGCTGCTTCGC |
| FTIP9_Y2H_R_1234 | CGGAATTCCGGGTACCAGACGAGGACGAGGT |
| FTIP9-BiFC_F | CTCAAGCTTCGAATTCTGCAATGGCGGCCGGTGCGCCC |
| FTIP9-BiFC_R | GATCCCGGGCCCGCGGTACCTCAGAGCATCCTGTCGGAGAGGCTGGG |
| GST-D14L_F | AAAGAATTCATGGGGATCGTGGAGGAGGCGCACA |
| GST-D14L_R | AAAGCGGCCGCTCCTAGACCGCAATGTCATGCTGGATGTGTCG |
| GST-FC1_F | AAAGAATTCATGCTTCCTTTCTTCGATTCCCCAA |
| GST-FC1_R | AAACTCGAGTCAGCAGTAGTGCCGCGAATTGG |
| GST-FTIP9_F | AAAGAATTCATGGCGGCCGGTGCGCCCC |

| | |
|---|---|
| GST-FTIP9_R | AAAGCGGCCGCTCGAGCATCCTGTCGGAGAGGCTGGGCAGC |
| HPTend5 | GATGGCTGTGTAGAAGTACT |
| KH002 | CAGTAGGATTCTGGTGTGT |
| KH002 | CAGTAGGATTCTGGTGTGT |
| M13F | CCCAGTCACGACGTTGTAAAACG |
| M13R | CAGGAAACAGCTATGAC |
| MBP-D14L_F | AAAGAATTCATGGGGATCGTGGAGGAGGCGCACA |
| MBP-D14L_R | AAATCTAGACTAGACCGCAATGTCATGCTGGATGTGTCGXBAI |
| MBP-FC1_F | AAAGAATTCATGCTTCCTTTCTTCGATTCCCCAA |
| MBP-FC1_R | AAATCTAGATCAGCAGTAGTGCCGCGAATTGG |
| MBP-FTIP9_F | AAAGAATTCATGGCGGCCGGTGCGCCCC |
| MBP-FTIP9_R | AAATCTAGAGAGCATCCTGTCGGAGAGGCTGGGCAGC |
| mubi1-5_new | ATTATTTTTGTGAACACGAGCA |
| mubiout | ATCTTCGTCCCATAGGTGTC |
| pGEX-3' | GGG CTG GCA AGC CAC GTT TGG TG |
| pGEX-5' | CCG GGA GCT GCA TGT GTC AGA GG |
| PGP1 | CCACGGCCAGTGAATTGTAAT |
| PGP2 | CCACGGCCAGTGAATTGTAAT |
| pOsU3-HindIII-F(P1)-Cas9 | GCCAAGCTTGTACGTTGGAAACCACGTGATG |
| RAP-F | TAACCACCCTTTTGGTAGCTT |
| RAP-R | TGTCAATGCATCCAAGTAAAC |
| sgRNA-XmaI-R(P2)_Cas9 | TATCCCGGGGCCATTTGTCTGCAGAATTGGC |
| T7 primer | TAATACGACTCACTATAGGG |

**Table 2. List of primers used in real-time PCR**

| Primer name | Sequence (5' to 3') |
|---|---|
| qD10_F | TCATCGCTGCTTTCCGACGTTC |
| qD10_R | TCCAAACCAGGAGCTTCCTCAAC |
| qD14_F | ACGTGATGATCTGCGTGATGCC |
| qD14_F | ACGTGATGATCTGCGTGATGCC |
| qD14_R | GGCTTTGGTTTGGCCAGCTAAC |
| qD14_R | GGCTTTGGTTTGGCCAGCTAAC |
| qD14L_F | AGTGTCGCCCAGACAATCTTCC |
| qD14L_R | TGGCATGGTACGGTGACAAGTG |
| qD17_F | CGATCCCACTTCACTTTCTACGAG |
| qD17_R | GATGTAGTGGGTGTCGGTGAAG |
| qD27_F | GGCCGTGTGAGGTTATGGAATC |
| qD27_R | TCTGGCATGGAATCTTGCAAAGG |
| qD3_F | ACACCGGCTACAACAAGGATTG |
| qD3_R | TGGAACTGATTGGTTGTTCCTTGG |
| qFC1_F | ATTCGCGGCACTACTGCTGATG |
| qFC1_R | TTAGTGCCGTACCGTTCGTTCG |
| qOsGT1_F | TCGGAGACGATGACCTGGTGTATG |
| qOsGT1_R | ACAGGCTGAACCACTCAACCAC |
| qOsWRKY94_F | TGCCATTGCTCAAAGAGGAGGAAG |
| qOsWRKY94_R | TGGATGAGGCGAACCCTTAATCG |
| qOsFTIP9_F | CAGATCAGATTCTGCGCCATCG |
| qOsFTIP9_R | TTTCTTGGCCTGGAAGCTCACG |

# Chapter 3

# Results

# Chapter 3 Results

## 3.1 Phylogenetic analysis of FTIP family

A phylogenetic tree of the FTIP family genes in different plant species was constructed to analyze the relationships among various FTIP genes, in order to provide insights into their functional grouping (Figure 1). Neighbour-joining method was employed using the Jones-Thornton-Taylor with the discrete Gamma distribution model. FTIPs from *Arabidopsis* and rice species were selected to compare with the homologues from lower plants (Figure 1). The phylogenetic tree showed five clades among rice and *Arabidopsis* members (Figure 1). In clade I, the reported *Arabidopsis FTIP1* (AT5G06850) was homologous to rice *OsFTIP1* (Os06g41090); and the *Arabidopsis FTIP2* (AT5G48060), the closest paralogue of *FTIP1*, was homologous to rice *OsFTIP2* (Os04g39680) (Figure 1). The focus of this study was the clade V, *OsFTIP9*, was homologous to *Arabidopsis FTIP15* (AT1G74720); while the two closest paralogues of rice *OsFTIP10* and *OsFTIP11* are homologues of *Arabidopsis FTIP14* (AT3G03680) and *Arabidopsis FTIP16* (AT5G17980) (Figure 1). Consistent with the close positioning in the phylogenetic tree, *OsFTIP9*, *OsFTIP10*, *OsFTIP11* all contained 4 C2 domains as well as a PRT_C domain, the structure of which indicated a possible association with membrane trafficking and transportation functions.


**Figure 1. Phylogenetic analysis of MCTPs from various plant species.**
Species backgrounds are represented by prefix in 2 letters for short (Os, *Oryza sativa*; Sm, *Selaginella mollendorffii*; AT, *Arabidopsis thaliana*; Pa, *Picea abies*; Pp, *Physcomitrella patens*). Jones-Thornton-Taylor (JTT) model with maximum-likelihood bootstraps inferred using LG+G model and discrete Gamma distribution (+G) model is used for the neighbor-joining method. For every node, a filled dot is used when all values are above 80% bootstrap support, otherwise, a circle is drawn if the values fall between 50% to 80% range. For values below 50%, dashes are used.

### 3.2 Generation of *Osftip9* mutant through CRISPR-Cas9

In order to obtain the knockout mutant of *Osftip9*, CRISPR-Cas9 system was employed to introduce mutations. Two specific target sites were chosen to ensure genome editing (Figure 2A). Targeting sites were chosen with a position preference of being near to the start codon, with the hope to obtain null alleles. Genotyping of the transgenic lines identified a mutant with a successful addition of 1bp at the position of 294bp counting from the start codon, named as *Osftip9-1* (Figure 2B). This mutation resulted in a frameshift, which eventually caused the early termination of translation (Figure 3). The genotyping screening also identified a heterozygous mutation (+A/+T) happened at the same position of the gene, named as *Osftip9-2*, the single addition of which resulted in similar mutated protein except for one amino acid difference (Figure 2B).

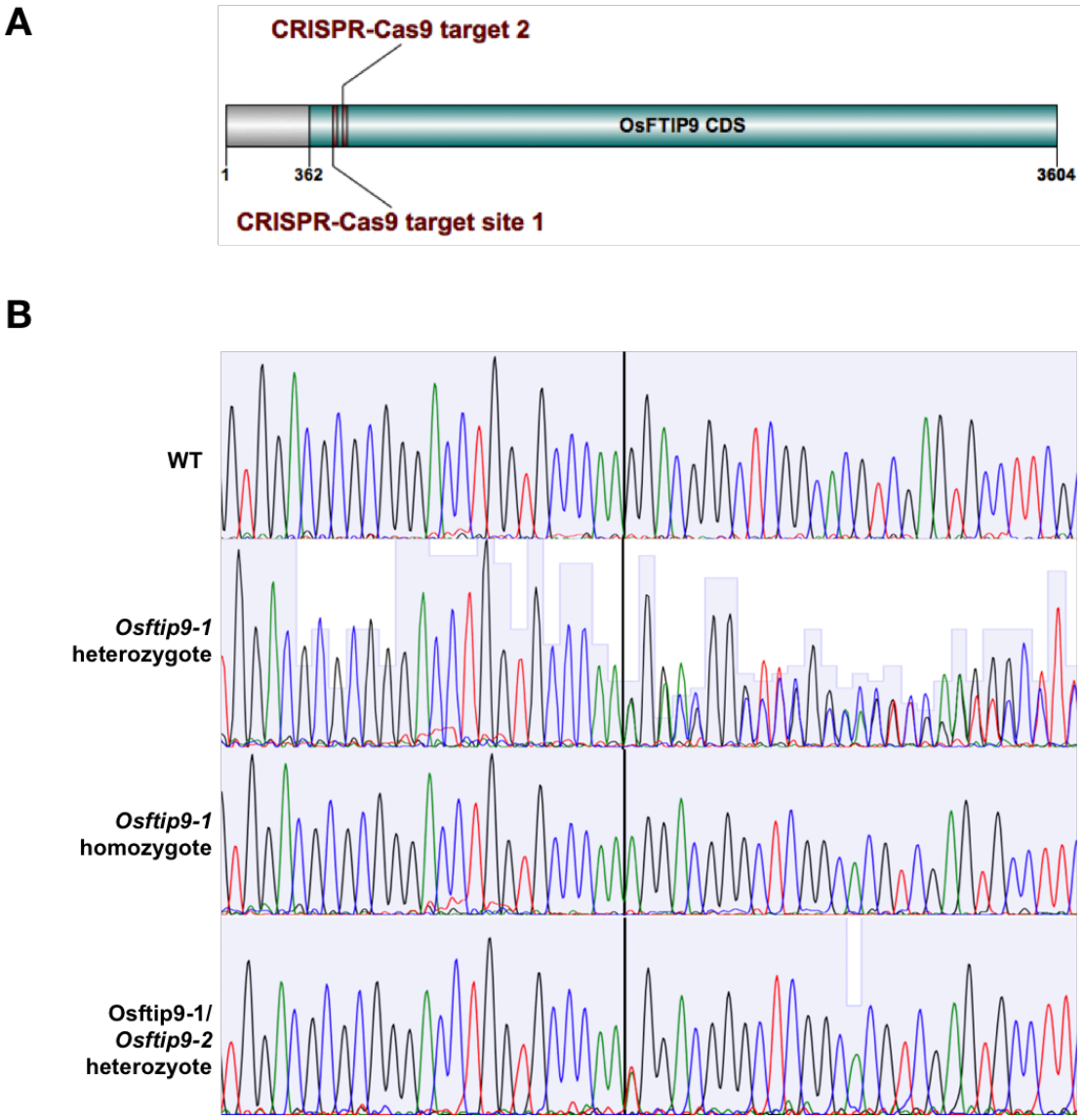


**Figure 2. Genotyping of *Osftip9* mutants generated using CRISPR-Cas9.**
(A). Schematic diagram of selections of target sites of CRISPR-Cas9 on *OsFTIP9*. Number indicates relative position. Grey, untranslated regions; green, exon; red, gene-specific sites selected for CRISPR-Cas9.
(B). Sequencing alignments of *Osftip9-1* heterozygous mutant, *Osftip9-1* homozygous mutant, *Osftip9-1/Osftip9-2* heterozygous mutant and WT. The sequences are aligned, the black line across all 4 panels indicates the mutation sites. Colour code for peaks: Red – Thymine; Black – Guanine; Green – Adenine; Blue – Cytosine.

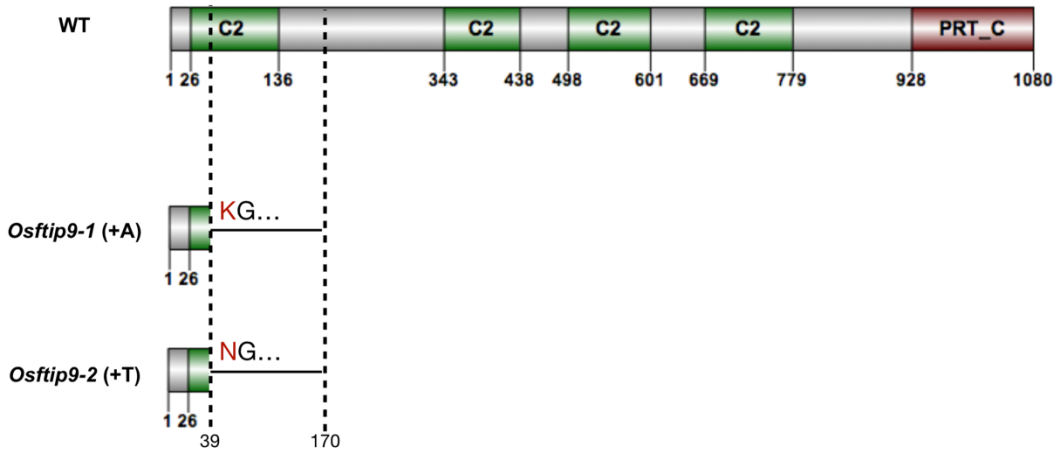


**Figure 3. Schematic representation of changes in OsFTIP9 coding proteins in created mutants.**

The predicted protein structures in *Osftip9-1* and *Osftip9-2*, with alignment to the WT OsFTIP9 protein. Green blocks, C2 (or part of C2) domains; red block, PRT_C domain. Dotted line aligns the start of misalignment of the mutated protein fragment to OsFTIP9. Solid lines, protein fragments different from OsFTIP9. Numbers mark relative position from N-terminal to C-terminal.

### 3.3 *Osftip9-1* knockout mutants show increased tiller number

The number of tillers of *Osftip9-1* knockout mutant was obviously higher than that of WT, which directly affected the architecture of the rice plant. The plant shape of *Osftip9-1* looked wider and more flourish, which was caused by the increased tiller number (Figure 4). In general, WT plants had around 10 to 11 tillers, while *Osftip9-1* generated more than 22 tillers (Figure 5B). The tillers could be classified into primary tillers and secondary tillers. The primary tillers are at the full height of the rice plant while the secondary tillers are always shorter. So we used the histogram to show the height distribution of all tillers of WT and *Osftip9-1*. Both *Osftip9-1* and WT had similar numbers of primary tillers at the height range of 60 to 80 cm. At the height below 55 cm, which was the range for secondary tillers, *Osftip9-1* had dramatically increased tillering ability (Figure 5A). The increased tillering number was doubled by the dramatically increased secondary tiller number (Figure 5A). More importantly, the tiller number phenotype was observed during the mature stage when tillering behaviour should be dormant. The continuous emergence of the secondary tillers in *Osftip9-1* indicated a lowered tillering dormancy.

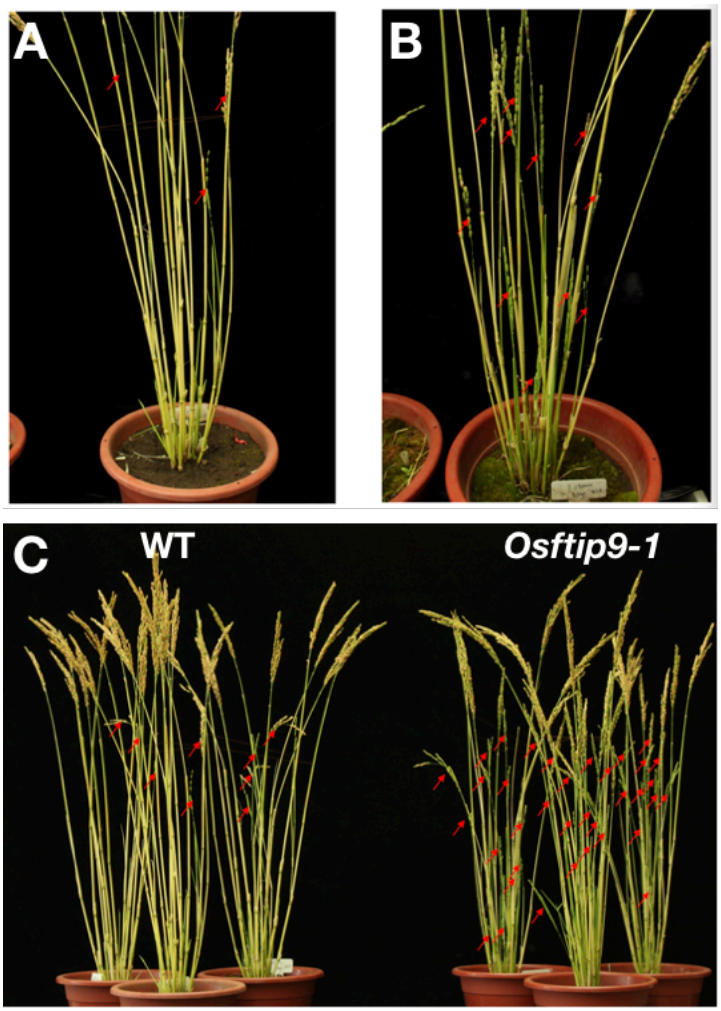


**Figure 4. Phenotypes of *Osftip9-1* in comparison with WT.**

(A, B). Phenotypes of *Osftip9-1* (A) and WT (B) at 120 days old. Leaves and sheaths are removed for better display of the tillers. Red arrows point out the observable secondary tillers in each plant.

(C). Overall plant architecture exhibition of *Osftip9-1* with reference to WT at 120 day-old. Leaves and sheaths are removed for better display of the tillers. Red arrows point out the observable secondary tillers in each plant.

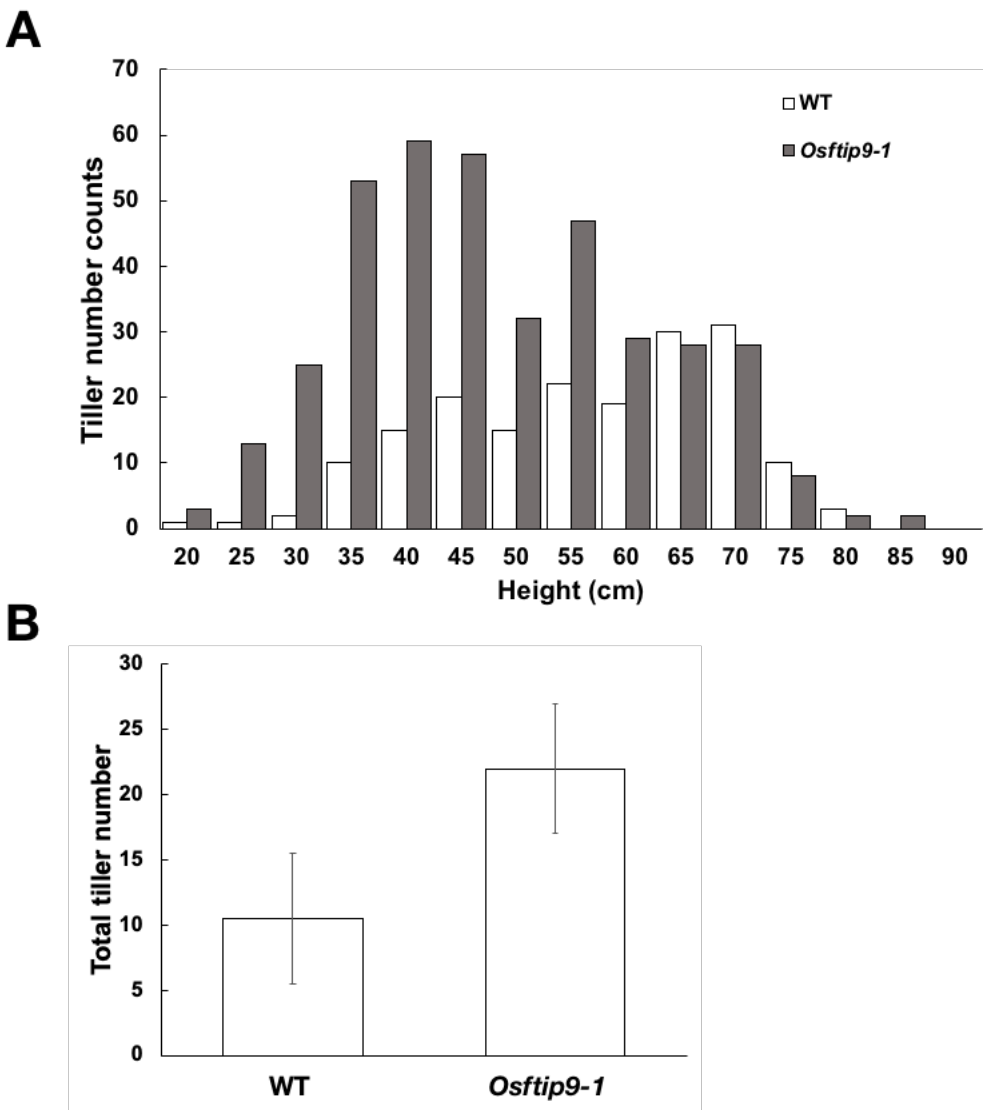


**Figure 5. Statistical analysis of tillering ability of *Osftip9-1* in comparison with WT.** (A). Tiller height distribution of *Osftip9-1* and WT by histogram. 15 pots of rice plants were analysed for each genetic background. Height of a tiller is measured from the ground to the tip of the panicle at 120 days old. Grey bars, *Osftip9-1*; white bars, WT. (B). Total tiller number for each plant of *Osftip9-1* and WT analyzed in (A). Data are shown as means±SD.

## 3.4 Generation of *OsFTIP9* over-expression and knockdown lines

### 3.4.1 *Pro35S:OsFTIP9* induces co-suppression of *OsFTIP9*

*Pro35S:OsFTIP9* was delivered into WT calluses followed by tissue culture process. However, after several rounds of *agrobacterium*-mediated transformation and tissue culture, we failed to obtain transgenic lines with increased expression of *OsFTIP9*. Instead, all survived transgenic lines exhibited co-suppression expression, as detected by the real-time PCR (Figure 6A). All obtained co-suppression lines exhibited lowered expression to less than 20% of WT, and the corresponding tiller numbers of the co-suppression lines exhibited a similar trend as *Osftip9-1*, in that there were more tillers than that of WT (Figure 6B).

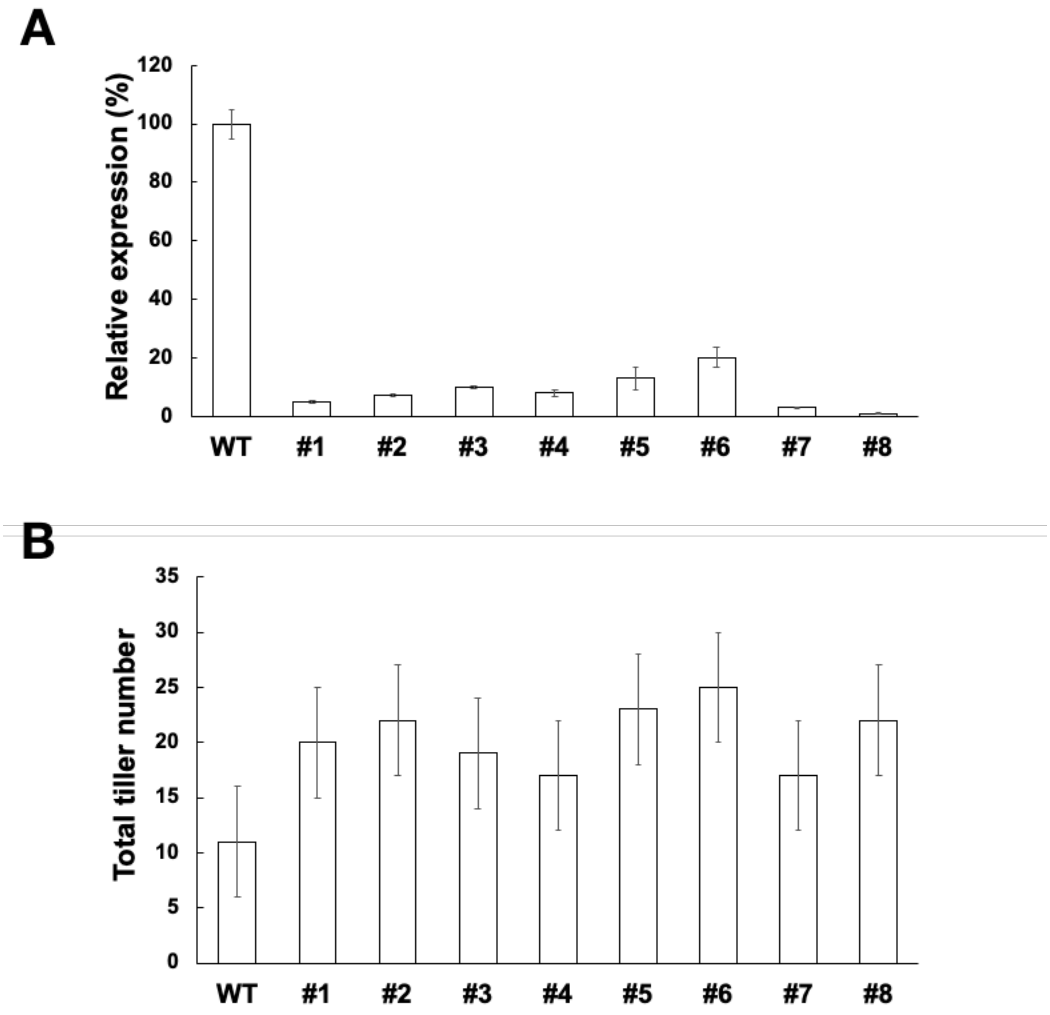


**Figure 6. Overexpression of *OsFTIP9* induces co-supression of *OsFTIP9*.**

(A). Quantitative real-time PCR analysis of *OsFTIP9* transcription levels in transgenic lines containing *Pro35S:OsFTIP9*. Results are normalized using the expression level of *UBQ*. Three biological replicates are performed. # number represents each transgenic line. Data are shown as means±SD.

(B). Total tiller number for each line in (A). # number represents each transgenic line. Tillers are counted at 120 days old. Data are shown as means±SD.

### 3.4.2 Knockdown of *OsFTIP9* exhibits similar tillering defects to *Osftip9-1*

The transcription of *OsFTIP9* was knocked down through RNA interference (RNAi), and the transcription levels of the transgenic lines were detected by real-time PCR. Quite a number of transgenic lines were obtained and they exhibited lowered expression levels of *OsFTIP9* to various levels, ranging from 80% to less than 10% as compared to WT (Figure 7A).

Among those transgenic lines, homologous lines with single-copy insertion were selected based on the segregation ratio. Similar to *Osftip9-1* mutants, *OsFTIP9* knockdown lines produced higher tiller numbers than WT (Figure 7B). Tiller numbers corresponded to the knockdown levels of *OsFTIP9*, in that the lower the expression was knocked down, the higher fold of tillers they generated (Figure 7B).

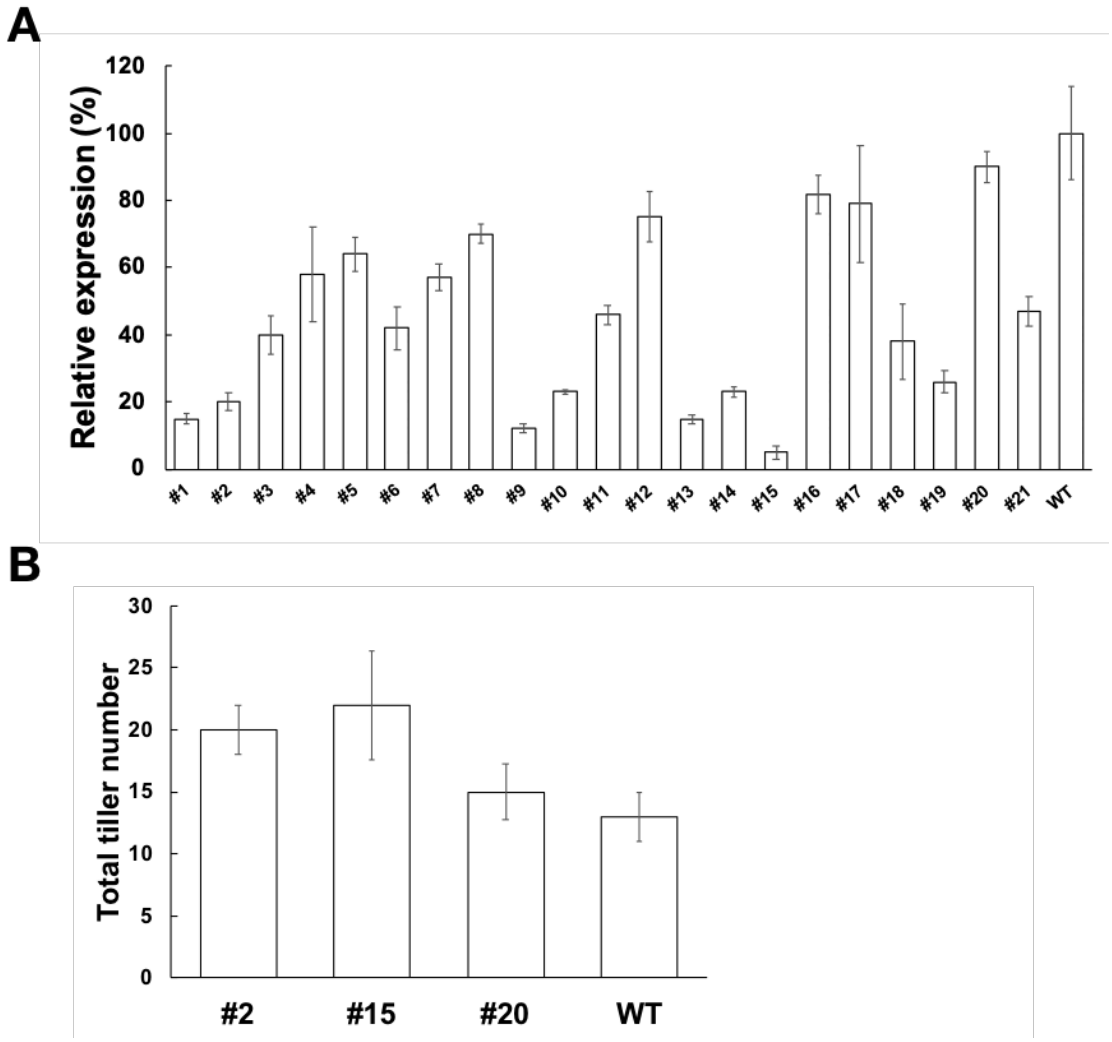


**Figure 7. Generation of *OsFTIP9* knockdown lines through RNAi.**

(A). Quantitative real-time PCR analysis of *OsFTIP9* transcription levels in *Osftip9* RNAi lines. Results are normalized using the expression level of *UBQ*. Three biological replicates are performed. # number represents each transgenic line. Data are shown as means±SD.

(B). Total tiller numbers of selected transgenic lines from (A). # numbers represent each transgenic line. Data are shown as means±SD.

### 3.5 Genomic fragment of *OsFTIP9* is able to rescue the tillering defects of *Osftip9-1*

In order to validate that the tillering phenotype was indeed caused by the mutation of *OsFTIP9*, the full genomic sequence of *OsFTIP9* was delivered into the *Osftip9-1* mutant. The genomic construct included 4kb 5' upstream and the entire 3kb coding sequence of *OsFTIP9*, excluding the terminator as the vestor contained a terminator positioned after the insertion. The tillering phenotypes of the transgenic lines were counted and we found that the increased tillering was recovered to a similar level of WT (Figure 8). This suggested that the tillering phenotype was caused by the mutation of *OsFTIP9* rather than other genes.

Taken all together, the loss-of-function mutant *Osftip9-1* exhibited increased secondary tillers, which was consistent with the phenotypes of *OsFTIP9* knockdown and co-suppression lines. And this was able to be rescued by the genomic *OsFTIP9*, confirming that *OsFTIP9* regulated the tillering phenotype.

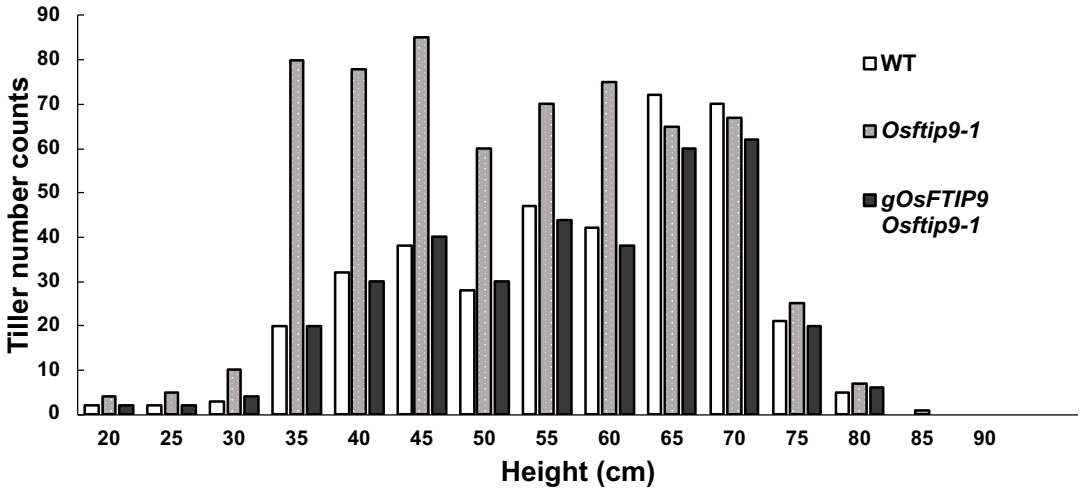


**Figure 8. Genomic *OsFTIP9* is able to rescue tillering defects of *Osftip9-1*.**
Tiller height distribution of *Osftip9-1*, *gOsFTIP9 Osftip9-1* and WT by histogram. 30 pots of rice plants for each genetic background were analyzed at 120 days old. Height of a tiller is measured from the ground to the tip of the panicle. Dotted grey bars, *Osftip9-1*; white bars, WT;black bars, *gOsFTIP9 Osftip9-1*.

### 3.6 Examination of mRNA expression of OsFTIP9 in the axillary buds by In situ hybridization

In order to gain more insights into the functions of *OsFTIP9*, we performed *in situ* hybridization using the WT bud tissue. Seedlings of 2 weeks after germination were used for sample collection. Sense and anti-sense probes targeting a gene-specific region of *OsFTIP9* were synthesized. The anti-sense probe detected that *OsFTIP9* was mainly expressed in the centre of the shoot apical meristem (SAM) as well as the tip of emerging axillary buds (Figure 9). While the lack of pigments in the slides applied with sense probe reinforced the validity of the signal (Figure 9). Seedlings of 3 weeks after germination were also examined, which showed the growing axillary buds with observable structures. The results had a similar expression pattern of *OsFTIP9* as 2-week-old seedlings (Figure 9).

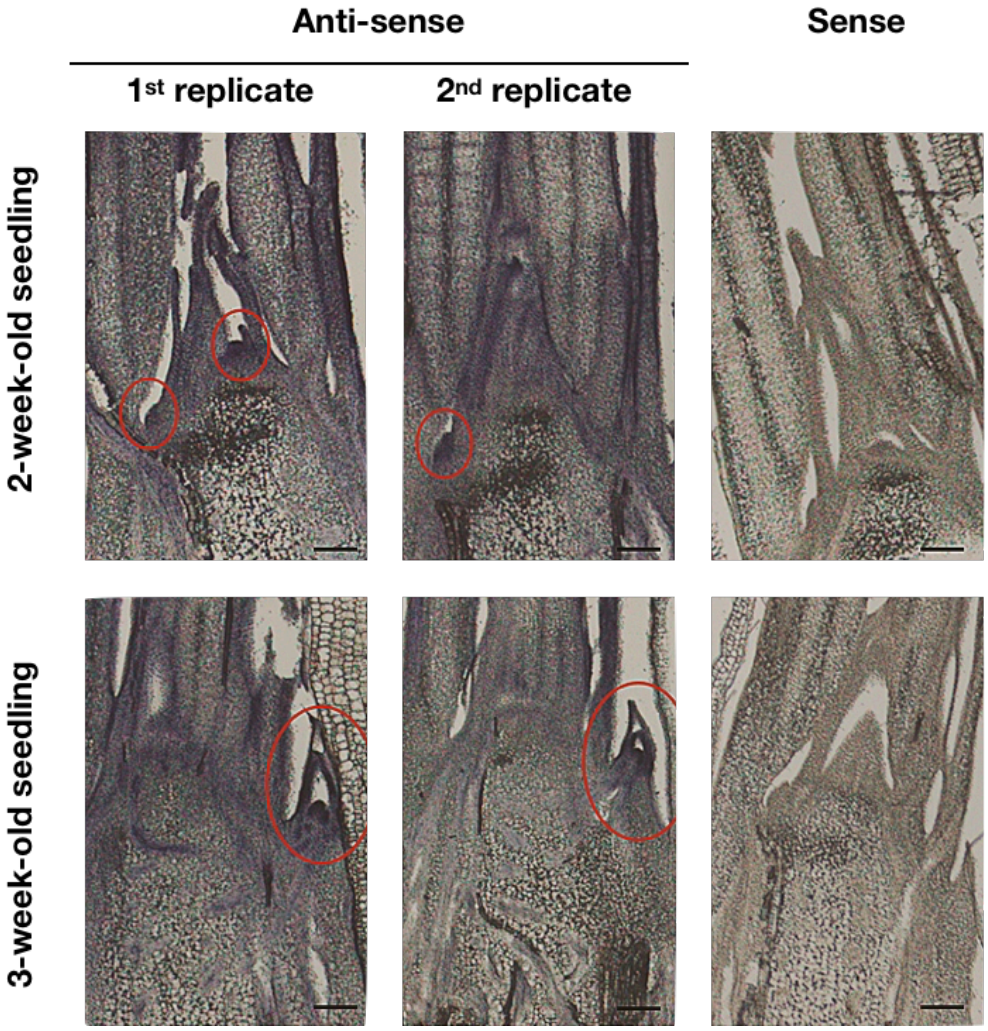


**Figure 9. *In situ* hybridization of *OsFTIP9* in the bud tissue.**

*In situ* hybridization analysis of the expression of *OsFTIP9* in the bud tissue. WT seedlings of 2-week-old have just emerging axillary buds, while 3-week-old seedlings have observable axillary buds, as shown in red circles. Scale bars, 100 μm.

### 3.7 Screening the interacting partners of OsFTIP9 through yeast two-hybird

To further understand how OsFTIP9 regulates the tillering behaviour in rice, we screened for its interacting partners through Y2H method. As memberane proteins are not suitable to be tested in Y2H, the PRT_C transmembrane domain was removed before being cloned into the pGBKT7 vector (Figure 10). The truncated forms of OsFTIP9 containing 1 to 4 C2 domains were cloned into the pGBKT7 vector, respectively. And thus, a mixture of baits were used to screen the pre-constructed rice cDNA library (Figure 10). This ensured that all potential interaction partners were screened out, which were to be validated one by one later.

Prior to the screening, various truncated C2 domains were constructed to pGBKT7 to test auto-activation. There was a weak auto-activation, and thus, 3-AT was added into the medium, which acted as a competitive inhibitor of what was produced by the reporter gene, *HIS3* gene (Liu et al., 2012). A series of nutritious media containing various concentrations of 3-AT were prepared and used to culture the yeast cells. And it was concluded that 5 mM 3-AT was an appropriate concentration that inhibited the auto-activation while allowing the growth of true interactive colonies.

The screening was done twice in order to collect as many colonies as possible, and for each round, around 800 colonies were picked. The colonies were then amplified with a pair of primers flanking the insertion fragment of potential prey proteins, followed by

sequencing analysis. Returned sequencing readings were checked using BLAST in the NCBI website in order to find out the corresponding gene, as the sequenced results might be fragmental. After two rounds of screening, a total of about 400 genes were obtained through BLAST, with 47 identical result hits and around 140 specific hits, part of which were listed in Table 3.

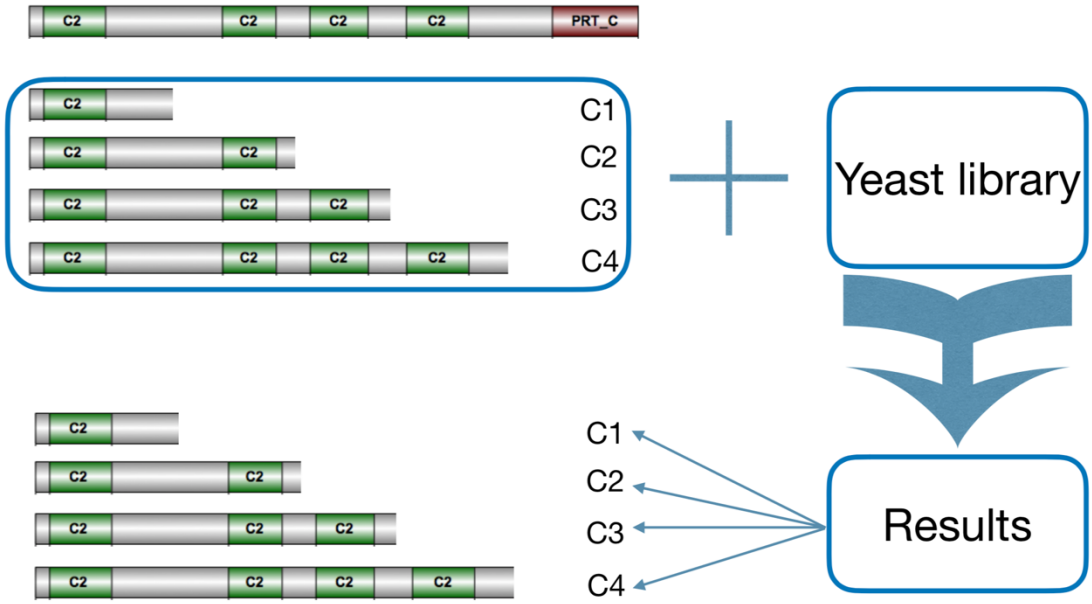


**Figure 10. Schematic representation of the Y2H screening process in searching for interacting partners of OsFTIP9.**

Schematic representation of the Y2H workflow to screen for OsFTIP9 interacting partners. Various truncated forms of OsFTIP9 (C1,C2,C3,C4) are mixed to mate with the yeast library. And the screening results are used to perform Y2H assay with each truncated form of OsFTIP9. Green blocks represent C2 domains; red block represents PRT_C domain. C1 to C4 indicate truncated fragments of OsFTIP9 containing various numbers of C2 domains.

**Table 3. A partial list of the candidates from Y2H screening**

| Loc No. | Brief Description |
|---|---|
| LOC_Os01g54810 | genomic\|lipase, putative, expressed |
| LOC_Os03g41060 | genomic\|GASR2 - Gibberellin-regulated GASA/GAST/Snakin family protein precursor, putative, expressed |
| LOC_Os02g02960 | genomic\|histone deacetylase complex subunit SAP18, putative, expressed |
| LOC_Os02g10480 | genomic\|stromal membrane-associated protein, putative, expressed |
| LOC_Os04g44870 | genomic\|C2 domain containing protein, putative, expressed |
| LOC_Os06g11990 | genomic\|expressed protein |
| LOC_Os02g42710 | genomic\|C2 domain containing protein, putative, expressed |
| LOC_Os03g10350 | genomic\|NPGR1, putative, expressed |
| LOC_Os03g11110 | genomic\|zinc finger family protein, putative, expressed |
| LOC_Os08g41950 | genomic\|OsMADS7 - MADS-box family gene with MIKCc type-box, expressed |
| LOC_Os10g01570 | genomic\|C-5 cytosine-specific DNA methylase, putative, expressed |
| LOC_Os03g25430 | genomic\|transcription regulator, putative, expressed |
| LOC_Os11g06934 | genomic\|expressed protein |
| LOC_Os02g42570 | genomic\|ferredoxin-thioredoxin reductase, variable chain, putative, expressed |
| LOC_Os01g60350 | genomic\|expressed protein |
| LOC_Os01g64350 | genomic\|expressed protein |
| LOC_Os04g33420 | genomic\|DNA-binding protein S1FA, putative, expressed |
| LOC_Os05g43252 | genomic\|expressed protein |
| LOC_Os06g23430 | genomic\|signal recognition particle 19 kDa protein, putative, expressed |
| LOC_Os07g49330 | genomic\|phospholipase C, putative, expressed |
| LOC_Os08g31769 | genomic\|expressed protein |
| LOC_Os09g28850 | genomic\|expressed protein |
| LOC_Os01g04030 | genomic\|signal peptidase complex subunit 3, putative, expressed |
| LOC_Os01g16090 | genomic\|RNA binding protein, putative, expressed |

### 3.8 Confirmation of interactions between OsFTIP9 and FC1, D14 & D14L

Three interacting candidates of special interest were selected from the screening pool, which were FC1, D14 & D14L. For *fc1* and *d14*, both mutants showed increased tillering ability; while D14L showed high similarity in terms of protein structure as D14, but D14L didn't affect tillering (Arite et al., 2009; Bennett et al., 2016; Minakuchi et al., 2010). In order to check whether they truly interacted with OsFTIP9, various methods were used as a crosscheck.

#### 3.8.1 Yeast two-hybrid assays show the interaction between OsFTIP9 and FC1, D14 & D14L

Y2H assays were firstly used to test the interaction, which could also detect the exact truncated form of OsFTIP9 that interacted with the candidate genes. To fulfil this purpose, BD constructs containing various numbers of C2 domains were delivered into the yeast competent cells respectively, and used separately as the baits for the assay, while on the other hand, the coding sequences of *FC1*, *D14* and *D14L* were cloned into the AD vector, followed by the delivery into yeast competent cells to be used as the preys.

The positive colonies growing on the DDO medium indicated the successful transformation of the yeast cells (Figure 11A). The growth on the TDO medium

detected the interaction: for FC1 and D14L, they interacted with the fragment containing three C2 domains (Figure 11B). While for D14, results showed that D14 interacted with the OsFTIP9 fragment containing two C2 domain. Yet it was not conclusive that D14 interacted with the three C2 domains, as the respective negative control also exhibited strong growth (Figure 12). All colonies did not grow on the QDO medium (Figure 11C & 12C).

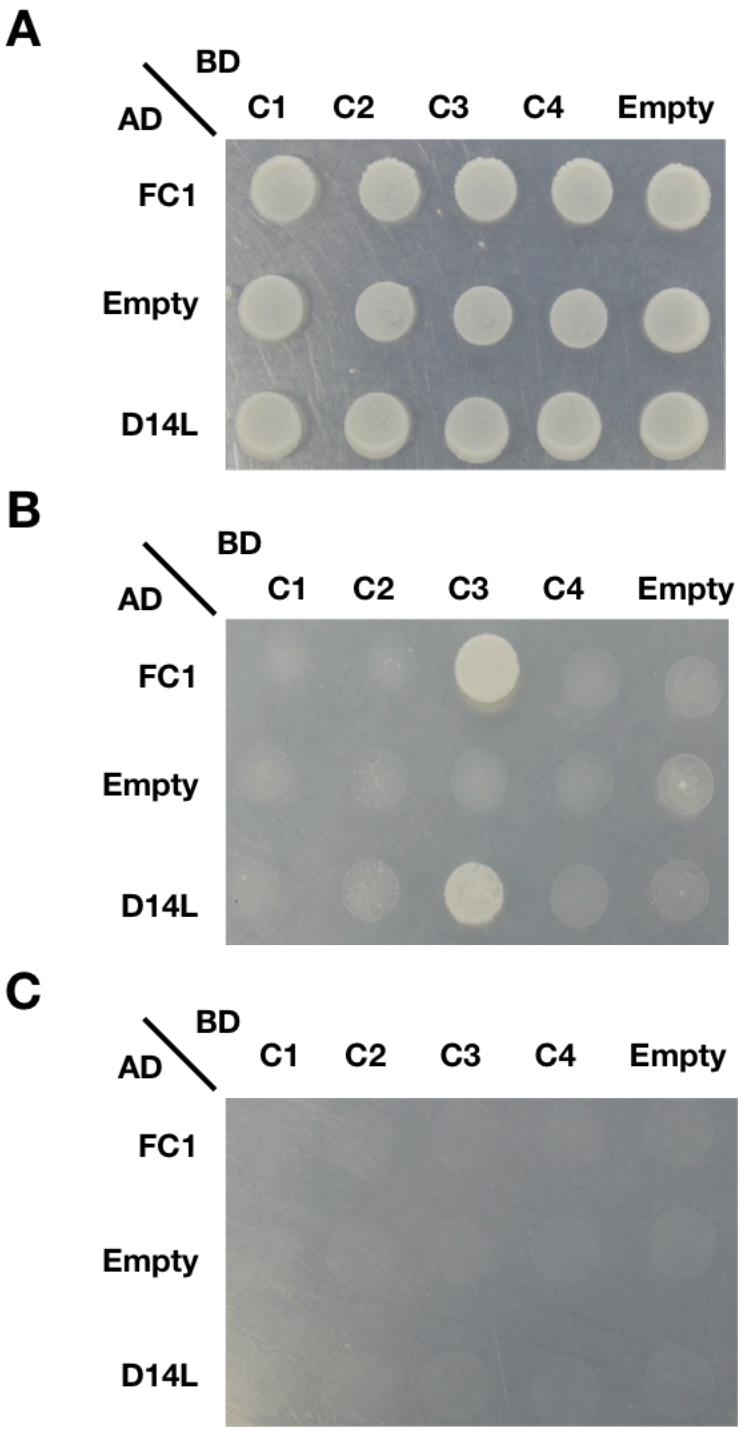


**Figure 11. Y2H assay shows interaction between truncated OsFTIP9 and FC1 or D14L.** Yeast cells after transformation grow on DDO (SD-Trp/-Leu) medium (A), TDO (SD-His/-Trp/-Leu) medium with 2mM 3-AT supply (B), and QDO (SD-His/-Trp/-Leu/-Ade) medium (C). Empty, yeast cells transformed with empty vector of AD or BD respectively.

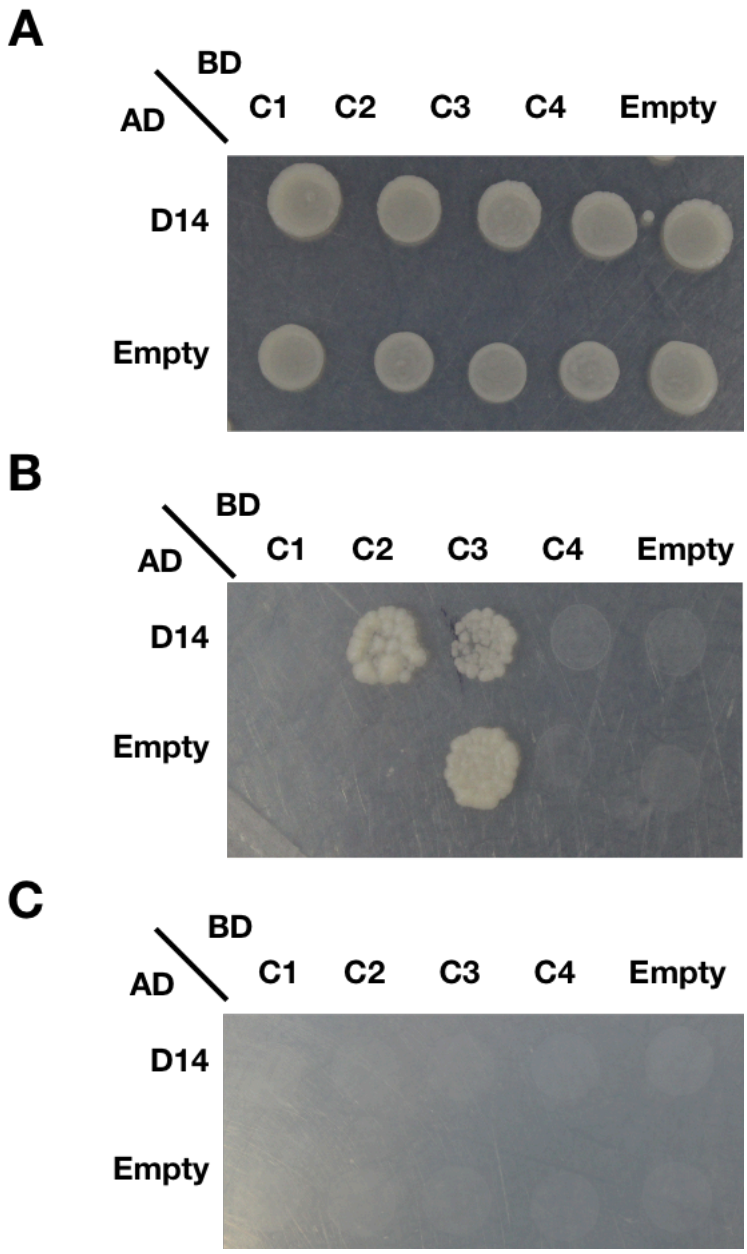


**Figure 12. Y2H assay shows interaction between truncated OsFTIP9 and D14.**
Yeast cells after transformation grow on DDO (SD-Trp/-Leu) medium (A), TDO (SD-His/-Trp/-Leu) medium supplied with 0.5mM 3-AT (B), QDO (SD-His/-Trp/-Leu/-Ade) medium (C). Empty, yeast cells transformed with empty vector of AD or BD respectively.

### 3.8.2 BiFC assays detect the interaction between OsFTIP9 and FC1, D14L

BiFC assay was used to further validate the interaction using rice protoplast cells. The coding sequence of *OsFTIP9* was cloned to be fused with nYFP fragment. In consideration of the transmembrane domain in the OsFTIP9 3' terminal, the nYFP was positioned in front of *OsFTIP9*. The coding sequences of *FC1* and *D14L* were then cloned to be fused with the cYFP fragment with the cYFP being positioned before *FC1* or *D14L*.

Rice protoplast cells were prepared accordingly and the vectors of various combinations were then delivered into the protoplast cells in sets. And they were stained with DAPI prior to the confocal microscopy observation.

For the test between OsFTIP9 and FC1, YFP signal was observed in the protoplast cells containing both *nYFP-OsFTIP9* and *cYFP-FC1*, and the DAPI staining confirmed that the signal was localized into the nucleus (Figure 13). All negative controls showed no YFP signals in the cells (Figure 13). The interaction test between OsFTIP9 and D14L exhibited the same results: the YFP signals were detected in the nucleus when *nYFP-OsFTIP9* and *cYFP-D14L* were both delivered into the protoplast cells (Figure 14).

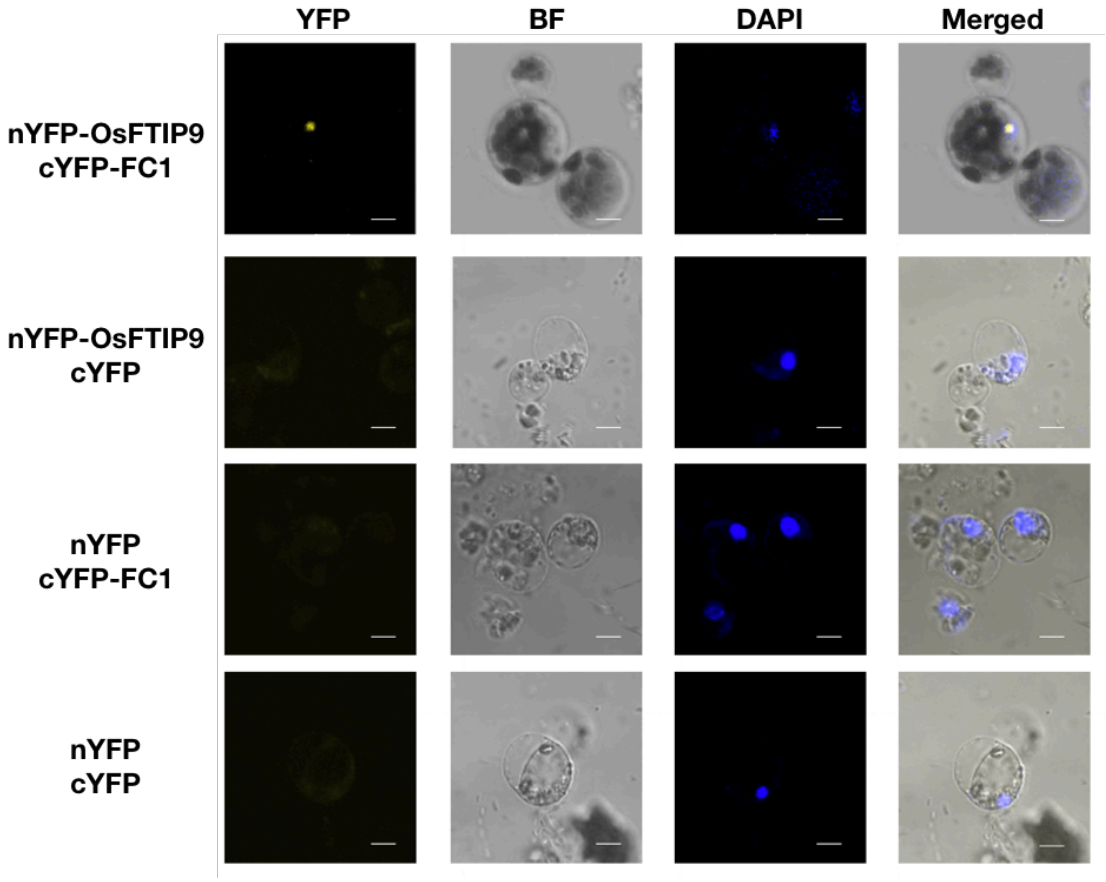


**Figure 13. BiFC analysis of interaction between OsFTIP9 and FC1.**
BiFC detects the interaction between OsFTIP9 and FC1. YFP, fluorescence of yellow fluorescent protein; BF, brightfield view; DAPI, inflourescence of 4',6-diamino-2-phenylindol; Merged, the merged view of YFP, BF, and DAPI. Scale Bars, 10 μm.

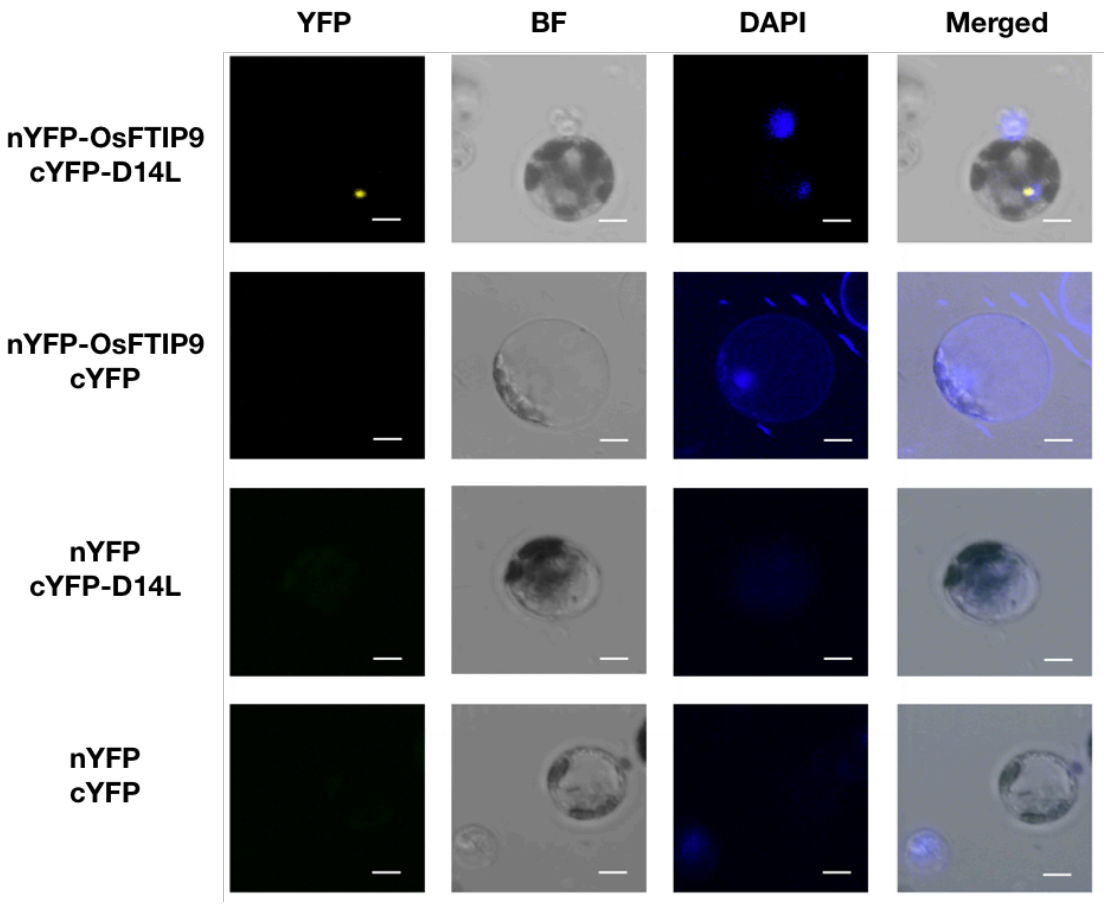


**Figure 14. BiFC analysis of interaction between OsFTIP9 and D14L.**
BiFC detects the interaction between OsFTIP9 and D14L. YFP, fluorescence of yellow fluorescent protein; BF, brightfield view; DAPI, inflourescence of 4',6-diamino-2-phenylindol; Merged, the merged view of YFP, BF, and DAPI. Scale Bars, 10 μm.

### 3.8.3 *In vitro* pull-down assays detect interactions between OsFTIP9 and FC1 & D14L

In order to further validate the interactions, *in vitro* pull-down assay was also performed. The coding sequence of *FC1* and *D14L* were cloned into the pMAL-c5X vector respectively, to produce MBP-FC1 or MBP-D14L fusion proteins. And the coding sequence of *OsFTIP9* was cloned into the pGEX-4T-1 in order to produce GST-OsFTIP9 fusion protein. The pull-down assay showed that both MBP-FC1 and MBP-D14L were able to be pulled down by GST-OsFTIP9 (Figure 15). Negative controls showed no interaction, except that GST pulled MBP-D14L down. Regarding the bait loading, GST-FTIP9 still had much stronger interaction with MBP-D14L than GST alone (Figure 15).

This conclusion was further reinforced when we swapped the tags: OsFTIP9 was fused with MBP, while FC1 and D14L were fused with GST. The pull-down assay again showed that GST-FC1 was able to be pulled down by MBP-OsFTIP9 while empty MBP could not (Figure 16). For GST-D14L and MBP-OsFTIP9, the pull down signal was much stronger then the affinity between GST-D14L and empty MBP (Figure 16).

Taken together, these results confirmed the interaction between OsFTIP9 with FC1 and D14L. While there was evidence showing interaction between OsFTIP9 and D14, the evidence was not as strong as that for FC1 and D14L.

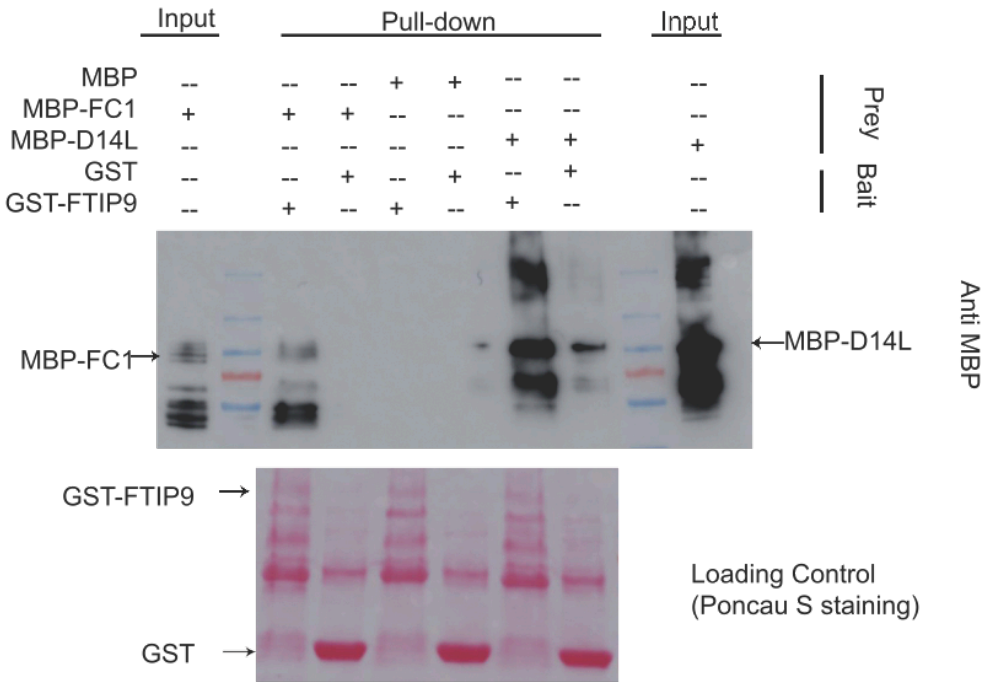


**Figure 15. *In vitro* GST pull-down assay of the interaction between OsFTIP9 and FC1 or D14L.**

*In vitro* pull-down assay analysis with GST-tagged OsFTIP9 and MBP-tagged FC1, MBP-tagged D14L. GST and MBP represent empty GST and MBP tags respectively. Immunoblot analysis uses Anti-MBP antibody, while GST-tagged proteins and GST are immobilized. Ponceau S is used for staining as the loading control.

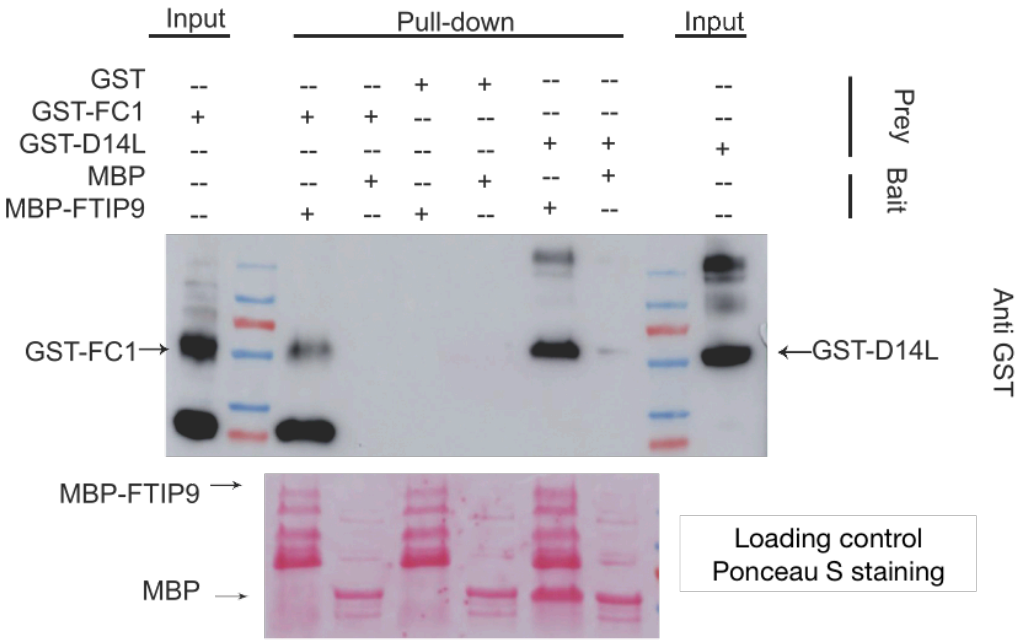


**Figure 16. *In vitro* MBP pull-down assay of the interaction between OsFTIP9 and FC1 or D14L.**

*In vitro* pull-down assay analysis with MBP-tagged OsFTIP9 and GST-tagged FC1, GST-tagged D14L. GST and MBP represent empty GST and MBP tags respectively. Immunoblot analysis uses Anti-GST antibody, while MBP-tagged proteins and MBP are immobilized. Ponceau S is used for staining as the loading control.

### 3.9 Expression patterns of *OsFTIP9* are largely overlapped with *FC1*, as compared with *D14* and *D14L*

To further gain insights into the functional link between *OsFTIP9* and the three candidate genes, we checked the mRNA expressions of these genes in different tissues of a rice plant. WT seedling of 14 days after germination were used and tested for bud, leaf and sheath tissues. Moreover, *fc1-2*, a loss-of-function mutant line obtained from Dr. Junko's lab, of same growth stage were also used to examine the expression pattern of *FC1* (Minakuchi et al., 2010).

It was found that *OsFTIP9* had the highest expression in the bud, which was more than 10X expression of that in leaf and sheath (Figure 17C). Such results were similar to the expression patterns of *FC1*, as it also showed the highest expression in the buds in WT (Figure 17A). The *FC1* expression in *fc1-2* was detectable, and its expression pattern was the same as that in the WT background (Figure 17B), suggesting that loss of *FC1* function in *fc1-2* was due to protein dysfunction rather than aborted transcription. While for *D14* and *D14L*, they showed the highest expression in the leaves, followed by the sheaths, and lastly the buds (Figure 17D, E). This indicated a closer association of *FC1* with *OsFTIP9*. Coupled with the validity of interaction results from Y2H assay, *in vitro* pull-down assay, and BiFC analysis, we chose to focus on the investigation of the interaction mechanism between OsFTIP9 and FC1.

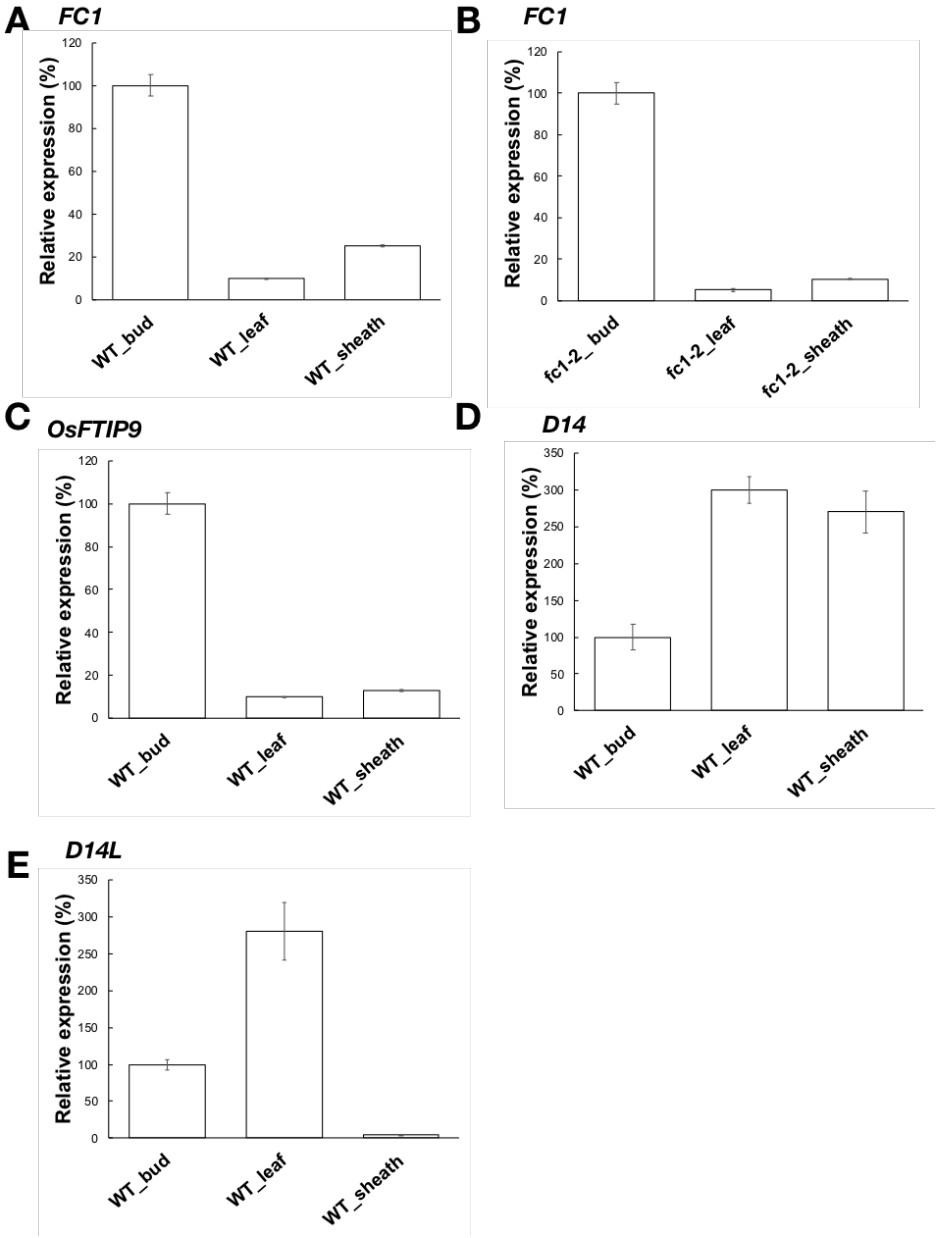


**Figure 17. mRNA expression patterns of *OsFTIP9*, *FC1*, *D14*, and *D14L* in various tissues.**

(A, B). Quantitative real-time PCR results of *FC1* transcription levels in various tissues in WT background (A) and *fc1-2* background (B). Results are normalized using the expression level of *UBQ*. Three biological replicates are performed. Error bars denote SD. 14-day-old seedlings are used for this experiment.

(C-E). Quantitative real-time PCR results of *OsFTIP9* (C), *D14* (D) and *D14L* (E) transcription levels in various tissues in WT background. Results are normalized using the expression level of *UBQ*. Three biological replicates are performed. Error bars denote SD. 14-day-old seedlings are used for this experiment.

### 3.10 Genotyping and phenotypic confirmation of fc1-2 and d14 mutants

In order to further study how OsFTIP9 controlled the tillering behaviour of rice, we obtained the available mutant seeds: *fc1-2* from Dr. Junko's lab in the University of Tokyo, and *d14* from Dr. Wang's lab in the Chinese Academy of Sciences (Arite et al., 2009; Minakuchi et al., 2010). The seeds were germinated in our lab together with WT as a control.

#### 3.10.1 A 27 bp deletion in *fc1-2* leads to increased tillering

The genomic DNA of *fc1-2* was extracted and a fragment spanning over the claimed mutation area was amplified by PCR. It was confirmed that *fc1-2* contained a total of 27 bp deletion in the TCP domain, which abolished the function of the protein, yet caused no frame shift for the downstream sequence (Figure 18A). The phenotype of *fc1-2* was also the same as published, as it exhibited elevated tillering ability as compared to WT (Figure 18C, D).

#### 3.10.2 A 1bp substitution in *d14* leads to increased tillering

The genotyping of *d14* was done using the same method as that of *fc1*-2. And it contained a single substitution in the claimed position, which changed the amino acid

sequence from Alanine to Glycine (Figure 18B). And notably, *d14* exhibited much stronger tillering ability and drastic dwarfism as compared to *fc1*-2 (Figure 18C, D).

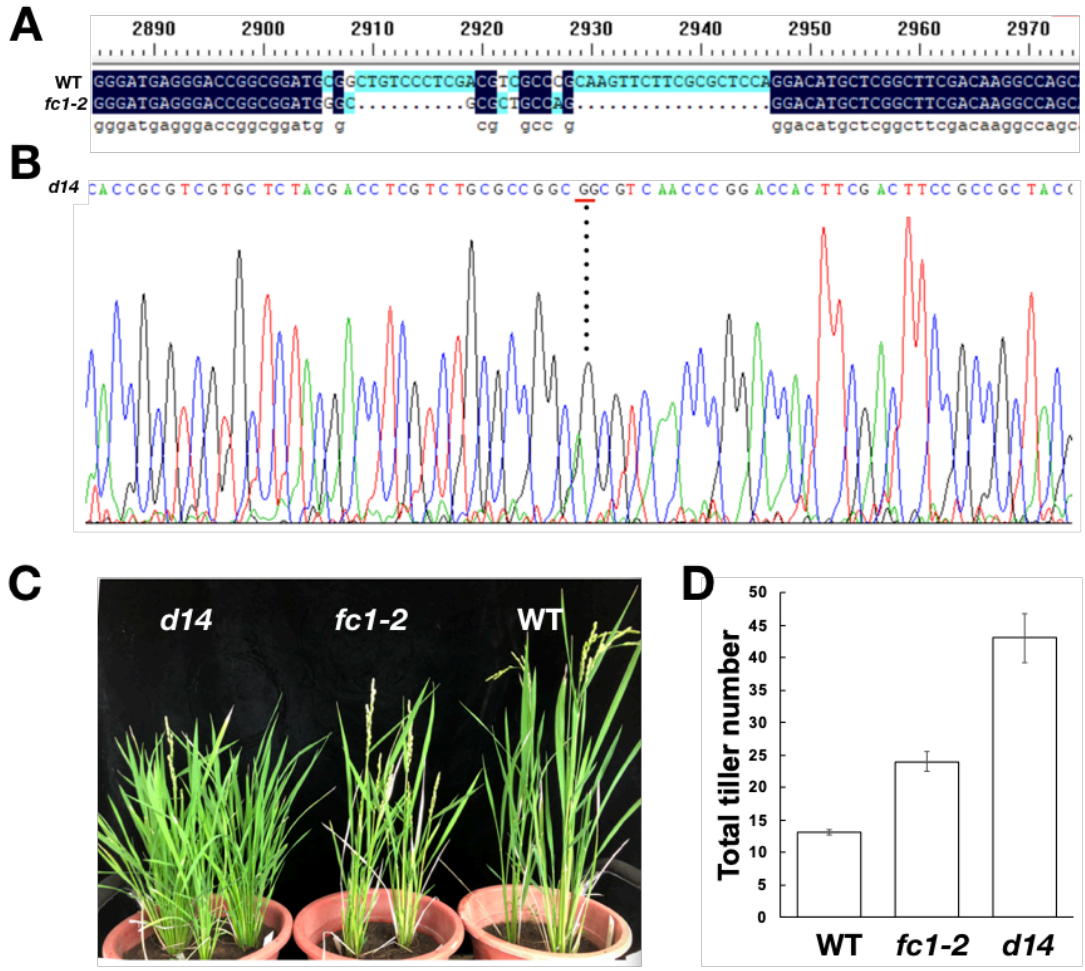


**Figure 18. Genotyping analysis and phenotypic exhibition of *fc1-2* and *d14*.**

(A). Sequence alignment of the mutation site of *fc1-2* to WT sequence. Number indicates relative position with reference to genomic *FC1*. Highlighted dark blue colour shows matching sequences.

(B). Sequencing result of *d14.* Dotted line points the single substitution position.

(C). Phenotypic exhibition of *fc1-2* and *d14* in comparison to WT plants. Plants are 90-day-old.

(D). Total tiller number counts for WT, *fc1-2* and *d14*. 15 pots of each type are counted. Data are shown as means±SD.

### 3.11 Knockdown of FC1 expression exhibits similar tillering phenotype as fc1-2

#### 3.11.1 Generation of *FC1* knockdown lines using RNA interference

Two targeting sites were chosen in the coding region of *FC1* with high specificity (Figure 19A). The respective constructs were delivered into WT calluses through *agrobacterium*-mediated transformation, followed by tissue culture process. We generated several transgenic lines from each targeted site and the transcription levels were detected through real-time PCR. It was showed that for both sites, the expression of *FC1* was downregulated to various levels, ranging from 10% to 80% of that of WT (Figure 19B).

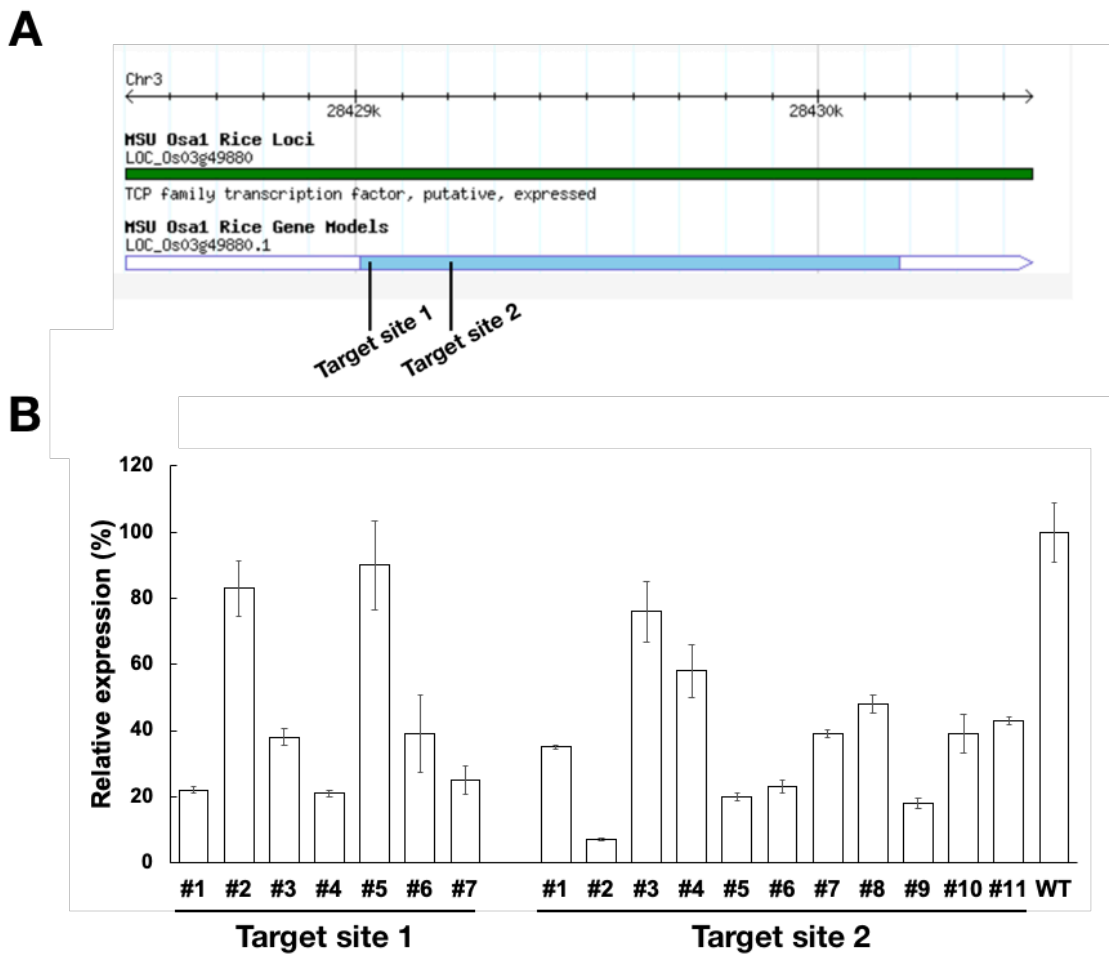


**Figure 19. Downregulation of *FC1* through RNAi.**

(A). Schematic representation of RNAi targeting sites for *FC1*. Blue block represents coding sequence of *FC1*.

(B). Quantitative real-time PCR analysis of *FC1* transcription levels in knockdown transgenic lines. Results are normalized using the expression level of *UBQ*. Three biological replicates are performed. # number represents each transgenic line. Data are shown as means±SD .

### 3.11.2 Downregulation of *FC1* leads to the increased tiller number

Among the knockdown lines, line #1 and #6 of target site 1 and line #5 and #7 of target site 2 were chose as representative lines for biochemical analysis. Homozygous lines with single insertion were chosen to be planted together with WT in order to confirm the phenotype. It was found that the tiller number was generally higher than that of WT. WT plants overall gave rise to around 10 tillers, while *FC1* RNAi lines generated from 15 to as much as 23 tillers, depending on the knockdown level. The tiller number increasing intensity was in line with the levels that *FC1* was supressed (Figure 20). This confirmed the phenotype of *FC1* as reported.

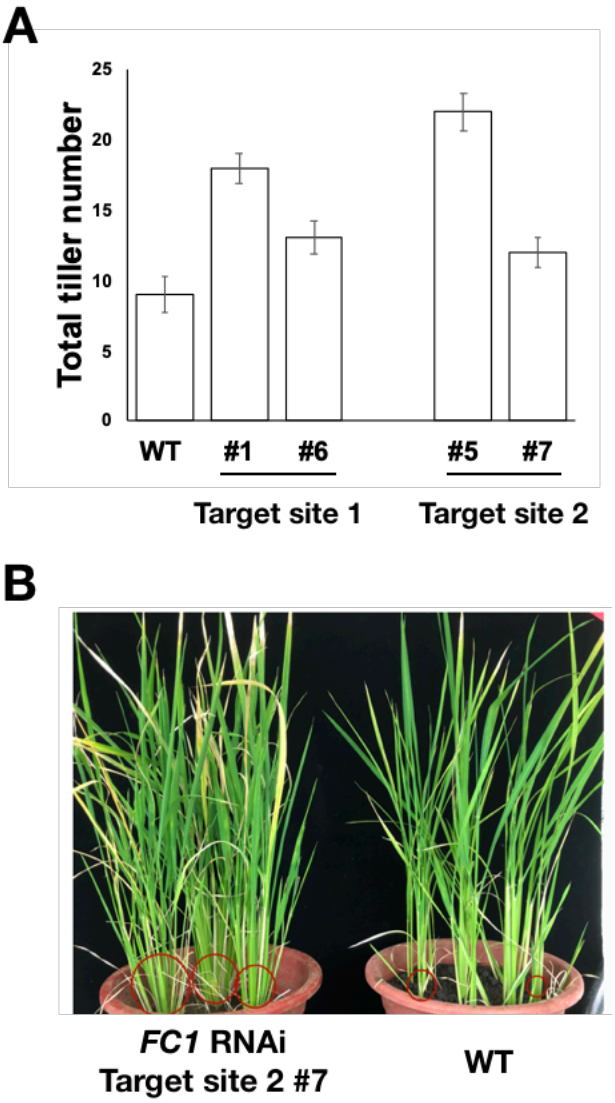


**Figure 20. *FC1* RNAi lines shows increased tiller numbers.**
(A). Total tiller number for selected *FC1* RNAi lines. # numbers represent each transgenic line from Figure 19B. Data are shown as means±SD.
(B). Plant architecture of *FC1* RNAi lines in comparison to WT. Red circles highlight the tillering difference.

### 3.12 Tissue-level expression pattern of FC1 is not affected in the *Osftip9-1* mutant

To test whether OsFTIP9 transported FC1 across different tissues, we tested whether the mutation of OsFTIP9 affected the distribution of FC1 protein at the tissue level. If OsFTIP9 transported FC1 protein among tissues, the absence of OsFTIP9 protein would result in a change in the expression pattern of FC1 at the tissue level.

#### 3.12.1 Generation and validation of rice FC1 antibody

To facilitate this test, we generated customized antibodies targeting the rice FC1 protein. Given the chance of antibody being unable to detect the endogenous FC1 protein, we generated three FC1 antibodies by different FC1 peptides. In order to validate whether the antibodies could successfully detect the FC1 proteins, we used all three antibodies to perform western blot with various samples. All three antibodies were able to detect the *in vitro* expressed MBP-FC1 (Figure 21). The absent affinity of empty MBP reflected that the bands detected in the MBP-FC1 lane were due to the FC1 recognition (Figure 21). When applying the 3 antibodies to detect endogenous FC1, all of them were able to detect signals in WT as well as in the *fc1-2* mutants, indicating that the mutated FC1 could also be recognized (Figure 21). The presence of the signal in *fc1-2* was due to two reasons: firstly, all three antibodies did not target the mutation sites of *fc1-2*, which happened at the conserved TCP domain; secondly, *fc1-2* containes a deletion of 27 bp, which does not cause any frameshift to the downstream sequence.

More interestingly, the signals in *fc1-2* were much stronger than that in WT (Figure 21). This might suggest the existence of a feedback loop for FC1, yet it awaits further investigation. And for the sake of convenience, only one (#1) antibody was used for further experiments. Lastly, all three antibodies failed to detect any signals in the leaves of neither WT or *fc1-2*, indicating that the FC1 protein expression levels were too low to be detected in the leaf tissue.

To the fact that *fc1-2* could not serve as a negative control, we also used the *FC1* RNAi lines of various knockdown levels for the western blot, and it was showed that the protein signal strength corresponded to the *FC1* mRNA levels (Figure 22). This further validated that all three FC1 antibodies were able to detect endogenous FC1 protein with adequate sensitivity and specificity.

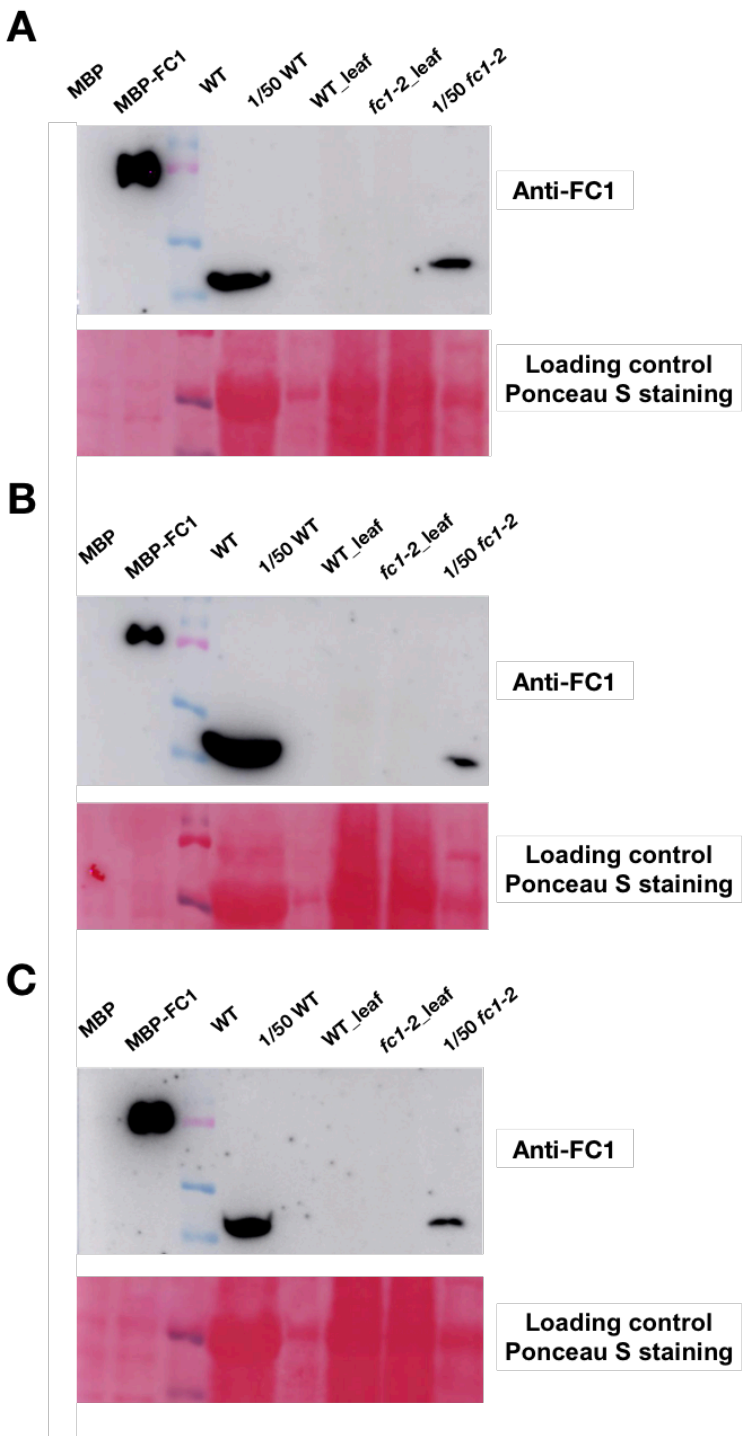


**Figure 21. FC1 protein is detectable by FC1 antibodies.**
(A)-(C). Anti-FC1 antibodies verification. #1 FC1 antibody (A), #2 FC1 antibody (B) and #3 FC1 antibody (C) are used to perform Western blot with various samples. Ponceau S stains loading amount; all seedlings are 10-day-old.

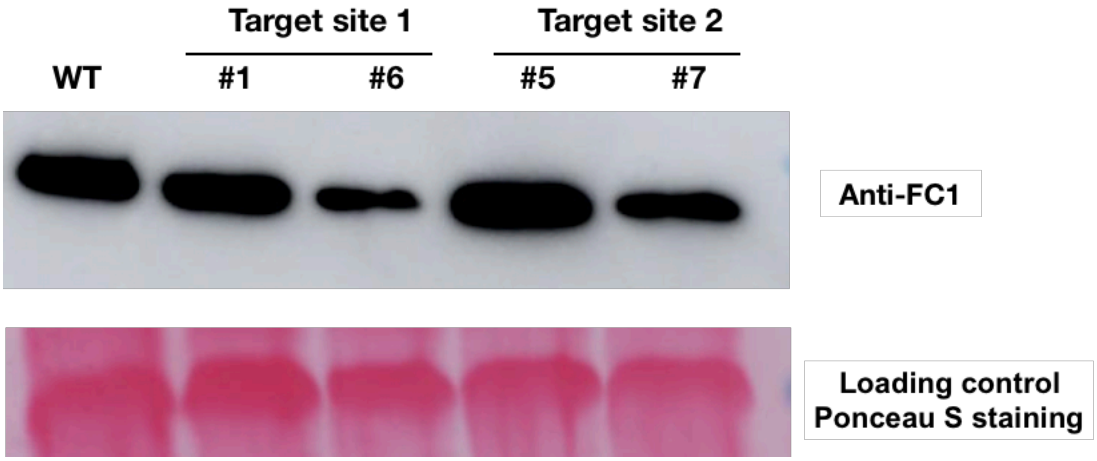


**Figure 22. Validation of FC1 antibodies with *FC1* RNAi lines.**
Validation of #1 FC1 antibody with selected *FC1* RNAi lines and WT. All seedlings used are 10-day-old. #number corresponds to transgenic lines in Figure 19B. All proteins are loaded in equal amount. Ponceau S staining is used as loading control.

### 3.12.2 Bradford assay and Ponceau S staining serve as loading references

We searched for appropriate loading reference among tissues. There were generally three kinds of loading references: firstly, Ponceau S staining for Rubisco large subunit (RbcL); secondly, housekeeping protein antibody detection; lastly, Bradford assay normalization for total protein. It was found that the two available antibodies targeting housekeeping proteins, anti-HSP70 and anti-histone, were not suitable to be used. The anti-HSP70 antibody showed inconsistant signal detection results in various tissue, especially for the mature plants, while anti-histone failed to detect the signals (data not showed). We then used the Bradford assay to directly detect the concentrations of the total protein loading. And the results were stained with Ponceau S as a crosscheck. We grounded the whole rice seedings of WT and *fc1*-2, and the concentration of the total extracted protein were normalized by the Bradford assay and then diluted to equal concentration. Equal amount of total extracted protein from WT and *fc1*-2 were loaded in a series of 10µl, 20µl, 40µl and 50µl and the Ponceau S staining also showed equal strength between WT and *fc1*-2 within each tissue type (Figure 23A). This confirmed the accuracy of Bradford Assay normalization. We then used proteins extracted from various tissue of rice plants from heading stage as well as the 10-day-old stage, and normalized the concentration using Bradford assay. The Ponceau S staining exhibited differentiated signal strength, which was extremely strong in the leaf tissue because of the abundant presence of RbcL. All other tissues are generally at the similar level (Figure 23B).

Taken together, we concluded that available antibodies targeting the housekeeping proteins were not applicable; Bradford assay was able to generate accurate measurement of protein concentration; Ponceau S staining was applicable except for the leaf tissue.

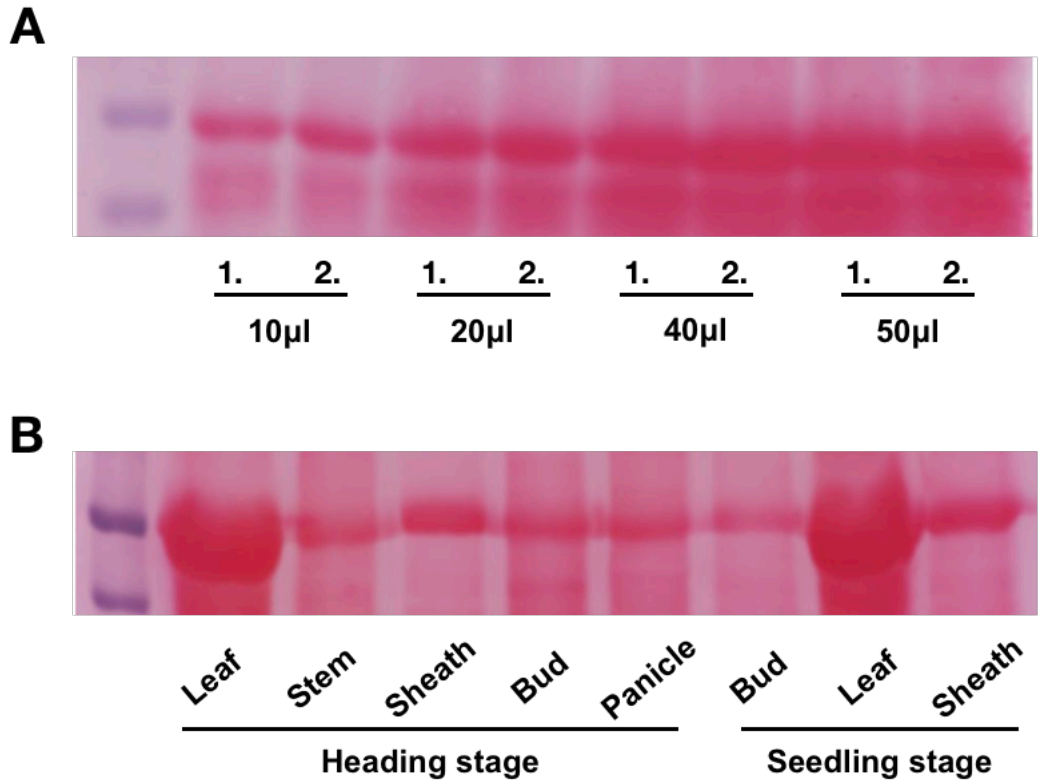


**Figure 23. Loading reference tests with Bradford assay and Ponceau S staining.**
(A). Ponceau S staining of whole proteins extracted from young seedlings at various loeading amounts. 1. WT seedlings; 2. *fc1-2* seedlings. Seedlings of 10-day-old are used to extract the whole protein. Concentrations of protein extracted from 1. and 2. are normalized using Bradford assay.
(B). Ponceau S staining of various tissues at different stages. WT seedlings of 10-day-old are used to extract the proteins. Different protein extracts are normalized using Bradford assay and loaded in equal amounts.

### 3.12.3 FC1 protein distribution in the tissue level is not affected in the *Osftip9-1* mutant

In order to find out whether OsFTIP9 transported FC1 among tissues, we examined the expression patterns of FC1 in the WT and *Osftip9-1* backgrounds. It was found that FC1 protein had the highest expression in the bud tissue at the heading stage. And the amounts of FC1 in the stem and panicle at heading stage were comparable to that in the bud of seedlings of 10 days old. The FC1 protein expression level remained low at the sheath tissue at both seedling stage and heading stage (Figure 24A). FC1 protein from different tissues of *Osftip9-1* at seedling and heading stages were also checked using the same FC1 antibody, and the results showed similar pattern to that of WT (Figure 24A, B). This indicated that the expression of FC1 at the tissue level was not affected by the mutation of OsFTIP9, which further suggested that OsFTIP9 might not transport FC1 protein from one tissue to another.

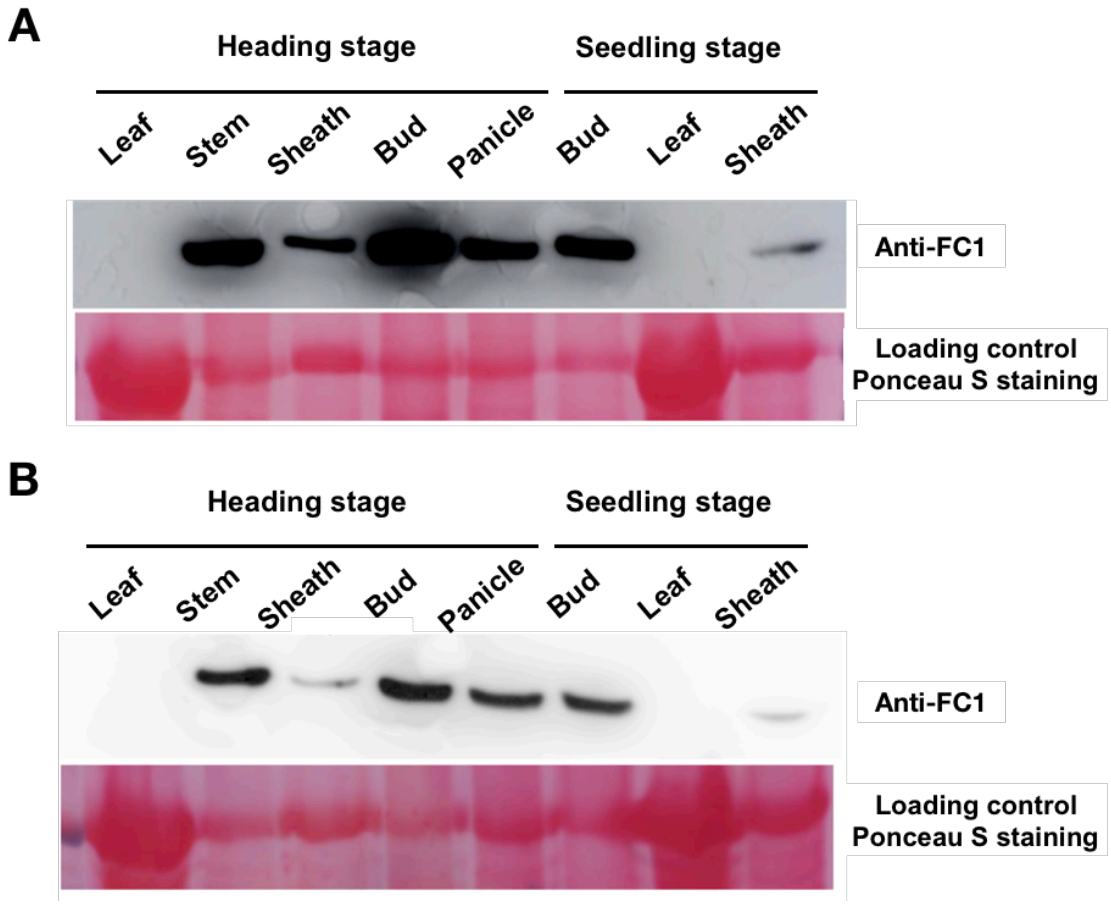


**Figure 24. Protein distribution patterns of FC1 in WT and *Osftip9-1*.**
(A, B). Examination of FC1 protein expression in various tissues at different stages, under the background of WT (A) and *Osftip9-1* (B). Seedling stage refers to 10-day-old, heading stage refers to 110-day-old. Different protein extracts are normalized using Bradford assay and loaded in equal amounts. Ponceau S staining serves as loading reference.

### 3.13 OsFTIP9 affects the stability of FC1 protein

From the above section, a reduced FC1 expression level in *Osftip9-1* was found after normalizing the total protein amounts to WT (Figure 24A, B). In order to find out whether OsFTIP9 also regulated the stability of FC1, we detected the FC1 expression level in the total protein extracted from WT and *Osftip9-1* 10-day-old seedlings. It was found that the expression level of FC1 was higher in WT seedlings than that in *Osftip9-1*, which indicated that the presence of OsFTIP9 protein might help maintain the FC1 protein level for its normal functions (Figure 25.).

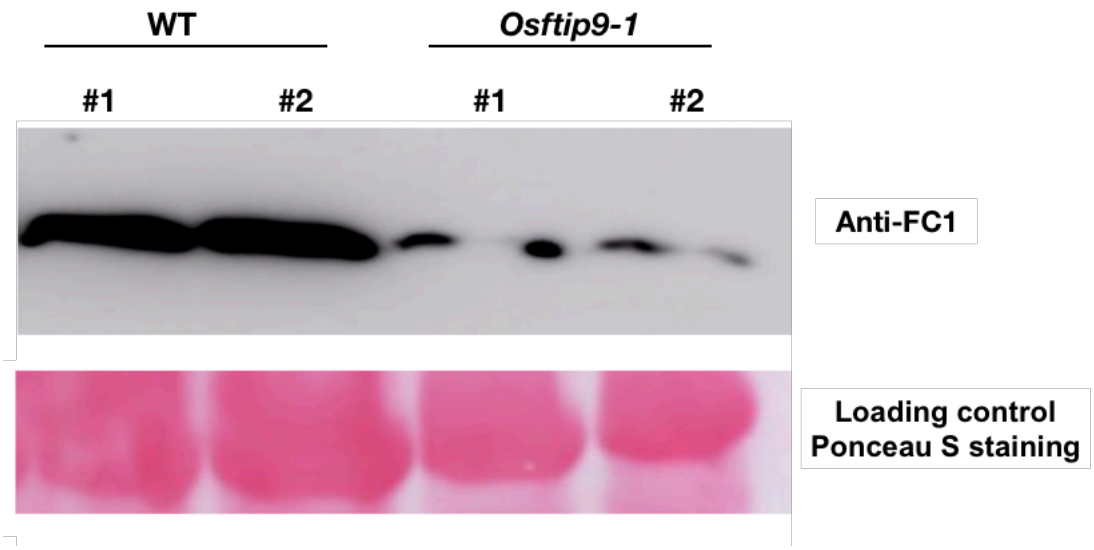


**Figure 25. FC1 protein level is reduced in *Osftip9-1*.**
Protein expression level of FC1 in *Osftip9-1* was lower than WT. # 1, #2 represent proteins extracted from two biological replicates to exclude environmental and other random factors. 10-day-old seedlings are used for protein extraction. Leaves are removed before protein extraction. Different protein extracts are normalized using Bradford assay and loaded in equal amount. Ponceau S staining serves as a loading reference.

### 3.14 Mutation of OsFTIP9 affects the subcellular localization of FC1

Given previous findings that OsFTIP9 might not transport FC1 from one tissue to another, we excluded the possibility of macromolecular trafficking in the long distance. And thus, we checked whether OsFTIP9 transported FC1 at the subcellular level.

#### 3.14.1 FC1-mCherry is localized in the nucleus

FC1 was fused with mCherry at C-terminal and transiently expressed in rice protoplast cells. The protoplasts were then examined under the confocal microscopy, and the mCherry fluorescence signal was found in the nucleus, which was confirmed by overlapping with DAPI signals (Figure 26). This suggested that FC1 was localized in the nucleus, which was consistent with the role of FC1 being a transcription factor.

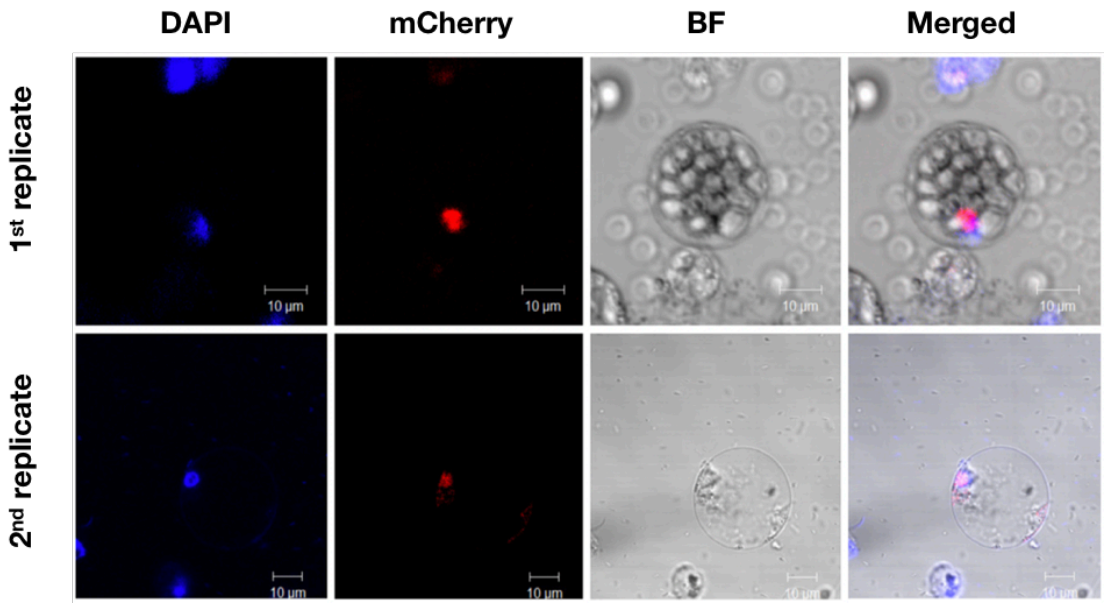


**Figure 26. FC1-mCherry is localized in the nucleus.**
FC1-mCherry was localized in the nucleus in rice WT protoplast cells. DAPI, inflourescence of 4',6-diamino-2-phenylindol; mCherry, fluorescence of mCherry protein; BF, brightfield view; Merged, the merged view of mCherry, BF, and DAPI. Scale Bars, 10 μm.

### 3.14.2 FC1 is localized in the whole protoplast cell of *Osftip9-1* mutant

In order to found out whether OsFTIP9 affected the FC1 localization in the subcellular level, we also delivered the *FC1-mCherry* into the protoplast cells derived from *Osftip9-1* mutant. After same time of culturing, the mCherry fluorescence signal was observed inside the whole cell, which was different from the localization in WT cells (Figure 27). This suggested that OsFTIP9 affected the subcellular localization of FC1, as FC1 failed to be fully localized in the nucleus in the absence of OsFTIP9. This further suggested that OsFTIP9 might be responsible of transporting FC1 into the nucleus.

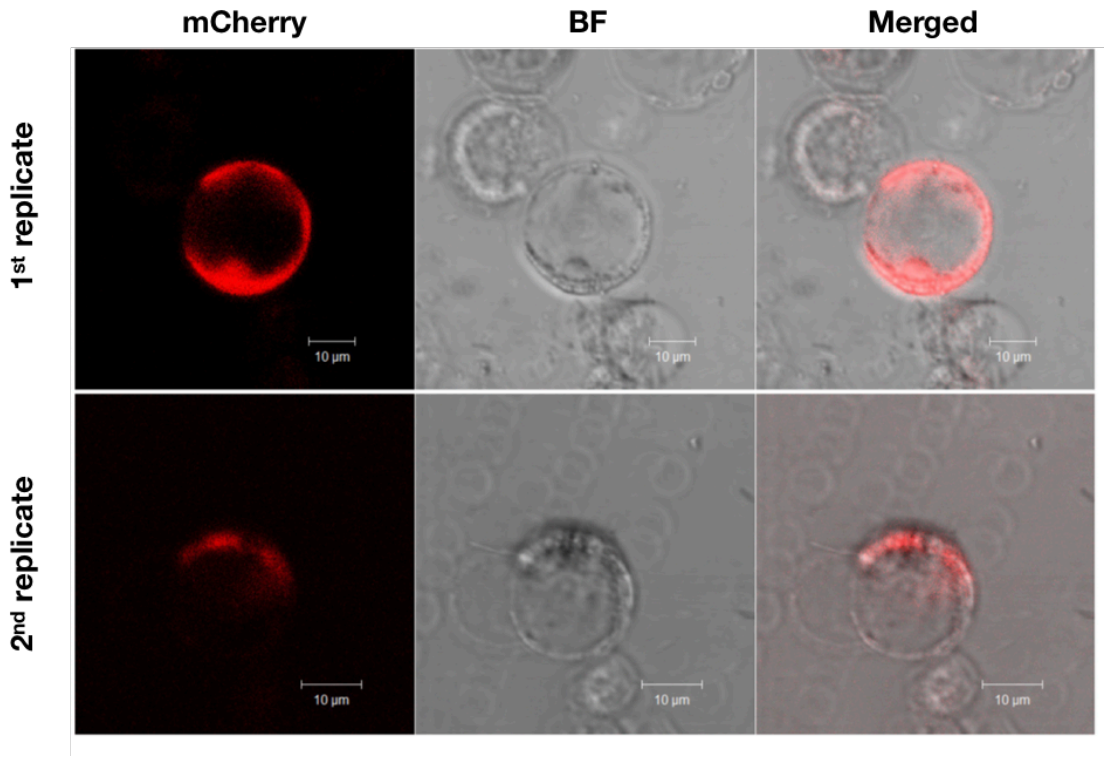


**Figure 27. FC1-mCherry is localized in the whole cell in *Osftip9-1* mutant.**
FC1-mCherry was localzed in the whole cell in the rice *Osftip9-1* protoplast cells. mCherry, fluorescence of mCherry protein; BF, brightfield view; Merged, the merged view of mCherry, BF, and DAPI. Scale Bars, 10 μm.

### 3.15 The expressions of *FC1* downstream genes are reduced in the *Osftip9-1* and *fc1-2* mutants

Given the hypothesis that OsFTIP9 might participate in the localisation process of FC1 into the nucleus, and FC1 controlled its downstream genes, we checked the expressions of some reported genes that were downstream of FC1.

*OsGT1* was homologous to the maize *GT1* gene, which was the downstream target of ZmTB1. *OsGT1* was potentially a downstream target of FC1, as FC1 was homologous to the maize TB1 (Zhang et al., 2004). And more importantly, GT1 was reported to inhibit the tillering function, meaning that the deficiency of OsGT1 may cause increased tillering ability (Zhang et al., 2004). It was the same story for *D14* as it was also reported as a downstream target of FC1, and functioned to inhibit rice tillering (Arite et al., 2009). *OsGT1* and *D14* were reported downstream targets of FC1 . The expressions of these genes were then tested in the background of *fc1-2* and *Osftip9-1* as compared to WT, and they exhibited dramatically decreased transcription levels (Figure 28A-C). All of them were negative regulators for rice tillering, thus their downregulations in *Osftip9-1* and *fc1-2* were consistent with the phenotype.

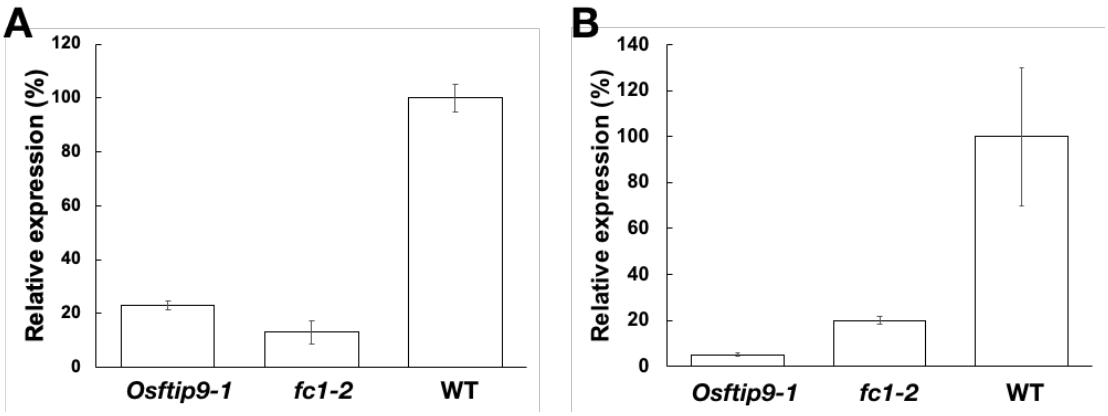


**Figure 28. Expression levels of *D14* and *OsGT1* in *Ostip9-1*, *fc1-2* and WT.**
(A, B). Quantitative real-time PCR analysis of transcription levels of *D14* (A) and *OsGT1* (B) in *Osftip9-1* and *fc1-2* mutants as compared to WT. Results are normalized using the expression level of *UBQ*. Three biological replicates are performed. Data are shown as means±SD.

# Chapter 4

# Discussion

# Chapter 4 Discussion

## 4.1 OsFTIP9 regulates rice tillering berhaviour in the late heading stage

Tiller development largely determines the architecture of a rice plant, which eventually determines the yield. It has long been a substantial trait in the domestication from wild species to different varieties of commercial rice, which suite the production needs (Doebley, Gaut, & Smith, 2006). The Asian rice is one of the typical domesticated rice with desired traits, including shattering, pericarp colour and tiller architecture (C. Li, Zhou, & Sang, 2006; Z. Lin et al., 2007; Sweeney, Thomson, Pfeil, & McCouch, 2006). The erect growth of rice largely benefits the farming of rice, thus boosts the agriculture production. On one hand, the required land for rice farming is largely reduced given the more erect architecture, which is critical for the modern conflicts between land usage and nature conservation. On the other hand, such an architecture increased the photosynthesis efficiency, which eventually increases the grain yield in terms of quality and quantity (Tan et al., 2008).

In this study, we showed that OsFTIP9 had a great impact over the architecture of a rice plant, by controlling the tiller numbers. Loss-of-function mutant *Osftip9* and *OsFTIP9* RNAi lines exhibited an elevated tiller number to almost 2 times. However, this was actually not the trait preferred for the development of rice cultivars, mainly because the extra tillers were secondary tillers developed from the axillary buds at the relatively late

heading stage. This phenotype causes several problems: firstly, the presence of the secondary tillers increased the space a rice plant requires to grow with; secondly, the nutrition was actually consumed by the development of the axillary buds instead of being totally dedicated to the ripening of rice grains; thirdly, the continuous emergence of secondary tillers causes extra trouble in harvesting.

Although *Osftip9* has inferior trait itself, the significant tiller phenotype of *Osftip9* supports that *OsFTIP9* could be a hereto uncharacterized target for agricultural engineering. We failed to obtain functional constitutive overexpression lines of *OsFTIP9* due to probably callus defects in this study, but theoretically, tissue-specific or stage-specific overexpression of *OsFTIP9* might improve the rice architecture as if it bypasses the callus defects. This research sheds light on the development of better rice cultivars that has better synchronised panicle development and ultimate number of tillers. The biomass of a rice plant might also be altered as tiller number directly corresponds to the biomass of rice.

### 4.2 OsFTIP9 may regulate FC1 entering into the nucleus

It was proposed that auxin plays a role in suppression axillary buds emergence. Several genetic links have been established on how apically derived auxin eventually functions in the bottom part of the rice plant. One pathway is through the regulation of

isopentenyltransferase (IPT) genes (Tanaka et al. 2006): It was hypothesized that auxin could inhibit the synthesis of CK, and thus, once auxin was absent from the stem tissue, the accumulation of CK was further transported to the axillary buds, which eventually functioned to inhibit the function of FC1. A recent link between SLs and auxin was also established through the expression of carotenoid cleavage dioxygenases (CCDs) (Foo et al. 2005, Arite et al. 2007, Heyward et al. 2009). The mRNAs of *CCDs* were found to correspond to the increase of SLs synthesis, and furthermore, treatment of exogenous SLs on the axillary buds was able to abolish the emergence and growth of axillary buds in mutants with elevated tillering phenotypes (Brewer et al. 2009, Heyward et al. 2009). Based on the available research information, one possible model was that auxin was apically derived and functions in two independent pathways: on one hand, auxin negatively regulates CK; on the other hand, auxin promotes the function of SLs. CK was eventually transported to the bud area, which negatively regulates FC1. While for SLs, they are proposed to promote FC1, yet it awaits for further elucidation given the unclear linkage.

FC1 is a transcription factor that acts very downstream of the pathway controlling rice tillering. It functions to inhibit the outgrowth of axillary buds by regulating the transcription of its downstream genes. Our research showed that OsFTIP9 might be responsible for transporting FC1 into the nucleus for its function inside. We showed that the subcellular localization of FC1 was merely inside the nucleus, but it spread to the entire cell in the *Osftip9* mutant. While we did check the possibility of OsFTIP9

transporting in larger scales, such as intercellular or across tissues, we found no such evidence with all experiments supporting the absence of long-distance transportation. It makes sense for the existence of the solely micro-scale transportation as the transcription of FC1 is in the axillary bud tissue rather than any other tissues. Besides, evidence showed that the presence of OsFTIP9 might help stabilize FC1 protein by unknown mechanisms. Taken all these pieces of evidence together, we showed that OsFTIP9 might function in transporting FC1 into the nucleus, which adds a key piece of knowledge of how FC1 could be regulated.

Now, we still have insufficient evidence to link OsFTIP9 with upstream phytohormones such as SLs, auxin and CK. FC1 is involved in SLs signalling, but the phenotype of *fc1* mutants are distinctive with SL-related mutants except for high tillering ability. SL-related mutants, like *d3*, *d14*, *d10*, *d17* and *d27*, have common dwarfisms, however *fc1* and *Osftip9* have normal plant height. This suggests that OsFTIP9-FC1 module is not simply part of a chain of SLs signalling, though it has inextricable interaction with SL. Our *in vitro* assays had revealed the potential interaction of OsFTIP9 with D14/D14L, but the functional evidences is still lacking. Besides, any possibility of CK or auxin regulation occurs via OsFTIP9 is still worth investigation.

### 4.3 OsFTIP9 might constitute a conserved function of MCTP family proteins in protein trafficking

The C2 domain was firstly reported as the binding site for the $Ca^{2+}$ ion, in the protein kinase C (PKCs), which consists of about 130 residues. Apart from the protein structure of a C2 domain that allows it to function as a docking site, researchers do have reported more than 220 proteins with C2 domains that possess a function of signal transduction or membrane trafficking (Nalefski & Falke, 1996; Rizo & Sudhof, 1998). As mentioned, a C2 domain contains a β-sandwich sheet that is made of 8 antiparallel strands, joint by loops (Essen, Perisic, Lynch, Katan, & Williams, 1997; Perisic, Fong, Lynch, Bycroft, & Williams, 1998; Sutton, Davletov, Berghuis, Sudhof, & Sprang, 1995; Sutton & Sprang, 1998)(49, 126, 165, 166). While the $Ca^{2+}$ binding site consists of several ligands for the $Ca^{2+}$ ions. It was found that most $Ca^{2+}$-dependent C2 domains had a binding capability of 2 or 3 ions (Sutton & Sprang, 1998). C2 domains have higher variety in terms of sequence homology, as compared to the relatively conserved C1 domains, mainly attributing to the different loop regions (Cho & Stahelin, 2005). It is proposed that the diversity of the C2 domain homology leads to the high functional diversity in various processes.

For MCTPs, they consist of several C2 domains coupled with transmembrane domains. The presence of the transmembrane domains enables MCTP to travel through the membranes, such as nuclear membranes and other membranes, and the presence of

several C2 domains enables them to function as a docking site for its interacting proteins (Nalefski & Falke, 1996; Rizo & Sudhof, 1998). Such a proteomic structure combination strongly indicates that MCTP may be an important protein transporter through membrane trafficking.

In this study, we showed that OsFTIP9 interacted with several proteins with similar phenotypes in tiller number generation. After comprehensive analysis and investigation, we chose to focus on the study the interaction between OsFTIP9 and FC1, which is a published gene playing a role downstream of CK and SLs. FC1 is a transcription factor that regulates the expression of several marker genes, yet its detailed upstream controlling mechanism remains to be elucidated. We confirmed the existence of the protein-protein interaction between these two genes, and furthermore, the absence of OsFTIP9 leads to the failure of FC1 being localized to the nucleus. This suggested that OsFTIP9 plays a role in the trafficking of FC1.

The study of macromolecular trafficking proteins has been advanced through research over the fields of structural, biophysical, computational and cell research. They provide insightful, comprehensive analysis and uncover how peripheral proteins differ in the membrane-binding mechanisms in various important developmental processes. Our study shed light on the MCTP functions in one area of transporting an important transcription factor, which eventually affects the rice tillering berhaviour. This contributes to an important regulatory mechanism that ultimately determined the rice

yield, which provides insights for resolving food scarcity problems by producing better rice cultivars. With the increasing availability of genome sequence from various species, we hope that more function of MCTPs could be uncovered in various important biological processes.

### 4.4 Proposed model and future studies

With all the experimental results presented, a potetional signal pathway can be proposed. OsFTIP9 protein may be responsible for transporting FC1 from the cytosome to the nucleus, where FC1, as a transcription factor, functions to regulate the transcription of the downstream genes. One of the potiential downstream gene that is regulated by FC1 under this pathway is *OsGT1* and *D14*, of which the proteins suppress the tillering behavior in rice. This model explains the phenotype that the loss-of-funtion *Osftip9* exhibited increased tiller number: in the ansence of OsFTIP9, FC1 was not recruited into the nucleus. The cascading effect was that the transcription of FC1 downstream genes were not regulated properly.

This model awaits further validation through more experinemts, in order to complete the current story. Due to the limited timeframe of this PhD research course, some experiments were yet to be completed at the time point when this thesis was drafted. Given the absence of those ongiong experiments' results, the current story still stands, yet we still would like to list the future research directions: first, *gOsFTIP9-4HA* will

be delivered into *Osftip9-1* in order to examine whether the tillering phenotype can be rescued by *gOsFTIP9-4HA*. This helps comfirm that the loss of OsFTIP9 causes the increased tiller number. Second, in order to further validate the interaction between OsFTIP9 and FC1, Co-IP will be performed once *gOsFTIP9-4HA Osftip9-1* is obtained, using the validated FC1 antibody. This further confirms the interaction *in vivo*. Third, double mutant of *Osftip9-1 fc1-2* will be produced, in order to compare the phenotypes with *Osftip9-1* and *fc1-2*, respectively. This will indicate the position of these two genes in the proposed signaling patheway. Forth, there are also several experiments that can be carried out to augment the current evidence set, one of which is to check the sub-cellular localization of OsFTIP9. OsFTIP9 is hypothesized to be also localized into the nucleus or the nuclear membrane, for it to transport FC1 into the nucleus. OsFTIP9 can either function as a docking site to recruit FC1 onto the nuclear membrane, or a cargo transporter to carry FC1 into the nucleus.

From a broader perspective, this signaling pathway could be further expaned towards the upstream regulators. It remains unknown that what are the regulators regulating OsFTIP9, and whethere there are any other proteins that function together with OsFTIP9 in order to form a complex, or OsFTIP9 functions alone. Yet these are another set of stories that requires a co mprehensive design of studies.

# References

**Arite, T., Iwata, H., Ohshima, K., Maekawa, M., Nakajima, M., Kojima, M., Sakakibara. H., Kyozuka, J.** (2007). DWARF10, an RMS1/MAX4/DAD1 ortholog, controls lateral bud outgrowth in rice. *Plant J, 51*(6), 1019-1029.

**Arite, T., Umehara, M., Ishikawa, S., Hanada, A., Maekawa, M., Yamaguchi, S., & Kyozuka, J.** (2009). d14, a strigolactone-insensitive mutant of rice, shows an accelerated outgrowth of tillers. *Plant Cell Physiol, 50*(8), 1416-1424.

**Bennett, T., Liang, Y., Seale, M., Ward, S., Muller, D., & Leyser, O.** (2016). Strigolactone regulates shoot development through a core signalling pathway. *Biol Open, 5*(12), 1806-1820.

**Bennett, T., Sieberer, T., Willett, B., Booker, J., Luschnig, C., & Leyser, O.** (2006). The Arabidopsis MAX pathway controls shoot branching by regulating auxin transport. *Curr Biol, 16*(6), 553-563.

**Bernier, G., & Perilleux, C.** (2005). A physiological overview of the genetics of flowering time control. *Plant Biotechnol J, 3*(1), 3-16.

**Bowman, J. L., & Eshed, Y.** (2000). Formation and maintenance of the shoot apical meristem. *Trends Plant Sci, 5*(3), 110-115.

**Brewer, P. B., Dun, E. A., Gui, R., Mason, M. G., & Beveridge, C. A.** (2015). Strigolactone inhibition of branching independent of polar auxin transport. *Plant Physiol, 168*(4), 1820-1829.

**Cho, W., & Stahelin, R. V.** (2005). Membrane-protein interactions in cell signaling

and membrane trafficking. *Annu Rev Biophys Biomol Struct, 34*, 119-151.

**Cook, C. E., Whichard, L. P., Turner, B., Wall, M. E., & Egley, G. H.** (1966). Germination of Witchweed (Striga lutea Lour.): Isolation and Properties of a Potent Stimulant. *Science, 154*(3753), 1189-1190.

**Corbesier, L., Vincent, C., Jang, S., Fornara, F., Fan, Q., Searle, I., Giakountis, A., Farrona, S., Gissot, L., Turnbull, C., Coupland, G.** (2007). FT protein movement contributes to long-distance signaling in floral induction of Arabidopsis. *Science, 316*(5827), 1030-1033.

**De Cuyper, C., Fromentin, J., Yocgo, R. E., De Keyser, A., Guillotin, B., Kunert, K., Boyer, F. D., Goormachtig, S.** (2015). From lateral root density to nodule number, the strigolactone analogue GR24 shapes the root architecture of Medicago truncatula. *J Exp Bot, 66*(13), 4091.

**Doebley, J. F., Gaut, B. S., & Smith, B. D.** (2006). The molecular genetics of crop domestication. *Cell, 127*(7), 1309-1321.

**Domagalska, M. A., & Leyser, O.** (2011). Signal integration in the control of shoot branching. *Nat Rev Mol Cell Biol, 12*(4), 211-221.

**Dun, E. A., de Saint Germain, A., Rameau, C., & Beveridge, C. A.** (2012). Antagonistic action of strigolactone and cytokinin in bud outgrowth control. *Plant Physiol, 158*(1), 487-498.

**Epel, B. L.** (1994). Plasmodesmata: composition, structure and trafficking. *Plant Mol Biol, 26*(5), 1343-1356.

**Essen, L. O., Perisic, O., Lynch, D. E., Katan, M., & Williams, R. L.** (1997). A ternary metal binding site in the C2 domain of phosphoinositide-specific phospholipase C-delta1. *Biochemistry, 36*(10), 2753-2762.

**Fulton, L., Batoux, M., Vaddepalli, P., Yadav, R. K., Busch, W., Andersen, S. U., Jeong, S., Lohman, J. U., Schneitz, K.** (2009). DETORQUEO, QUIRKY, and ZERZAUST represent novel components involved in organ development mediated by the receptor-like kinase STRUBBELIG in Arabidopsis thaliana. *PLoS Genet, 5*(1), e1000355.

**Gomez-Roldan, V., Fermas, S., Brewer, P. B., Puech-Pages, V., Dun, E. A., Pillot, J. P., Letisse, F., Matusova, R., Danoun, S., Portais, J. C., Bouwmeester, H., Becard, G., Beveridge, C. A, Rameau, C., Rochange, S. F.** (2008). Strigolactone inhibition of shoot branching. *Nature, 455*(7210), 189-194.

**Greb, T., Clarenz, O., Schafer, E., Muller, D., Herrero, R., Schmitz, G., & Theres, K.** (2003). Molecular analysis of the LATERAL SUPPRESSOR gene in Arabidopsis reveals a conserved control mechanism for axillary meristem formation. *Genes Dev, 17*(9), 1175-1187.

**Hastings, M. H., & Follett, B. K.** (2001). Toward a molecular biological calendar? *J Biol Rhythms, 16*(4), 424-430.

**Ishikawa, S., Maekawa, M., Arite, T., Onishi, K., Takamure, I., & Kyozuka, J.** (2005). Suppression of tiller bud activity in tillering dwarf mutants of rice. *Plant Cell Physiol, 46*(1), 79-86.

**Jaeger, K. E., & Wigge, P. A.** (2007). FT protein acts as a long-range signal in

Arabidopsis. *Curr Biol, 17*(12), 1050-1054.

**Khush, G. S.** (2005). What it will take to feed 5.0 billion rice consumers in 2030. *Plant molecular biology, 59*(1), 1-6.

**Komatsu, K., Maekawa, M., Ujiie, S., Satake, Y., Furutani, I., Okamoto, H., Shimamoto, K., Kyozuka, J.** (2003). LAX and SPA: major regulators of shoot branching in rice. *Proc Natl Acad Sci U S A, 100*(20), 11765-11770.

**Levy, Y. Y., & Dean, C.** (1998). The transition to flowering. *Plant Cell, 10*(12), 1973-1990.

**Li, C., Zhou, A., & Sang, T.** (2006). Rice domestication by reducing shattering. *Science, 311*(5769), 1936-1939.

**Li, X., Qian, Q., Fu, Z., Wang, Y., Xiong, G., Zeng, D., Wang, X., Liu, X., Teng, S., Horishi, F., Yuan, M., Luo, D., Han, B., Li, J.** (2003). Control of tillering in rice. *Nature, 422*(6932), 618-621.

**Liang, W., Shang, F., Lin, Q., Lou, C., & Zhang, J.** (2014). Tillering and panicle branching genes in rice. *Gene, 537*(1), 1-5.

**Lin, M. K., Belanger, H., Lee, Y. J., Varkonyi-Gasic, E., Taoka, K., Miura, E., Xoconostle-Cázares, B., Gendler, K., Jorgensen, R. A., Phinney, B., Lough, T. J., Lucas, W. J.** (2007). FLOWERING LOCUS T protein may act as the long-distance florigenic signal in the cucurbits. *Plant Cell, 19*(5), 1488-1506.

**Lin, Q., Wang, D., Dong, H., Gu, S., Cheng, Z., Gong, J., Qin, R., Jiang, L., Li, G., Wang, J. L., Wu, F., Guo, X., Zhang, X., Lei, C., Wang, H, Wan, J.** (2012). Rice

APC/C(TE) controls tillering by mediating the degradation of MONOCULM 1. *Nat Commun, 3*, 752.

**Lin, Z., Griffith, M. E., Li, X., Zhu, Z., Tan, L., Fu, Y., Zhang, W., Wang, X., Xie, D., Sun, C.** (2007). Origin of seed shattering in rice (Oryza sativa L.). *Planta, 226*(1), 11-20.

**Liu, L., Li, C., Song, S., Teo, Z. W. N., Shen, L., Wang, Y., Jackson, D., Yu, H.** (2018). FTIP-Dependent STM Trafficking Regulates Shoot Meristem Development in Arabidopsis. *Cell Rep, 23*(6), 1879-1890.

**Liu, L., Liu, C., Hou, X., Xi, W., Shen, L., Tao, Z., Wang, Y., Yu, H.** (2012). FTIP1 is an essential regulator required for florigen transport. *PLoS Biol, 10*(4), e1001313.

**Liu, L., Zhu, Y., Shen, L., & Yu, H.** (2013). Emerging insights into florigen transport. *Curr Opin Plant Biol, 16*(5), 607-613.

**Martin-Trillo, M., & Cubas, P.** (2010). TCP genes: a family snapshot ten years later. *Trends Plant Sci, 15*(1), 31-39.

**Mastsuo, T., & Hoshikawa, K. Science of the rice plant. vol. 1, morphology.**

**Mathieu, J., Warthmann, N., Kuttner, F., & Schmid, M.** (2007). Export of FT protein from phloem companion cells is sufficient for floral induction in Arabidopsis. *Curr Biol, 17*(12), 1055-1060.

**Minakuchi, K., Kameoka, H., Yasuno, N., Umehara, M., Luo, L., Kobayashi, K., Hanada, A., Ueno, K., Asami, T., Yamaguchi, S., Kyozuka, J.** (2010). FINE CULM1 (FC1) works downstream of strigolactones to inhibit the outgrowth of axillary buds in

rice. *Plant Cell Physiol, 51*(7), 1127-1135.

**Nalefski, E. A., & Falke, J. J.** (1996). The C2 domain calcium-binding motif: structural and functional diversity. *Protein Sci, 5*(12), 2375-2390.

**Oikawa, T., & Kyozuka, J.** (2009). Two-Step Regulation of LAX PANICLE1 Protein Accumulation in Axillary Meristem Formation in Rice. *Plant Cell, 21*(4), 1095-1108.

**Perisic, O., Fong, S., Lynch, D. E., Bycroft, M., & Williams, R. L.** (1998). Crystal structure of a calcium-phospholipid binding domain from cytosolic phospholipase A2. *J Biol Chem, 273*(3), 1596-1604.

**Prusinkiewicz, P., Crawford, S., Smith, R. S., Ljung, K., Bennett, T., Ongaro, V., & Leyser, O.** (2009). Control of bud activation by an auxin transport switch. *Proc Natl Acad Sci U S A, 106*(41), 17431-17436.

**Pysh, L. D., Wysocka-Diller, J. W., Camilleri, C., Bouchez, D., & Benfey, P. N. (**1999). The GRAS gene family in Arabidopsis: sequence characterization and basic expression analysis of the SCARECROW-LIKE genes. *Plant J, 18*(1), 111-119.

**Rizo, J., & Sudhof, T. C.** (1998). C2-domains, structure and function of a universal $Ca^{2+}$-binding domain. *J Biol Chem, 273*(26), 15879-15882.

**Schumacher, K., Schmitt, T., Rossberg, M., Schmitz, G., & Theres, K.** (1999). The Lateral suppressor (Ls) gene of tomato encodes a new member of the VHIID protein family. *Proc Natl Acad Sci U S A, 96*(1), 290-295.

**Song, S., Chen, Y., Liu, L., See, Y. H. B., Mao, C., Gan, Y., & Yu, H.** (2018a). Author Correction: OsFTIP7 determines auxin-mediated anther dehiscence in rice. *Nat Plants,*

*4*(12), 1124.

**Song, S., Chen, Y., Liu, L., Wang, Y., Bao, S., Zhou, X., Teo, Z. W., Mao, C., Gan, Y., Yu, H.** (2017). OsFTIP1-Mediated Regulation of Florigen Transport in Rice Is Negatively Regulated by the Ubiquitin-Like Domain Kinase OsUbDKgamma4. *Plant Cell, 29*(3), 491-507.

**Sutton, R. B., Davletov, B. A., Berghuis, A. M., Sudhof, T. C., & Sprang, S. R.** (1995). Structure of the first C2 domain of synaptotagmin I: a novel $Ca^{2+}$/phospholipid-binding fold. *Cell, 80*(6), 929-938.

**Sutton, R. B., & Sprang, S. R.** (1998). Structure of the protein kinase Cbeta phospholipid-binding C2 domain complexed with $Ca^{2+}$. *Structure, 6*(11), 1395-1405.

Sweeney, M. T., Thomson, M. J., Pfeil, B. E., & McCouch, S. (2006). Caught red-handed: Rc encodes a basic helix-loop-helix protein conditioning red pericarp in rice. *Plant Cell, 18*(2), 283-294.

**Tabuchi, H., Zhang, Y., Hattori, S., Omae, M., Shimizu-Sato, S., Oikawa, T., Qian, Q., Nishimura, M., Kitano, H., Xie, H., Fang, X., Yoshida, H., Kyozuka, J., Chen, F., Sato, Y.** (2011). LAX PANICLE2 of rice encodes a novel nuclear protein and regulates the formation of axillary meristems. *Plant Cell, 23*(9), 3276-3287.

**Tamaki, S., Matsuo, S., Wong, H. L., Yokoi, S., & Shimamoto, K.** (2007). Hd3a protein is a mobile flowering signal in rice. *Science, 316*(5827), 1033-1036.

**Tan, L., Li, X., Liu, F., Sun, X., Li, C., Zhu, Z., Fu, Y., Cai, H., Wang, X., Xie, D., Sun, C.** (2008). Control of a key transition from prostrate to erect growth in rice domestication. *Nat Genet, 40*(11), 1360-1364.

**Umehara, M., Hanada, A., Yoshida, S., Akiyama, K., Arite, T., Takeda-Kamiya, N., Magome, H., Kamiya, Y., Shirasu, K., Yoneyama, K., Kyozuka, J., Yamaguchi, S.** (2008). Inhibition of shoot branching by new terpenoid plant hormones. *Nature, 455*(7210), 195-200.

**Vaddepalli, P., Herrmann, A., Fulton, L., Oelschner, M., Hillmer, S., Stratil, T. F., Fastner, A., Hammes, U. Z., Ott, T., Robinson, D. G., Schneitz, K.** (2014). The C2-domain protein QUIRKY and the receptor-like kinase STRUBBELIG localize to plasmodesmata and mediate tissue morphogenesis in

**Wang, Y., & Li, J.** (2005). The plant architecture of rice (Oryza sativa). *Plant Mol Biol, 59*(1), 75-84.

**Waters, M. T., Gutjahr, C., Bennett, T., & Nelson, D. C.** (2017). Strigolactone Signaling and Evolution. *Annu Rev Plant Biol, 68*, 291-322.

**Xu, C., Wang, Y., Yu, Y., Duan, J., Liao, Z., Xiong, G., Meng, X., Liu, G., Qian, Q., Li, J.** (2012). Degradation of MONOCULM 1 by APC/C(TAD1) regulates rice tillering. *Nat Commun, 3*, 750.

**Xu, Y., McCouch, S. R., & Shen, Z.** (1998). Transgressive segregation of tiller angle in rice caused by complementary gene action. *Crop sci, 38*(1), 12-19.

**Yao, R., Ming, Z., Yan, L., Li, S., Wang, F., Ma, S., Yu, C., Yang, M., Chen, L., Chen, L., Li, Y., Yan, C., Miao, D., Sun, Z., Yan, J， Sun, Y., Wan, L., Chu, J., Fan, S., He, W., Deng, H., Nan, F， Li, J., Rao, Z., Luo, Z., Xie, D.** (2016). DWARF14 is a non-canonical hormone receptor for strigolactone. *Nature, 536*(7617), 469-473.

**Yuan, Z., Gao, S., Xue, D. W., Luo, D., Li, L. T., Ding, S. Y., Yao, X., Wilson, Z. A.,**

**Qian, Q., Zhang, D. B.** (2009). RETARDED PALEA1 controls palea development and floral zygomorphy in rice. *Plant Physiol, 149*(1), 235-244.

**Zeevaart, J. A.** (1962). Physiology of Flowering: Flowering is hormonally controlled, but the nature of the hormone remains to be elucidated. *Science, 137*(3532), 723-731.

**Zhang, M. Y., Bourbouloux, A., Cagnac, O., Srikanth, C. V., Rentsch, D., Bachhawat, A. K., & Delrot, S.** (2004). A novel family of transporters mediating the transport of glutathione derivatives in plants. *Plant Physiol, 134*(1), 482-491.

# Appendix

## Publication during Graduate Course

Shiyong Song, Ying Chen, Lu Liu, Yanwen Wang, Shengjie Bao, **Xuan Zhou**, Zhi Wei Norman Teo, Chuanzao Mao, Yinbo Gan, Hao Yu. (2017). OsFTIP1-Mediated Regulation of Florigen Transport in Rice Is Negatively Regulated by the Ubiquitin-Like Domain Kinase OsUbDKgamma4. **Plant Cell***, 29*(3), 491-507.